

Springer Theses

Recognizing Outstanding Ph.D. Research

Magdalena Zych

Quantum Systems Under Gravitational Time Dilation



Springer

Springer Theses

Recognizing Outstanding Ph.D. Research

Aims and Scope

The series “Springer Theses” brings together a selection of the very best Ph.D. theses from around the world and across the physical sciences. Nominated and endorsed by two recognized specialists, each published volume has been selected for its scientific excellence and the high impact of its contents for the pertinent field of research. For greater accessibility to non-specialists, the published versions include an extended introduction, as well as a foreword by the student's supervisor explaining the special relevance of the work for the field. As a whole, the series will provide a valuable resource both for newcomers to the research fields described, and for other scientists seeking detailed background information on special questions. Finally, it provides an accredited documentation of the valuable contributions made by today's younger generation of scientists.

Theses are accepted into the series by invited nomination only and must fulfill all of the following criteria

- They must be written in good English.
- The topic should fall within the confines of Chemistry, Physics, Earth Sciences, Engineering and related interdisciplinary fields such as Materials, Nanoscience, Chemical Engineering, Complex Systems and Biophysics.
- The work reported in the thesis must represent a significant scientific advance.
- If the thesis includes previously published material, permission to reproduce this must be gained from the respective copyright holder.
- They must have been examined and passed during the 12 months prior to nomination.
- Each thesis should include a foreword by the supervisor outlining the significance of its content.
- The theses should have a clearly defined structure including an introduction accessible to scientists not expert in that particular field.

More information about this series at <http://www.springer.com/series/8790>

Magdalena Zych

Quantum Systems Under Gravitational Time Dilation

Doctoral Thesis accepted by
University of Vienna, Vienna, Austria



Springer

Author

Magdalena Zych
Centre for Engineered Quantum Systems,
School of Mathematics and Physics
The University of Queensland
Brisbane, QLD
Australia

Supervisor

Prof. Časlav Brukner
Institute for Quantum Optics and Quantum
Information, University of Vienna
Vienna
Austria

ISSN 2190-5053

Springer Theses

ISBN 978-3-319-53191-5

DOI 10.1007/978-3-319-53192-2

ISSN 2190-5061 (electronic)

ISBN 978-3-319-53192-2 (eBook)

Library of Congress Control Number: 2017930278

© Springer International Publishing AG 2017

This work is subject to copyright. All rights are reserved by the Publisher, whether the whole or part of the material is concerned, specifically the rights of translation, reprinting, reuse of illustrations, recitation, broadcasting, reproduction on microfilms or in any other physical way, and transmission or information storage and retrieval, electronic adaptation, computer software, or by similar or dissimilar methodology now known or hereafter developed.

The use of general descriptive names, registered names, trademarks, service marks, etc. in this publication does not imply, even in the absence of a specific statement, that such names are exempt from the relevant protective laws and regulations and therefore free for general use.

The publisher, the authors and the editors are safe to assume that the advice and information in this book are believed to be true and accurate at the date of publication. Neither the publisher nor the authors or the editors give a warranty, express or implied, with respect to the material contained herein or for any errors or omissions that may have been made. The publisher remains neutral with regard to jurisdictional claims in published maps and institutional affiliations.

Printed on acid-free paper

This Springer imprint is published by Springer Nature

The registered company is Springer International Publishing AG

The registered company address is: Gewerbestrasse 11, 6330 Cham, Switzerland

Supervisor's Foreword

Time in physics is unambiguously operationally defined as “what a clock shows”. Accordingly, time is defined through other quantities, such as spin precession in a magnetic field, which can serve as a reference clock. The status of time varies in different theories in physics. In Newtonian physics and non-relativistic quantum mechanics, time flows at the same rate for all clocks. According to general relativity, however, clocks tick slower when they are closer to a massive body and faster if they are placed further away from the massive body. This time dilation effect results in a so-called “twin paradox”: if one twin moves out to live at a higher altitude, they will age faster than the other twin, who remains on the ground. This effect was verified with remarkable accuracy in general relativistic experiments, but never in conjunction with genuine quantum effects such as quantum superposition or entanglement.

In her work, Magdalena Zych considers a single clock that is brought into a quantum superposition of two locations—one closer and one further away from a massive body. The single quantum clock then takes the role of both “twins” from the classical paradox. *What is the time as shown by the clock?* Taking this problem as a starting point, the author proposes several original and ingenious ways to probe the notion of time at the interplay between quantum theory and general relativity. This topic is in the focus of the research conducted at the University of Vienna and the Institute for Quantum Optics and Quantum Information (IQOQI).

The author investigates a matter and an optical interferometer where time dilation induced by different gravitational potentials in the two arms of the interferometer lead to a decrease in visibility of the quantum interference patterns. The innovative aspect of this experiment as compared to typical atom interferometer setups lies in the clock that is used. While standard setups induce a phase shift explainable with Newtonian gravity, Zych’s experimental proposal employs an internal time-evolving degree of freedom to work as a clock. In consequence, relativistic time of the clock becomes a “which-path” witness. As a result of Bohr’s complementarity principle, a loss in the visibility of the interference pattern occurs.

The origin of this loss lies in the entanglement between the internal states of the clock and its spatial position.

Zych then argues that the entanglement induced by the time dilation affects the coherence of spatial superpositions of generic composite systems, for which the revival time of coherence increases with the size of the system. For macroscopic systems, this effectively leads to a new decoherence mechanism. In this way, the author demonstrates that gravity plays a certain role in the transition from the quantum world to the classical world.

The formalism developed by Magdalena Zych for composite quantum systems in gravity relies on the metric nature of gravity, and in particular on the Einstein Equivalence Principle (EEP). The weak version of the principle states the equivalence between rest, inertial and gravitational mass-energies. However, in quantum mechanics, even non-relativistic, quantized internal energies contribute to the total mass-energies. In her work, the author proposes a “quantum weak EEP” to state the equivalence between the rest, inertial and gravitational internal energy *operators* and explores ways to test it in experiment.

Finally, the author considers a situation where the temporal order between a set of events A is entangled with the temporal order between a set of events B . Here, the order of events is defined operationally with respect to physical “clocks”. Zych goes on to show that combined quantum and general relativistic effects allow a violation of a Bell-like inequality for temporal order. An experimental violation of the inequality would question the mere possibility of defining temporal order prior to and independent of measurement.

Readers geared towards theory will delight in the stringent, precise and detailed way in which Magdalena Zych lays out her arguments. But also experimentalists will appreciate the analysis as the author never leaves the ground of operationally justified concepts and understands well experimental constraints.

Ever since in 2012, the Nobel Prize in Physics was awarded to Serge Haroche and David J. Wineland for their independent development of revolutionary experimental methods for the control of individual quantum systems, the development of quantum technologies has seen a drastic rise. We have good reason to believe that soon, we will be able to enter the joined regime of quantum and relativistic physics, breaking new ground in the study of the notion of time. When we arrive at that waypoint, Magdalena Zych's thesis will have been among the most important first steps in the right direction.

Vienna, Austria
December 2016

Prof. Časlav Brukner

Abstract

The regime where quantum mechanics and general relativity jointly apply is not yet completely understood and remains beyond reach of our experimental capabilities. Therefore, there is a fundamental interest in finding feasible experiments that could probe the interplay between quantum and general relativistic phenomena.

This thesis explores how time dilation affects internal dynamics of quantum particles—topic largely overlooked in theoretical research. Crucially, such particles can be seen as ideal “clocks”—and the thesis thus focuses on new quantum effects from proper time in interference experiments with “clocks”. The framework developed to that purpose also reveals that new experimental paradigm is necessary to tests the very validity of the metric picture of gravity at the interplay with quantum mechanics. In contrast to the present understanding, its validity in quantum theory does not follow from its validity in the classical limit, and relevant for the difference is the quantisation of the internal states of test particles—and not of their position. The operational approach to “clocks” is finally extended to a scenario where a large mass in a quantum superposition state influences the causal relations between the “clocks”. The resulting causal structure is non-classical: temporal order between a pair of time-like events can become entangled with the order between another pair of time-like events. This permits for a violation of Bell-like inequality formulated here for temporal order. On the one hand this shows quantitatively how temporal relations can exhibit quantum features. On the other—that such scenarios can be described within standard quantum theory and general relativity and no inconsistencies arise.

New physical effects of time dilation in quantum mechanics derived in this work can be within reach of the near future interference experiments with “clocks” implemented in electrons, atoms, also photons. The operational approach to proper time at the interplay with quantum theory might further lead to a new framework describing non-perturbative effects of quantum gravity.

Acknowledgements

My deep appreciations goes to Časlav Brukner for his support, engagement and guidance throughout the years. Discussions of quantum foundations in the Währinger Park between Časlav and people he gathered around were a game-changing experience, when I first visited Vienna as an Erwin Schrödinger Fellow.

I am therefore forever indebted to people without whom I would never venture onto the scientific path: Profs. Piotr Kosiński and Paweł Maślanka—mentors of my undergraduate studies in Łódź. I am grateful for their encouragement and support, and for introducing me to research activities still in my undergraduate years—a rare opportunity which I deeply appreciate.

I extend gratitude to the members of my doctoral thesis advisory committee, Markus Aspelmeyer and Daniel Greenberger. Markus' enthusiasm and passion for fundamental questions resulted in many stimulating discussions. Danny Greenberger is one of the most original thinkers I had the chance to meet. Working with Danny during my visit in New York was an amazing scientific adventure and personally a mile stone—also thank to his wife Suzy. I will always cherish the memory of playing truant one day with Danny in the Natural History Museum.

I was lucky to cross my paths with Fabio Costa and Igor Pikovski, fellow Ph.D. students. Many thanks to both of you for the amazing time spent working, discussing and travelling together—I continue to draw inspiration from our meeting!

From the many people with whom I enjoyed important discussions during the last years I would like to thank especially Janet Anders, Markus Arndt, Yuri Bonder, Jörg Frölich, Christopher Hilweg, Radek Łapkiewicz, Juan Leon, Francesco Massa, Holger Müller, Tomasz Paterek, William Plick, Sven Ramelow, Carlo Rovelli, Sahar Sahebdivan, Philip Walther, Reinhard Werner, Marcin Wieśniak, Jakob Yngvason, Anton Zeilinger, Marek Żukowski. I owe special thanks to Harvey Brown for his fascinating lectures and to Timothy C. Ralph for drawing our attention to Shapiro delay and the resulting fruitful collaboration.

I should not miss the opportunity to thank all colleagues from my group, in particular for the greatly heated debates that make the Brukner's group journal club so special. Thank you Mateus Araújo, Veronika Baumann, Esteban Castro,

Borivoje Dakic, Adrien Feix, Flaminia Giacomini, Johannes Kofler, Ognian Oreshkov, Jacques Pienaar, Tobias Schäfer, Mark Williamson.

I acknowledge the doctoral program Complex Quantum Systems (CoQuS) and the Austrian Academy of Science (ÖAW) for financial support and in particular Christiane Losert for her great help on countless occasions.

I thank my parents for their unconditional support and my brother for friendship and continuing inspiration.

Contents

1	Introduction	1
	References	6
2	Classical Clocks in General Relativity	9
2.1	Point Particles with Internal Degrees of Freedom	9
2.1.1	Hamiltonian	9
2.1.2	Lagrangian	11
2.1.3	Energy-Momentum Tensor	13
2.1.4	Routhian or Point Particles as Ideal Clocks	14
2.1.5	Low Energy and Non-relativistic Limits and Symmetries of the Framework	17
2.2	Derivation of the Point-Particle Framework	22
2.2.1	Effective Dynamics of Relativistic N-Particle Systems	22
2.2.2	Quantitative Discussion of the Approximations	25
2.3	Relevance of the Framework for Experiments	26
	References	28
3	Quantum Clocks in General Relativity	29
3.1	Quantisation of the Composite Point-Particle Framework	29
3.2	Low-Energy and Non-relativistic Limits, and Symmetries of the Framework	31
3.3	Mass Superselection Rule in the Context of Composite Particles	34
	References	35
4	Quantum Complementarity and Time Dilation	37
4.1	Quantum Complementarity—Interferometric Visibility Versus Which-Way Information	37
4.2	Which-Way Information from Time Dilation—Gedankenexperiment	43
	References	46

5	Interference of “Clocks”—Experimental Proposals	47
5.1	Massive Particle as a “clock”	47
5.1.1	Time Dilation Effects for Massive Quantum Systems	47
5.1.2	Two-Level Quantum System as a Clock	50
5.1.3	Quantitative Predictions	53
5.1.4	Discussion	55
5.2	Photons as Clocks	56
5.2.1	Gravitational Time Dilation for Light—Shapiro Delay	57
5.2.2	Gaussian Photon Wave-Packet as a Clock	59
5.2.3	Quantitative Predictions	61
5.2.4	Discussion	63
5.3	General Relativistic and Quantum Aspects of the Proposals	65
	References	67
6	Decoherence from Time Dilation	71
6.1	Visibility for General Internal States	71
6.2	Visibility and Decoherence Time for Thermal States	73
6.3	Ideas for Experimental Verification	75
6.4	Discussion	76
	References	78
7	Quantum Formulation of the Einstein Equivalence Principle	81
7.1	Motivation	81
7.2	Quantum Formulation and Test Theory of the EEP	83
7.3	Testing the Quantum Formulation of the EEP	87
7.3.1	Testing the Quantum Formulation of the WEP	88
7.3.2	Testing the Quantum Formulation of the LPI and LLI	90
7.4	Discussion	94
	References	95
8	Clocks Beyond Classical Space-Time	99
8.1	Superpositions of Temporal Order	99
8.2	Bell Inequalities for Temporal Order	103
8.2.1	Violation of Bell Inequalities for Temporal Order	106
8.3	Discussion	110
	References	113
9	Conclusions and Outlook	115
	References	117
	Appendix A	119
	Appendix B	121
	Appendix C	123
	Appendix D	127

Contents	xiii
Appendix E	129
Appendix F	137

Chapter 1

Introduction

The understanding of nature has been radically changed by the advent of quantum mechanics and general relativity. Quantum theory questions the view that physical quantities have pre-defined local values independent of the experimental context, merely revealed in the measurement [1–3]; while general relativity forces us to abandon the understanding of space-time as a passive and absolute arena. Instead, it describes the space-time as a physical system whose dynamics depends on the presence of matter and whose geometry gives rise to the phenomenon of gravity [4] (see also textbooks [5–7], for the philosophy of special and general relativity see [8, 9]). And thus, for example, the worldview in which particles follow definite paths in space, and which in free fall are accelerated by the gravitational force, has been entirely overthrown: Quantum mechanics describes the particles as following in superposition all paths in space, and the “classical trajectory” can be recovered as the one where extreme constructive interference of the paths occur [10]. General relativity renders the notion of a gravitational force obsolete and describes free fall as an inertial motion along a straight line, albeit in a space-time that is curved by massive objects.

The two theories do not only provide a different perspective on the known phenomena, but also predict new effects, counterintuitive from the perspective of the preceding paradigm. Initially, when no intuition is yet developed for a novel framework, its distinctive effects often seem “paradoxical”. The Einstein-Podolski-Rosen (EPR) “paradox” [11] in quantum theory or the twin paradox in relativity [7] are the well known examples. Crucial for resolving such “paradoxes” is an operational approach often exemplified by *thought experiments*: hypothetical—but in principle realisable—experimental scenarios. Operational approach helps to understand the theories’ foundations, built the physical intuition and ultimately, to develop the theory further.

Let us briefly recall how this approach worked for the EPR “paradox”. The EPR “paradox” is based on certain assumptions about what any “reasonable” (in the worldview of the authors) physical theory should satisfy. The authors considered a

(maximally) entangled state of two distant particles (two spins with zero total angular momentum, in the version due to Bohm [12]). Quantum theory predicts perfect correlations between such particles: any measurement outcome obtained on one of them allows predicting with certainty the outcome of the same observable measured on the other particle. One of the EPR assumptions was that of “locality”: due to the separation of the systems, they argued, one can assume that any manipulation on one of the particles should not affect the state of the other, and thus also outcomes of observations that can be made on it. The EPR concluded that exploiting perfect correlations between systems in an entangled state it is possible to determine with arbitrary precision—and without changing the state of a system—all its properties (by making corresponding measurements on its distant entangled partner). Their next assumption was that such properties should then be viewed as pertaining to the particle, and called them “elements of reality”. They defined as *complete* a theory that provides mathematical description of all “elements of reality”. But according to quantum theory not all properties of a system are simultaneously defined with arbitrary precision—this is known as quantum complementarity. The conclusion of the EPR was that quantum theory (or a quantum state, to be more precise) is not a complete description of Nature. Bell’s theorem [1] can then be seen as a formalisation of the assumptions of the EPR and application of the resulting structure to a concrete experiment. The theorem states that a certain inequality (particularly simple to derive in the so-called CHSH form [13]) is obeyed by results of measurements on two systems in *any* theory that satisfies the assumptions of the EPR. He also showed that quantum theory allows for a violation of this bound. Crucially, experiments also do violate the Bell inequality [14, 15] (note also the most recent experiments, realised with making as few assumptions as possible, so called “loophole-free” Bell tests: [16–18]). EPR would thus need to conclude that no reasonable theory can describe Nature, that can account for the results of experiments. Bell’s result, while mathematically very simple, led to deep insights into philosophy of physics, as well as into the structure of quantum theory. In particular, it brought to light the significance of correlations, which according to quantum mechanics can be stronger than those allowed by classical physics [19]. Ultimately, Bell’s approach led to the development of the field of quantum information [20]. The key lesson for us here is that by considering operationally well-defined scenario Bell showed that theories incorporating the EPR assumptions (whether they are complete or not) and the quantum theory give different predictions. It could then be resolved by experiments which of the two accounts of “reality” agrees with observations.

It might be difficult to imagine that the famous traveling twins, from the “twin paradox”, indeed were thought challenge the self-consistency of relativity still in the 1970s. The journal *Nature* [21–23] as well as *Physics Today* published heated debates between time-dilation sceptics [24] and their colleagues who offered various explanations to the recurring questions: why the difference between the proper time intervals in the observer’s own and a different inertial frame is not in contradiction with the reciprocity of Lorentz transformations, or why proper time cannot be described by a single-valued function in relativity without getting rid of virtually all relativistic effects [25]. An operational approach to answering the question about

physical reality of the twin paradox is to focus on a scenario where the twins take different world lines connecting two common events (start and end of their respective journeys). The reason is that only if the twins' path meet again the question: Who is older *now*? makes physically sense. Space-like separated events do not have physically well-defined time order in relativity—it is one of the key aspects of the theory, not a “technical detail”. Various explanations of the twin paradox published in the course of the above mentioned debates helped understanding the physical significance of the proper time and pin-point its most relevant aspect: that the time elapsing for an observer or object is determined by the “length” of their world line in space-time. Such an understanding of the proper time provides powerful intuition, allowing us to immediately resolve the apparent paradox of the travelling twins. It is also at the heart of all time-dilation experiments, where pairs of clocks, such as decaying particles, atoms or ions, are put on different trajectories and then compared [26–29]. Finally, the reality of the twin paradox routinely impacts our modern communication technologies, such as the Global Positioning System. There are two key messages from the twin paradox debate for the present work. First, that clocks taken along different paths in space in general do show different times when brought together. Second, that asking what time two *distant* clocks show “now” is not a well posed question, because the notion of “now” is not unique. Depending on the way the “present” is defined¹ one will obtain a different answer—simply because different ways of defining “now” in the end correspond to different physical situations, different experiments.

The regime where quantum mechanics and general relativity jointly apply gives rise to further puzzles, above those present in either of the frameworks alone. At high energies (comparable with the particle's rest mass-energy mc^2) the very notion of a particle is replaced with a state of a quantum field [30], which generally does not contain a definite number of particles. Even the above notion of a particle becomes questionable when the space-time curvature cannot be neglected [31]. The regime of quantum fields in curved space-time also has its paradoxes, such as the black hole information paradox. Here, the assumption of unitarity of quantum theory and the existence of thermal radiation from black holes, the Hawking radiation [32, 33], assumed to lead to a complete evaporation of a Black Hole, seem to be in contradiction. Though fiercely debated for five decades, the black-hole-information paradox remains largely unresolved (see e.g. [34, 35] for a review). It is speculated that for its explanation it is necessary to describe gravity as a quantum theory.

The framework of quantum gravity is expected to bring a further great paradigm shift. No such complete framework has yet been developed and various attempts are profoundly disparate, both in their mathematical approaches and in their physical conjectures [36]. The crucial obstacle is the lack of any experimental results that could guide the development of the theory. Note, however, that even predictions of quantum field theory in curved space-time—such as the above mentioned Hawking radiation, or effects of the space-time curvature on ultrarelativistic particles [37, 38]—are beyond present day experimental capabilities.

¹More technically: what foliation of space-time into space like hypersurfaces one considers.

It is indeed a striking fact that all experiments performed to date, where both quantum mechanics and gravity are relevant, are fully compatible with the non-metric, Newtonian gravity—which has so thoroughly been disproved for classical systems (see e.g. [39]). The first experiment measuring the effect of gravity on a quantum system was performed by Colella, Overhauser, and Werner (COW) [40]. In this experiment single neutrons travel in a superposition along two paths at different heights above the Earth. Due to the different gravitational potential along the paths—and thus a difference in the potential energy—a relative phase is acquired between the superposed amplitudes of the neutron. This relative phase is measured from the interference pattern observed when the amplitudes are recombined. Today, analogous experiments with so called atomic fountains [41] are used to perform high-precision measurements of the gravitational acceleration g [42–44] and of the gravitational constant G [45, 46]. In different type of experiments, neutrons were trapped in a gravitational well—created by Earth gravitational potential and a horizontal mirror. Neutrons trapped above the mirror showed quantisation of the energy levels in agreement with the predictions of non-relativistic quantum mechanics [47]. By “shaking” carefully the mirror it was further possible to induce and measure oscillations (so called Rabi oscillations) of the neutrons between the gravitational levels [48]. All these effects are fully accounted for by a non-relativistic Schrödinger equation with Newtonian gravitational potential.

Moreover, in all to date performed tests of general relativity, the degrees of freedom relevant for the observation of general relativistic effects can be fully described by the laws of classical physics. To give just a few examples relevant to this thesis: The seminal Pound-Rebka redshift experiment [49] showed that the frequency of gamma rays emitted from an iron foil placed on top of a 22.5 m tower (at Harvard’s Jefferson Laboratory) is higher as compared to the frequency of gamma rays that can be absorbed by an identical foil placed at the foot of the tower. Their result is fully explained by the theory of classical electromagnetic waves (the gamma rays) in curved space-time, which predicts the gravitational redshift of light climbing up the gravitational potential and a corresponding blue-shift of light that “descends” down. Another example is the Shapiro effect [50, 51]—the slow-down of light in the presence of a massive object. Also this effect is fully understood within classical electrodynamics in curved space-time. The first high precision experiment testing the twin paradox—or time dilation—with precise atomic clocks was the Hafele-Keating experiment [26, 27]. In this test, the time difference accrued between initially synchronised Caesium-beam clocks taken along different trajectories on board of commercial planes was measured. There results are fully described in terms of difference in the proper lengths between the classical world lines of the atomic clocks.² Thus, not only the quantum gravity or quantum field theory in curved space-time remain

²While to describe internal states of the Caesium atoms, or modern high-precision atomic clocks [29] quantum theory is unquestionably required, time dilation measured with the use of such clocks depends on their centre of mass—which in all to-date experiments was consistent with a classical description.

untested—even the regime where classical general relativity and quantum mechanics both play a role has never been subject to experimental verification.

A new take on this problem has recently come from the field of relativistic quantum information [52]. With a pragmatic goal of understanding the relation between quantum information and relativity this field has sparked new proposals for quantum optics experiments at large-distance scales, where effects of space-time curvature would become relevant, see e.g. Ref. [53] for a review. Nevertheless, the gap between experimental and theoretical advance in the research area so fundamental to modern physics persists.

This thesis proposes yet a different approach: it asks whether there are both quantum and general relativistic effects that could be observed in low-energy quantum systems subject to weak gravitational effects, on earth? The answer to this question is “yes” and the main result of the thesis are the predictions of such novel effects, a theoretical framework to quantitatively describe them, and ideas how to test these effects with matter wave interferometers in earth-based experiments. The effects described in the Thesis are related to time dilation and how it affects quantum coherence. Their discovery was enabled by a thoroughly operational treatment of time: which is here considered only in relation to actual physical systems that can measure it. The thesis thus starts with developing a framework to describe *ideal* relativistic quantum “clocks” (quantum systems with internal dynamical degrees of freedom, such as atoms, molecules, electronic or neutron spins; the framework is also extended to photons). It is then shown that when the “clocks” display quantum features, like quantum interference or entanglement, new physical effects arise due to time dilation—effects which do not appear for classical relativistic clocks nor for quantum clocks subject to non-relativistic, Newtonian gravity. Physical regime where these effects are measurable is rapidly getting closer to our experimental capabilities and might thus allow for first tests of the interplay between quantum mechanics and general relativity.

Chapter 2 introduces a framework of point-like relativistic particles with internal degrees of freedom in classical physics. It shows how the regime arises as a limit of a generic bound system. It is then shown that such particles can be seen as ideal relativistic classical clocks. Key conceptual features and regime of validity of the framework are discussed. In particular, it is shown how the universality of time dilation arises from the perspective of the dynamics of the clocks—these considerations hold for the quantum case as well, and are directly relevant for the main results of the thesis. Chapter 3 presents the quantisation of the relativistic “clock” framework. It derives the Hamiltonian of an ideal quantum “clock” under weak relativistic gravity. Chapter 4 introduces a quantum version of the twin paradox—a thought experiment in which a single quantum “clock” takes in superposition two paths along which different amounts of proper time elapse. The framework developed in Chap. 4 is used to derive new effects arising in the quantum twin paradox scenario. An interpretation of these effects is discussed, in terms of quantum complementarity between possibility of observing interference and the amount of “which-way” information available due to time dilation. Chapter 5 presents experimental proposals aimed at probing the new effects of time dilation with massive and massless systems.

Chapter 6 generalises the analysis of the previous chapters to the case of quantum systems in generic states—not only in specific “clock-states”. The results show that universality of time dilation leads to a universal decoherence mechanism, which affects coherence in the external degrees of freedom of highly complex system. While the first chapters assume validity of the metric description of gravity in the regime where quantum effects are relevant, Chap. 7 discusses the conditions necessary for this to be the case. The results show that validity of the metric picture of gravity—i.e. of the Einstein Equivalence Principle (EEP)—in quantum theory does not follow from its validity in classical physics: testing it constraining more parameters in conceptually different tests. Chapter 8 extends the operational approach developed for clocks and applies it to space-time events: which are here defined with respect to physical systems used as clocks (which can mark the position and time coordinates of the events). A thought experiment is then proposed where due to quantum state of a large mass, the temporal order between a pair of time-like events in the resulting space-time becomes entangled with the order between another pair of time-like events. This chapter shows that, on the one hand, temporal order of events cannot be classically pre-defined independently of the experimental context, and on the other—that even scenarios where space-time is provably non-classical can be consistently described within the standard quantum theory and general relativity, contrary to a common view [54–57].

References

1. J.S. Bell, On the Einstein-Podolsky-Rosen paradox. *Physics* **1**, 195–200 (1964)
2. J. Bell, *Speakable and Unsayable in Quantum Mechanics: Collected Papers on Quantum Philosophy* (Cambridge University Press, 2004)
3. R.A. Bertlmann, A. Zeilinger, *Quantum (un) Speakables: from Bell to Quantum Information* (Springer Science and Business Media, 2013)
4. A. Einstein, The foundation of the general theory of relativity. *Ann. Phys.* **40**, 284–337 (1916)
5. S.M. Carroll, *Spacetime and Geometry. An Introduction to General Relativity*, vol 1 (Addison-Wesley, 2004)
6. C.W. Misner, K.S. Thorne, J.A. Wheeler, *Gravitation* (Macmillan, 1973)
7. S. Weinberg, *Gravitation and Cosmology: Principle and Applications of General Theory of Relativity* (Wiley, New York, 1972)
8. A. Einstein, L. Infeld, *The Evolution of Physics: the Growth of Ideas from Early Concepts to Relativity and Quanta* (An Essandess paperback, Simon and Schuster, 1961)
9. H. Brown, *Physical Relativity:space-time Structure from a Dynamical Perspective: Space-time Structure from a Dynamical Perspective*, Oxford Scholarship Online. *PhiloSophy Module* (Clarendon Press, 2005)
10. R.P. Feynman, R.B. Leighton, M. Sands, *The Feynman Lectures on Physics*. Quantum Mechanics, vol 3 (Addison-Wesley, Inc., Reading, Mass.-London, 1965q)
11. A. Einstein, B. Podolsky, N. Rosen, Can quantum-mechanical description of physical reality be considered complete? *Phys. Rev.* **47**, 777–780 (1935)
12. D. Bohm, *Quantum Theory* (Courier Corporation, 1951)
13. J.F. Clauser, M.A. Horne, A. Shimony, R.A. Holt, Proposed experiment to test local hidden-variable theories. *Phys. Rev. Lett.* **23**, 880–884 (1969)

14. S.J. Freedman, J.F. Clauser, Experimental test of local hidden-variable theories. *Phys. Rev. Lett.* **28**, 938–941 (1972)
15. A. Aspect, P. Grangier, G. Roger, Experimental test of local hidden-variable theories via Bell's theorem. *Phys. Rev. Lett.* **47**, 460–463 (1981)
16. B. Hensen, H. Bernien, A. Dréau, A. Reiserer, N. Kalb, M. Blok, J. Ruitenbergh, R. Vermeulen, R. Schouten, C. Abellán et al., Loophole-free Bell inequality violation using electron spins separated by 1.3 kilometres. *Nature* **526**, 682–686 (2015)
17. M. Giustina, M.A.M. Versteegh, S. Wengerowsky, J. Handsteiner, A. Hochrainer, K. Phelan, F. Steinlechner, J. Kofler, J.-A. Larsson, C. Abellán, W. Amaya, V. Pruneri, M.W. Mitchell, J. Beyer, T. Gerrits, A.E. Lita, L.K. Shalm, S.W. Nam, T. Scheidl, R. Ursin, B. Wittmann, A. Zeilinger, Significant-loophole-free test of Bell's theorem with entangled photons. *Phys. Rev. Lett.* **115**, 250401 (2015)
18. L.K. Shalm, E. Meyer-Scott, B.G. Christensen, P. Bierhorst, M.A. Wayne, M.J. Stevens, T. Gerrits, S. Glancy, D.R. Hamel, M.S. Allman, K.J. Coakley, S.D. Dyer, C. Hodge, A.E. Lita, V.B. Verma, C. Lambrocco, E. Tortorici, A.L. Migdall, Y. Zhang, D.R. Kumor, W.H. Farr, F. Marsili, M.D. Shaw, J.A. Stern, C. Abellán, W. Amaya, V. Pruneri, T. Jennewein, M.W. Mitchell, P.G. Kwiat, J.C. Bienfang, R.P. Mirin, E. Knill, S.W. Nam, Strong loophole-free test of local realism*. *Phys. Rev. Lett.* **115**, 250402 (2015)
19. B. Dakić, Č. Brukner, Quantum Theory and Beyond: Is Entanglement Special?, in *Deep Beauty—Understanding the Quantum World through Mathematical Innovation*, ed. by H. Halvorson, (American Institute of Physics, 2011) pp. 365–392
20. M.A. Nielsen, I.L. Chuang, *Quantum Computation and Quantum Information: 10th Anniversary Edition*, 10th edn. (Cambridge University Press, New York, NY, USA, 2011)
21. H. Dingle, The case against special relativity. *Nature* **216**, 119–122 (1967)
22. W.H. McCrea, Why the special theory of relativity is correct. *Nature* **216**, 122–124 (1967)
23. F.J.M. Farley, Is the special theory right or wrong?: experimental verifications of the theory of relativity. *Nature* **217**, 17–18 (1968)
24. J. Terrell, R.K. Adair, R.W. Williams, F.C. Michel, D.A. Ljung, D. Greenberger, J.P. Matthesen, V. Korenman, T.W. Noonan, R. Price, V. Sandberg, P.H. Polak, S.R. de Groot, G. Lüders, J. G. Fletcher, M. Sachs, Atom interferometers and the gravitational redshift. *Phys. Today* **25**, 9 (1972)
25. D.M. Greenberger, The reality of the twin paradox effect. *Am. J. Phys.* **40**, 750–754 (1972)
26. J.C. Hafele, R.E. Keating, Around-the-world atomic clocks: predicted relativistic time gains. *Science* **177**, 166–168 (1972)
27. J.C. Hafele, R.E. Keating, Around-the-world atomic clocks: Observed relativistic time gains. *Science* **177**, 168–170 (1972)
28. C.-W. Chou, D. Hume, T. Rosenband, D. Wineland, Optical clocks and relativity. *Science* **329**, 1630–1633 (2010)
29. T.L. Nicholson, S.L. Campbell, R.B. Hutson, G.E. Marti, B. Bloom, R. McNally, W. Zhang, M. Barrett, M. Safronova, G. Strouse, W. Tew, J. Ye, Systematic evaluation of an atomic clock at 2×10^{-18} total uncertainty. *Nat. Comm.* **6**, 6896 (2015)
30. S. Weinberg, *The Quantum Theory of Fields*, vol. 2 (Cambridge University Press, 1996)
31. D. Colosi, C. Rovelli, What is a particle? *Class. Quantum Gravity* **47**, 245–252 (2009)
32. S.W. Hawking, Black hole explosions. *Nature* **248**, 30–31 (1974)
33. S.W. Hawking, Particle creation by black holes. *Commun. Math. Phys.* **43**, 199–220 (1975)
34. D. Harlow, Jerusalem Lectures on Black Holes and Quantum Information, [arXiv:1409.1231](https://arxiv.org/abs/1409.1231) [hep-th]
35. S.D. Mathur, The information paradox: a pedagogical introduction. *Class. Quantum Gravity* **26**, 224001 (2009)
36. C. Kiefer, *Quantum Gravity (General) and Applications* (Springer, Berlin Heidelberg, 2009)
37. K. Konno, M. Kasai, General relativistic effects of gravity in quantum mechanics: a case of ultrarelativistic, spin 1/2 particles. *Progress Theoret. Phys.* **100**, 1145–1157 (1998)
38. S. Dimopoulos, P.W. Graham, J.M. Hogan, M.A. Kasevich, General relativistic effects in atom interferometry. *Phys. Rev. D* **78**, 042003 (2008)

39. C.M. Will, The confrontation between general relativity and experiment. *Living Rev. Relativ.* **17**, 4 (2014), [arXiv:1403.7377](https://arxiv.org/abs/1403.7377) [bibgr-qc]
40. R. Colella, A. Overhauser, S. Werner, Observation of gravitationally induced quantum interference. *Phys. Rev. Lett.* **34**, 1472–1474 (1975)
41. S. Chu, Nobel lecture: the manipulation of neutral particles. *Rev. Mod. Phys.* **70**, 685–706 (1998)
42. A. Peters, K.Y. Chung, S. Chu, Measurement of gravitational acceleration by dropping atoms. *Nature* **400**, 849–852 (1999)
43. S. Fray, C.A. Diez, T.W. Hänsch, M. Weitz, Atomic interferometer with amplitude gratings of light and its applications to atom based tests of the equivalence principle. *Phys. Rev. Lett.* **93**, 240404 (2004)
44. H. Müller, S.-W. Chiow, S. Herrmann, S. Chu, K.-Y. Chung, Atom-interferometry tests of the isotropy of post-Newtonian gravity. *Phys. Rev. Lett.* **100**, 031101 (2008)
45. G. Rosi, F. Sorrentino, L. Cacciapuoti, M. Prevedelli, G. Tino, Precision measurement of the Newtonian gravitational constant using cold atoms. *Nature* **510**, 518–521 (2014)
46. G.M. Tino, Testing gravity with atom interferometry, in *Proceedings of the International School of Physics—Enrico Fermi*, eds. by G.M. Tino, M.A. Kasevich (2014) pp. 457–493
47. V.V. Nesvizhevsky, H.G. Börner, A.K. Petukhov, H. Abele, S. Baeßler, F.J. Rueß, T. Stöferle, A. Westphal, A.M. Gagarski, G.A. Petrov et al., Quantum states of neutrons in the Earth’s gravitational field. *Nature* **415**, 297–299 (2002)
48. T. Jenke, P. Geltenbort, H. Lemmel, H. Abele, Realization of a gravity-resonance-spectroscopy technique. *Nature Phys.* **7**, 468–472 (2011)
49. R. Pound, G. Rebka, Apparent weight of photons. *Phys. Rev. Lett.* **4**, 337–341 (1960)
50. I.I. Shapiro, Fourth test of general relativity. *Phys. Rev. Lett.* **13**, 789–791 (1964)
51. I.I. Shapiro, M.E. Ash, R.P. Ingalls, W.B. Smith, D.B. Campbell, R.B. Dyce, R.F. Jurgens, G.H. Pettengill, Fourth test of general relativity: new radar result. *Phys. Rev. Lett.* **26**, 1132–1135 (1971)
52. R.B. Mann, T.C. Ralph, Relativistic quantum information. *Class. Quantum Gravity* **29** (2012)
53. D. Rideout, T. Jennewein, G. Amelino-Camelia, T.F. Demarie, B.L. Higgins, A. Kempf, A. Kent, R. Laflamme, X. Ma, R.B. Mann et al., Fundamental quantum optics experiments conceivable with satellites-reaching relativistic distances and velocities. *Class. Quantum Gravity* **29**, 224011 (2012)
54. L. Diósi, Models for universal reduction of macroscopic quantum fluctuations. *Phys. Rev. A* **40**, 1165 (1989)
55. R. Penrose, On gravity’s role in quantum state reduction. *Gen. Relativ. Gravit.* **28**, 581–600 (1996)
56. L. Diósi, Intrinsic time-uncertainties and decoherence: comparison of 4 models. *Braz. J. Phys.* **35**, 260–265 (2005)
57. P.C.E. Stamp, Environmental decoherence versus intrinsic decoherence. *Phil. Trans. R. Soc. A* **370**, 4429–4453 (2012)

Chapter 2

Classical Clocks in General Relativity

This chapter discusses the regime of point-like systems with internal degrees of freedom in general relativity. First, a heuristic derivation of the framework is given and the focus is on the consistency and general properties of the formalism. It is shown that the framework has a well-behaved action, its own symmetry group and that in the non-relativistic limit it reduces to the Newtonian theory. The interpretation of the framework as describing ideal clocks is then presented. The second part of the chapter sketches a derivation of the composite particle framework. It shows how the framework naturally arises as a description of a generic many particle system that is sufficiently well-localised. Crucial approximations involved in the derivation are quantitatively discussed. Finally, relevance of the framework for tests of general relativity is reviewed in the light of time dilation and redshift experiments.

For simplicity, space-time is assumed to be static, with metric tensor $g_{\mu\nu}$ satisfying $g_{0i} = g_{i0} = 0$ and $g_{ij} = g_{ji}$ for $i, j = 1, 2, 3$, metric is dimensionless with signature $(-+++)$.

2.1 Point Particles with Internal Degrees of Freedom

2.1.1 Hamiltonian

In general relativity a point particle following a world line $x^\mu(t)$ (where, for now, t shall be considered an arbitrary parameterisation of the world line) can be described by a covariant momentum four-vector $p_\mu(x)$, where $x \equiv x^\mu$, and this short notation will be used hereafter (for coordinates as well as for the momenta). Energy of the

Section 2.1.5 includes excerpts from *Quantum formulation of the Einstein Equivalence Principle*, M. Zych and Č. Brukner, [arXiv:1502.00971](https://arxiv.org/abs/1502.00971) (2015).

particle is described by the component p_0 and the three-momentum—by components p_j , $j = 1, 2, 3$. From the covariance of the momentum four-vector p_μ follows that the scalar product $p_\mu p^\mu = \sum_{\mu\nu} p_\mu(x) g^{\mu\nu}(x) p_\nu(x)$ is a coordinate invariant quantity. In particular, in the coordinates in which the particle is at rest $p'_j = \frac{\partial x^v}{\partial x'^j} p_\nu = 0$ for $j = 1, 2, 3$ this invariant reads:

$$p_\mu p^\mu = p'_0 g'^{00} p'_0 \quad (2.1)$$

(the x -dependence of the quantities will hereafter be omitted whenever it does not lead to ambiguities). The time component x'^0 is not fixed by the requirement that the particle is at rest with respect to this new coordinates. Taking this component to be the proper time along the particle's world line results in $g'^{00} = \eta^{00} = -1$, where $\eta_{\mu\nu}$ is the Minkowski metric. This natural choice of the time parameter will be adopted hereafter.

The total rest frame energy is given by cp'_0 . It comprises not only the energy stemming from the rest mass mc^2 of the system but also any binding or kinetic energies of the internal degrees of freedom and thus also the particle's internal Hamiltonian H_{int} . It can thus be written as

$$cp'_0 = mc^2 + H_{int} \equiv H_{rest}.$$

On the other hand, p_0 describes dynamics of the particle with respect to the initial, arbitrary, time coordinate and includes energy of the internal as well as the external degrees of freedom. It constitutes the total Hamiltonian of the system relative to the arbitrary but fixed coordinates and will be denoted by $H \equiv cp_0$. From the Eq. (2.1) the total Hamiltonian of a point-like relativistic particle with internal degrees of is found to be

$$H = \sqrt{\frac{-c^2 p_j p^j + g'^{00} H_{rest}^2}{g^{00}}}$$

Incorporating that $g'^{00} = -1$ in the “primed” coordinate system, and that $g_{00} = (g'^{00})^{-1}$ for a static metric, the Hamiltonian takes the form

$$H = \sqrt{-g_{00}(c^2 p_j p^j + H_{rest}^2)}. \quad (2.2)$$

The Hamiltonian in Eq. (2.2) generalises that of an elementary massive particle of mass m , which reads $H_m = \sqrt{-g_{00}(c^2 p_j p^j + mc^2)}$, by including the total internal mass-energy $mc^2 + H_{int}$ rather than just the rest mass parameter mc^2 . Systems that can be described with the formalism of point-like particles with internal degrees of freedom include atoms or molecules (see also Sect. 2.2), for which large contribution to the rest mass is given by binding energies between atoms, nucleons, quarks, etc. (from the perspective of the standard model of particle physics all masses reduce to the energy of the Higgs field). Note, that in general relativity, there is no unique distinction

between the “mass” and “energy” and the above can be seen as an expression of the mass-energy equivalence. It will be discussed in the Sect. 2.1.5 how the definition of the mass and the split between mass and energy arise in the non-relativistic limit. Such a split depends on the context in which the system is discussed (energy scale, type and precision of measurements, etc.) and entails that the lowest energy of the internal Hamiltonian H_{int} is zero.

2.1.2 Lagrangian

The regime of point-like composed particles is as an effective approximation to the underlying elementary physics (and the next section will discuss this in detail), therefore, it is worth showing that such an effective description presents a fully consistent theory. Below the Lagrangian for a point-like relativistic system with internal degrees of freedom is derived from the Hamiltonian in Eq. (2.2). It is then shown that such a Lagrangian gives rise to a scalar action and thus to covariantly conserved energy-momentum tensor, consistent with the Hamiltonian derived in Eq. (2.2).

Hamiltonian of a system with N degrees of freedom is defined over a phase space $(x_1, \dots, x_N; p_1, \dots, p_N)$, whereas Lagrangian is described in a configuration space $(x_1, \dots, x_N; \dot{x}_1, \dots, \dot{x}_N)$, where $\dot{x}_n^\mu \equiv \frac{dx_n^\mu}{dt}$, $n = 1, \dots, N$. Given a Hamiltonian $H(x_1, \dots, x_N; p_1, \dots, p_N)$ its corresponding Lagrangian $L(x_1, \dots, x_N; \dot{x}_1, \dots, \dot{x}_N)$, giving fully equivalent descriptions of the system, is obtained via a Legendre transform:

$$L = \sum_n p_{ni} \dot{x}_n^i - H; \quad (2.3)$$

where \dot{x}_n^i and p_{ni} are 3-velocities and 3-momenta, respectively, $i = 1, 2, 3$, and

$$\dot{x}_n^i := \frac{\partial H}{\partial p_{ni}}. \quad (2.4)$$

Velocity \dot{x}_n^i is called canonically conjugate to the momentum p_{ni} and by the virtue of Eq. (2.4) is defined with respect to the same time parameter with respect to which the Hamiltonian H is defined.

The Hamiltonian of a point-like particle with internal degrees of freedom $H = \sqrt{\frac{-c^2 p_j p^j + g^{00} H_{rest}^2}{g^{00}}}$, in Eq. (2.2), describes a system with an external degree of freedom, with momentum p_i , and with N internal degrees of freedom, whose coordinates and momenta will be denoted by q_k and w_k , respectively, $k = 1, \dots, N$. The dynamics of these internal degrees of freedom is given by internal energy, $H_{rest} \equiv H_{rest}(q_k, w_k)$, which implies that such defined w_k are defined with respect to the *rest frame* time coordinate. From Eq. (2.4), velocity \dot{x}^j conjugate to the external momentum p_j of the Hamiltonian H above reads

$$\dot{x}^j = \frac{-c^2 p^j}{g^{00} H} \quad (2.5)$$

and velocities \dot{q}_k canonically conjugate to w_k read

$$\dot{q}_k = \frac{g^{00} H_{rest}}{g^{00} H} \frac{\partial H_{rest}}{\partial w_k}. \quad (2.6)$$

From Eqs. (2.3), (2.5) and (2.6) follows

$$L = -\frac{c^2 p^j p_j}{H g^{00}} + \sum_k \frac{g^{00} H_{rest}}{g^{00} H} \frac{\partial H_{rest}}{\partial w_k} w_k - H.$$

Note, that the Legendre transform of the rest frame Hamiltonian H_{rest} with respect to internal momenta w_k is by definition the rest frame Lagrangian

$$L_{rest} = \sum_k \frac{\partial H_{rest}}{\partial w_k} w_k - H_{rest} \quad (2.7)$$

and thus

$$L = \frac{g^{00} H_{rest}}{g^{00} H} L_{rest}$$

From the above, Eq. (2.5) and from the explicit form of H follows that

$$c \frac{g^{00} H_{rest}}{g^{00} H} = \sqrt{g^{00} (g_{00} + \dot{x}^j \dot{x}_j)} = \sqrt{-g_{\mu\nu} \dot{x}^\mu \dot{x}^\nu}. \quad (2.8)$$

where the last equality incorporates that $g^{00} = -1$ and a time coordinate $x^0 = ct$ has been introduced such that $\dot{x}^0 = \frac{\partial H}{\partial p_0} = c$, which guarantees that the two pictures are indeed an equivalent description of the same physics and with respect to the same coordinates. Collecting the two formulas above, the final form of the Lagrangian follows:

$$L = L_{rest} \frac{1}{c} \sqrt{-g_{\mu\nu} \dot{x}^\mu \dot{x}^\nu} \equiv L_{rest} \dot{\tau}, \quad (2.9)$$

where it has been used that $\sqrt{-g_{\mu\nu} \dot{x}^\mu \dot{x}^\nu}/c$ is nothing but the derivative of the proper time element $d\tau := \sqrt{-g_{\mu\nu} dx^\mu dx^\nu}/c$ along the system's world line $x^\mu(t)$ with respect to the time parameter t .

Lagrangian L in Eq. (2.9) generalises that of a structureless massive particle with mass m , which reads $L_m = -mc^2 \dot{\tau}$. In particular, the rest frame Lagrangian L_{rest} has the form

$$L_{rest} = -mc^2 + L_{int},$$

which, follows from Eq. (2.7) with $H_{rest} = mc^2 + H_{int}$ and L_{int} arises as the Legendre transform of H_{int} . In a full analogy to the Hamiltonian description in Sect. 2.1.1 (see Eq. (2.2) and comments thereafter) the internal dynamics of a composed particle comprises the static part $-mc^2$ and the dynamical part L_{int} .

The action S corresponding to the Lagrangian L reads $S = \int L dt$ and using Eq. (2.9) it can be written as

$$S = \int L_{rest} d\tau. \quad (2.10)$$

The rest frame Lagrangian L_{rest} defined in Eq. (2.7) is a scalar (by definition, since the rest energy H_{rest} was defined as scalar) as well as the proper time element—and thus so is S in Eq. (2.10). This entails that the energy-momentum tensor $T^{\mu\nu}(x)$ of the system is covariantly conserved and that equations of motion resulting from such an action are generally covariant, see e.g. [1] for a general reference.

2.1.3 Energy-Momentum Tensor

Below an explicit form of the energy-momentum tensor of a point-like relativistic particle with internal dynamics is derived. The modern definition of the energy momentum tensor of a system with the Lagrangian L reads

$$T^{\mu\nu}(x) := \frac{-2}{\sqrt{-g}} \frac{\delta L}{\delta g_{\mu\nu}(x)}, \quad (2.11)$$

where $\frac{\delta}{\delta g_{\mu\nu}(x)}$ denotes a functional derivative with respect to the field $g_{\mu\nu}(x)$ and $g := \text{Det} g_{\mu\nu}$ (determinant of the matrix $g_{\mu\nu}$).

In order to obtain $T^{\mu\nu}$ for the Lagrangian $L = L_{rest} \dot{\tau}$ note, that the internal Lagrangian depends on the internal variables q_k and on their velocities with respect to the proper time τ : $L_{rest} = L_{rest}(q_k, \frac{q_k}{d\tau})$. This is evident from its definition in Eq. (2.7) and from the fact that $\frac{\partial H_{rest}}{\partial w_k} = \frac{dq_k}{d\tau}$ (which can be seen by substituting $\dot{\tau} = \frac{g^{00} H_{rest}}{g^{00} H}$, Eq. (2.8), into Eq. (2.6)). In order to compute the variation of the internal Lagrangian $\frac{\delta L_{rest}(q_k, dq_k/d\tau)}{\delta g_{\mu\nu}(x)}$ —which is not independent of the metric since $c\dot{\tau} = \sqrt{-g_{\mu\nu} \dot{x}^\mu \dot{x}^\nu}$ —it is convenient to use the relation $\frac{dq_k}{d\tau} = \frac{\dot{q}_k}{\dot{\tau}}$, which yields

$$\frac{\delta L_{rest}}{\delta g_{\mu\nu}(x)} = - \sum_k \frac{\partial L_{rest}}{\partial \frac{dq_k}{d\tau}} \frac{dq_k}{d\tau} \frac{1}{\dot{\tau}} \frac{\delta \dot{\tau}}{\delta g_{\mu\nu}(x)}.$$

The energy momentum tensor of the system is given by $T^{\mu\nu}(x) = \frac{-2}{\sqrt{-g}} (\frac{\delta L_{rest}}{\delta g_{\mu\nu}(x)} \dot{\tau} + L_{rest} \frac{\delta \dot{\tau}}{\delta g_{\mu\nu}(x)})$ and takes the form

$$T^{\mu\nu}(x) = \frac{2}{\sqrt{-g}} \left(\sum_k \frac{\partial L_{rest}}{\partial \frac{dq_k}{d\tau}} \frac{dq_k}{d\tau} - L_{rest} \right) \frac{\delta \dot{\tau}}{\delta g_{\mu\nu}(x)}$$

Note, that inverse Legendre transform, applied to a Lagrangian, gives the corresponding Hamiltonian, therefore

$$H_{rest} = \sum_k \frac{\partial L_{rest}}{\partial \frac{dq_k}{d\tau}} \frac{dq_k}{d\tau} - L_{rest}. \quad (2.12)$$

The variation of $\dot{\tau}$ with respect to the metric reads

$$\frac{\delta \dot{\tau}}{\delta g_{\mu\nu}(x)} = \frac{-\dot{x}^\mu \dot{x}^\nu}{2c^2 \dot{\tau}},$$

and the final form of the energy-momentum tensor for the considered system takes the form

$$T^{\mu\nu}(x) = \frac{-1}{\sqrt{-g}} H_{rest} \frac{\dot{x}^\mu \dot{x}^\nu}{c^2 \dot{\tau}}. \quad (2.13)$$

Such defined energy-momentum tensor is also metric energy-momentum. The corresponding four-momentum is given by $p_\mu = \sqrt{-g} T^0_\mu$ and in particular $\sqrt{-g} T^0_0 = -H_{rest} \frac{\dot{x}^0 \dot{x}^0 g_{00}}{\dot{\tau}}$ is the energy component, which is equal¹ to the Hamiltonian H , as can be checked by substituting $\dot{\tau} = \frac{g^{00} H_{rest}}{g^{00} H}$ (Eq. (2.8)), $x^0 = ct$ and $g^{00} = -1$.

The energy-momentum tensor in Eq. (2.13) generalises that of a point particle with mass m , which reads $T_m^{\mu\nu}(x) = \frac{-1}{\sqrt{-g}} m \frac{\dot{x}^\mu \dot{x}^\nu}{\dot{\tau}}$, analogously as for the case of Lagrangian and Hamiltonian, discussed in Sects. 2.1.2 and 2.1.1.

2.1.4 Routhian or Point Particles as Ideal Clocks

The relevance of here discussed physical regime lies in the fact that point-like systems with internal dynamics represent ideal clocks in relativity. Lagrangian of a point-like composed relativistic system obtained in Sect. 2.1.2 has a general, product form $L = L_{rest} \dot{\tau}$ (cf. 2.9) which already has an intuitive interpretation in terms of the time dilation of the internal dynamics of the system. However, in the context of time dilation experiments the frequency of clocks is often given in terms of energy while

¹For scalar particles the metric energy-momentum tensor coincides with the canonically defined via Noether's theorem (whose energy component coincides with the energy obtained from the Legendre transform of the Lagrangian). For other than spin zero scalar particles the two tensor differ (the canonical tensor is e.g. not symmetric), see e.g. [2] for further discussion. From the perspective of general relativity the metric energy-momentum is much more convenient: it is by definition covariantly conserved and constitutes the source term in the Einstein equations derived from the variational principle.

time dilation is expressed in terms of relative velocity and position in the gravitational potential between the rest reference frames of the clocks. Similar observation holds for redshift experiments. It is therefore convenient use a formalism where internal degrees of freedom are described by a Hamiltonian, whereas the external ones— by a Lagrangian (in configuration space). Such a formalism is provided by a Routhian.

Routhian is defined as a partial Legendre transform of the Lagrangian—with respect to a subset of degrees of freedom; it is therefore a Hamiltonian with respect to the Legendre-transformed ones and a Lagrangian with respect to the remaining ones. In particular, the Routhian considered here is

$$R := \sum_k \frac{\partial L}{\partial \dot{q}_k} \dot{q}_k - L, \quad (2.14)$$

and the notation is the same as in Sect. 2.1.2. The internal momentum w_k in terms of the configuration space variables reads

$$w_k = \frac{\partial L_{rest}}{\partial (dq_k/d\tau)} \equiv \frac{\partial L}{\partial \dot{q}_k}$$

and Eq. (2.14) takes the form

$$R = \left(\sum_k \frac{\partial L_{rest}}{\partial \frac{q_k}{d\tau}} \frac{q_k}{d\tau} - L_{rest} \right) \dot{\tau}.$$

Recall, that the expression in the bracket is the internal Hamiltonian, Eq. (2.12), and the Routhian can be written as:

$$R = H_{rest} \dot{\tau}. \quad (2.15)$$

The Routhian in Eq. (2.15) acts like a Hamiltonian on the internal degree of freedom and describes dynamics of a system with respect to a time parameter t . The speed of the time evolution of any internal observable a_i with respect to t is thus given by a Poisson bracket $\dot{a}_i = \{a_i, R\}$. Equivalently, using Eq. (2.15), one finds

$$\dot{a}_i = \{a_i, H_{rest}\} \dot{\tau}. \quad (2.16)$$

It immediately follows from Eq. (2.16) that $v_{rest} := \{a_i, H_{rest}\} = \frac{da_i}{d\tau}$, is the speed of the time evolution of a_i with respect to the proper time τ . Thus, internal degrees of freedom of the system moving along a world line γ will evolve as if the time elapsed during this evolution was the proper length of the world line $\tau_\gamma = \int_\gamma d\tau$:

$$a_i(t_f) - a_i(t_{in}) = \int_\gamma \dot{a}_i dt = \int_\gamma v_{rest} \dot{\tau} dt = v_{rest} \tau_\gamma, \quad (2.17)$$

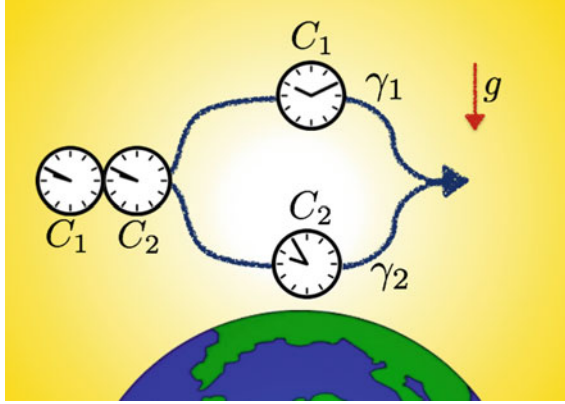


Fig. 2.1 Time dilation between two systems C_1 and C_2 moving along world lines γ_1 , γ_2 , respectively. The two systems have time evolving internal degrees of freedom and can thus be used as “clocks”. Prepared in the same internal configuration, the systems C_1 , C_2 evolve into different final states if the proper lengths of γ_1 and γ_2 differ, Eq. (2.18) (e.g. due to earth’s gravitational field g)—initially synchronised “clocks” taken along different paths generally show different times when brought together. Universality of this prediction gave rise to the formulation of the “twin paradox”—a Gedankenexperiment in which instead of synchronised clocks one considers twins, who set up on separate journeys and meet at a predefined future event, when it transpires that each of them has aged differently—by the amount of proper time which elapsed along their world line

where t_f and t_{in} are the values of the parameter t that correspond to the end points of γ , and for simplicity a constant speed of the internal dynamics has been assumed. Any two systems moving along different world lines γ_1 and γ_2 , e.g. as in Fig. 2.1, will thus exhibit a universal difference in their internal time evolution, equal to the proper time difference between their trajectories. Indeed, from Eq. (2.17) follows

$$\int_{\gamma_1} \dot{a}_i dt - \int_{\gamma_2} \dot{a}_i dt = v_{rest} \Delta\tau \quad (2.18)$$

where $\Delta\tau := \tau_{\gamma_1} - \tau_{\gamma_2}$.

Finally, note that for an observer using a time parameter t the system will evolve by a time interval $\int_{\gamma} dt$ and this observer will describe the system’s internal evolution as time dilated by a universal factor $\dot{\tau}$. Consequently, the internal Hamiltonian of the system will in such coordinates be “red-shifted” by the factor $\dot{\tau}$ and will read $H_{rest} \dot{\tau}$. Thus, time dilation is tantamount to the presence of interactions between the internal degrees of freedom (described by H_{rest}) and the external ones (described by $\dot{\tau}$), which originate from the specific form of general relativistic description of composed systems.

Dynamics of relativistic point-like systems allows an interoperation that such systems “measure” proper time along their world lines. Their internal evolution exhibits a universal time dilation when the systems are taken along different trajectories in space-time—only depending on the proper time difference between the trajectories

and not on the systems themselves. In this sense point-like systems with internal degrees of freedom can be seen as ideal clocks.

2.1.5 Low Energy and Non-relativistic Limits and Symmetries of the Framework

Point particles with internal degrees of freedom in the low energy and non-relativistic limits. In order to consider the non-relativistic limit of the framework, valid in some earth-based scenario, the Schwarzschild space time will be considered. To lowest order the metric components read [1]: $g_{00} \approx -(1 + 2\frac{\Phi(x)}{c^2})$, $g_{ij} \approx \delta_{ij}$, where $\Phi(x) = -\frac{Gm_e}{x}$ is the earth's gravitational potential (with G the Newton constant and m_e —the mass of earth) which immediately gives the low-energy limit of the Routhian, R_{le} :

$$H_{rest}\dot{\tau} \approx H_{rest} \left(1 - \frac{\vec{v}^2}{2c^2} + \frac{\Phi(x)}{c^2} \right) =: R_{le}, \quad (2.19)$$

with $\vec{v} := (\dot{x}^1, \dot{x}^2, \dot{x}^3)$ denoting the centre of mass velocity with respect to the laboratory reference frame. The corresponding Hamiltonian reads

$$H_{le} = H_{rest} + \frac{\vec{p}^2 c^2}{2H_{rest}} + H_{rest} \frac{\Phi(x)}{c^2} \quad (2.20)$$

and one could think that the Eq. (2.19) already gives the non-relativistic limit of the dynamics of a particle with a total mass $M := H_{rest}/c^2$. However, if the internal degrees of freedom are not stationary, Eqs (2.19), (2.20) will feature relativistic time dilation effects. In the Eq. (2.19) the terms $H_{rest}(1 - \frac{\vec{v}^2}{2c^2})$ and $H_{rest}(1 + \frac{\Phi(x)}{c^2})$ give rise to the lowest order special relativistic and gravitational time dilation of internal dynamics, respectively: time evolution of an internal observable a_i under R_{le} reads $v_{rest}(1 - \frac{\vec{v}^2}{2c^2} + \frac{\Phi(x)}{c^2})$ with $v_{rest} := \{a_i, H_{rest}\}$, cf. Sect. 2.1.4. From an operational perspective the theory of Newtonian particles with “dynamical mass” H_{rest}/c^2 —Eq. (2.20)—is not a consistent non-relativistic theory, in particular it does not give rise to the Euclidean space-time with absolute time. In order to find the consistent non-relativistic limit it is convenient to split the internal energy H_{rest} into a constant part E_{rest} —such that $\{a_i, E_{rest}\} = 0$ —and the remaining part which drives the dynamics of the internal degrees of freedom. The Routhian in Eq. (2.19) can equivalently be written as $R_{le} = H_{rest} + E_{rest} \left(-\frac{\vec{v}^2}{2c^2} + \frac{\Phi(x)}{c^2} \right) + (H_{rest} - E_{rest}) \left(-\frac{\vec{v}^2}{2c^2} + \frac{\Phi(x)}{c^2} \right)$. The first term, H_{rest} , results in the universal rate of internal evolution with no time dilation effects, as well as the second term proportional to E_{rest} and it is the last term proportional to $H_{rest} - E_{rest}$ which introduces time dilation. Therefore, the consistent non-relativistic limit is given by $H_{rest} + E_{rest} \left(-\frac{\vec{v}^2}{2c^2} + \frac{\Phi(x)}{c^2} \right)$ and arises

when the dynamical part of the internal energy is small, i.e. internal dynamics is slow. Moreover, the constant E_{rest} defines the mass parameter of the system $m := E_{rest}/c^2$ and $H_{rest} - E_{rest}$ is equivalent to H_{int} introduced earlier in this Chapter. The non-relativistic limit can thus equivalently be written as

$$R_{nr} = mc^2 + H_{int} - m \frac{\vec{v}^2}{2} + m\Phi(x). \quad (2.21)$$

Under R_{nr} the rate of the internal evolution is the same in any coordinates $\{a, R_{nr}\} = \{a, H_{int}\}$ and such a dynamical theory is consistent with the Euclidean space-time. Moreover, this shows that the non-relativistic limit of point particles with internal dynamics represents ideal clocks of the non-relativistic mechanics, as expected. With the definition of the mass parameter as $m = E_{rest}/c^2$ one also recovers the usual understanding of the non-relativistic limit as the zeroth order in $1/c^2$. The low-energy Hamiltonian in terms of $H_{rest} = mc^2 + H_{int}$ reads $H_{le} = mc^2 + H_{int} + \frac{\vec{p}^2}{2(m + H_{int}/c^2)} + (m + H_{int}/c^2)\Phi(x)$ and taking the non-relativistic limit gives the familiar Hamiltonian of the Newtonian dynamics

$$H_{nr} = mc^2 + H_{int} + \frac{\vec{p}^2}{2m} + m\Phi(x).$$

In summary, for composed systems the correct non-relativistic limit is described not only by small kinetic and potential energies of the external degree of freedom, but also by slow internal evolution—i.e. small *dynamical* part of the internal energy. The reason is that, in such a case the contributions of the dynamical part of the internal energy are relevant only in the rest energy term but can be neglected in the kinetic and potential energy terms (since these are already small in the considered limit), to which only the static part of the internal energy effectively contributes. This can be seen as the origin of the split between the mass and energy in the non-relativistic physics, which are fully equivalent in the relativistic theory. From this perspective the mass parameter of a non-elementary system can be *defined* as the static part of its internal energy, in appropriate units.²

Finally, note that for a non-relativistic limit of a theory to be at all meaningful, one needs to assume that the relevant measurements have finite precision. If one could measure internal states arbitrary precisely, time dilation of their evolution could never be neglected. The regime of *approximate* validity of the non-relativistic mechanics is thus operationally defined in the light of the available measurement precision—in this context *slow* internal dynamics means: slow enough that (over the considered, finite, time scales) the presence of the couplings that give rise to time dilation, leads to non-resolvable difference in the evolution of the internal states, which can thus be neglected.

²Of course the constant term mc^2 can be omitted as it has no physical meaning for the dynamics of the particle, neither in classical nor in the quantum theory. Such a constant energy term only acquires physical meaning when the gravitational potential produced by the system is considered.

Symmetries of the framework The symmetry group of a massive elementary relativistic particle is the Poincaré group and the mass parameter is just a property of the system. Configuration space of a point-particle whose internal coordinates are denoted q_k , $k = 1, \dots, N$ and the centre of mass coordinate is x will be denoted $(\{q_k\}_{k=1}^N; x^\mu)$. Transformations of x are generated by the Poincaré group, and they leave the dynamics invariant. In the framework of point particles the translations of the internal coordinates are generated by the internal energy operator (and are the only internal transformations considered here). Thus, by construction, the symmetry group of the framework of relativistic point particles with internal dynamics is a central extension of the Poincaré group: mass is generalised from a parameter to a generator, H_{rest}/c^2 , which commutes with all other group generators—it lies in the centre of the new group. The algebra of the Poincaré group is otherwise unchanged—this central extension is thus called trivial as it is a product of the Poincaré group and of the internal symmetry group (here only generated by the internal Hamiltonian). Analogously, in the non-relativistic limit, Eq. (2.21), the symmetry group of the framework is a product of the Galilei group and of the symmetry group of the internal dynamics (as well generated by internal Hamiltonian).

A non-trivial and physically relevant is the case of the low-energy regime, described by H_{le} , Eq. (2.20) or, equivalently, by the R_{le} , Eq. (2.19). This regime arises when the only observable relativistic effects are the time dilation effects on the internal evolution and the dynamics in such a regime is invariant under the corresponding limit of the relativistic transformations. In particular, the boost by w acts on the coordinates as $x'^i \approx x + wt$, $t' \approx (t + \frac{xw}{c^2})(1 - \frac{w^2}{c^2})^{-1}$ and leaves the dynamics invariant. This can be seen directly by applying the transformation above to the equation of motion for the internal coordinate, which in this limit reads $\dot{q}_k = \{q_k, H_{rest}\}(1 - \frac{v^2}{2c^2})$. Transformed to the “primed coordinates” defined above it reads $\frac{dq_k}{dt'} = \dot{q}_k \frac{dt}{dt'} \approx \{q_k, H_{rest}\}(1 - \frac{(v+w)^2}{2c^2})$ and finally note that, up to considered order, $H_{rest}(1 - \frac{(v+w)^2}{2c^2}) = R'_{le}$.

On the other hand H_{le} has the same form as the non-relativistic, Newtonian, Hamiltonian but with a dynamical mass, formally defined as $M := H_{rest}/c^2$ (compare the paragraph above) $H_{le} = Mc^2 + \frac{\vec{p}}{2M}$ (the gravitational interaction will be skipped in this section). Velocity of the internal coordinate under H_{le} reads

$$\dot{q}_k = v_0 c^2 (1 - \frac{\dot{\vec{x}}^2}{2c^2}), \quad (2.22)$$

where $\dot{\vec{x}}$ is canonically conjugate to \vec{p} , $v_0 := \{q_k, M\}$, and c^2 appears here merely for adjusting the units. Note, that Galilei group elements: translations and rotations of the external coordinate as well as translation of the time parameter leave the above invariant. Galilei boost by \vec{w} : $\vec{x}' = \vec{x} + \vec{w}t$ transforms Eq. (2.22) into

$$\dot{q}'_k = \dot{q}_k - v_0 \dot{\vec{x}} \vec{w} - v_0 \frac{1}{2} \vec{w}^2 \quad (2.23)$$

which gives [3]:

$$q'_k = q_k - v_0 \vec{w} \vec{x} - v_0 \frac{1}{2} \vec{w}^2 t + a_w \quad (2.24)$$

where a_w is a constant. The symmetry group $\tilde{\mathcal{G}}$ of the entire configuration space $(\{q_k\}, \vec{x}, t)$ thus comprises an element α of the internal symmetry group and an element g of the Galilei group \mathcal{G} . The latter comprises: spatial translations, parametrised by \vec{a} ; temporal translations b ; boosts \vec{w} ; and rotations R . An element $g \in \mathcal{G}$ will be denoted $g = (R, \vec{w}, \vec{a}, b)$. An element of the total symmetry group $\tilde{\mathcal{G}}$ is thus denoted by $\tilde{g} = (\alpha, g)$ and its action on of the configuration space of the system is

$$\tilde{g}(\{q_k\}, \vec{x}, t) = (\{q_k + \alpha - v_0 \vec{w} \vec{x} - v_0 \frac{1}{2} \vec{w}^2 t\}, R\vec{x} + \vec{w}t + \vec{a}, t + b). \quad (2.25)$$

The above general rule allows to consider the following combination of transformations from $\tilde{\mathcal{G}}$: a boost by \vec{w} then shift by \vec{a} , boost by $-\vec{w}$ and shift by $-\vec{a}$:

$$\begin{aligned} (\{q_k\}, \vec{x}, t) &\xrightarrow{\tilde{g}_{\vec{w}}} (\{q_k - v_0 \vec{w} \vec{x} - v_0 \frac{1}{2} \vec{w}^2 t\}, \vec{x} + \vec{w}t, t) \\ &\xrightarrow{\tilde{g}_{\vec{a}}} (\{q_k - v_0 \vec{w} \vec{x} - v_0 \frac{1}{2} \vec{w}^2 t\}, \vec{x} + \vec{w}t + \vec{a}, t) \\ &\xrightarrow{\tilde{g}_{-\vec{w}}} (\{q_k + v_0 \vec{w} \vec{a}\}, \vec{x} + \vec{a}, t) \\ &\xrightarrow{\tilde{g}_{-\vec{a}}} (\{q_k + v_0 \vec{w} \vec{a}\}, \vec{x}, t). \end{aligned} \quad (2.26)$$

The transformation $\tilde{g} = \tilde{g}_{-\vec{a}} \tilde{g}_{-\vec{w}} \tilde{g}_{\vec{a}} \tilde{g}_{\vec{w}} = (\vec{w} \vec{a}, g_{-\vec{a}} g_{-\vec{w}} g_{\vec{a}} g_{\vec{w}}) = (\vec{w} \vec{a}, id_{\mathcal{G}})$ is not identity in $\tilde{\mathcal{G}}$ although the Galilei group elements themselves add up to the identity of the Galilei group $id_{\mathcal{G}}$. This means that the group $\tilde{\mathcal{G}}$ does not factor into a product of the two groups, as it was in the non-relativistic limit. Furthermore, the above chain of transformations shows that in $\tilde{\mathcal{G}}$ the generator of spatial translations P and of the boosts K satisfy

$$PK - KP \propto M \quad (2.27)$$

(since M is the generator of internal shifts). In the Galilei group itself the right hand side of Eq. (2.27) vanishes. The remaining commutators of the algebra $\tilde{\mathcal{G}}$ are the same as those in \mathcal{G} and M commutes with other elements of $\tilde{\mathcal{G}}$, which immediately follows from the Eq. (2.25). Thus, $\tilde{\mathcal{G}}$ is a non-trivial central extension of the Galilei group. The above results agree with Ref. [3], which showed that assuming dynamical mass in Galilei invariant physics results in dynamics which is invariant under the central extension of the Galilei group. This is fully consistent with the fact that the limit of the Poincaré group (with mass as a parameter) is central extension of the Galilei group (with mass parameter on the right hand side of the Eq. (2.27)) and not the Galilei group itself [4, 5].

Note, that from the perspective of the group structure the operationally well defined non-relativistic limit corresponds to the system whose symmetry group is a product of the Galilei and the internal symmetry group. On the other hand, the discussion of the previous paragraph shows that the non-relativistic limit corresponds to the case when the internal energy (or the “dynamical mass”) is effectively static (in the kinetic and potential energy terms) and can be understood as a parameter. However, this still leaves the right hand side of Eq. (2.27) non-zero: $PK - KP \propto M \rightarrow \text{const.} \equiv m$, which formally is again a structure of a central extension of the Galilei group and not the Galilei group. This is only an apparent discrepancy: with $PK - KP \propto m$ the transformations of the external coordinate would not induce any non-trivial transformations on the internal coordinates—a constant generator m has vanishing Poisson brackets with any function.³ In other words, the limit $M \rightarrow m$ in the commutator above entails that the transformation law for internal coordinates, Eq. (2.24), reduces to $q'_k = q_k + \alpha$. The Hamiltonian leading to such a transformation law is $H_{rest} + \frac{\vec{p}^2}{2m}$ —i.e. the fully non-relativistic one. As long as the generator m is (approximately) a constant, transformations of the configuration space resulting from a central extension of the Galilei group are indistinguishable from those originating from the group with $PK - KP = 0$ i.e. from the Galilei group. Thus, also from the symmetry-group perspective a consistent non-relativistic limit for a theory of “Newtonian” particles with a “dynamical mass” is obtained when the dynamical contribution to the mass can be neglected (everywhere apart from the rest energy term).

The Hamiltonian H_{le} viewed as the low energy limit of a relativistic system with internal degrees of freedom is invariant under the Poincaré group (to lowest order) and viewed as the theory of “Newtonian” particles with “dynamical mass”—is invariant under a non-trivial central extension of the Galilei group.⁴ These two approaches are operationally undistinguishable. The framework of “Newtonian” particles with “dynamical mass” and its corresponding symmetry group—non-trivial central extensions of the Galilei group with central element M —thus have a natural physical interpretation, in terms of low-energy relativistic systems with internal degrees of freedom. In particular the “dynamical mass” M can be interpreted as the total internal mass-energy of the system, in appropriate units. Central extensions of the Galilei group and the corresponding models of “Newtonian” particles with “dynamical mass” were studied before in the literature—mostly from a formal perspective in the context of quantum mechanics [3, 6, 7], or in the context of discussing mass as independent degree of freedom [8–11].

From the operational point of view adopted in this thesis, central extensions of the Galilei group do not describe the non-relativistic physics. Recall, that the non-

³With the $PK - KP \propto \text{const.}$ the v_0 which appears in the “kinetic terms” of Eq. (2.25) satisfies $v_0 = \{q_k, \text{const.}\} \rightarrow 0$, whereas the v_0 in the rest energy term is not constrained by requirement imposed on the commutator.

⁴Note that the transformation law for internal coordinates induced by requiring Galilei invariance, Eq. (2.23), matches the low-velocity limit of the relativistic transformation, which reads $\dot{q}'_k = \dot{q}_k \frac{dt}{dt'} \approx \dot{q}_k - v_0 \dot{x} w - v_0 \frac{w^2}{2}$, where $\frac{dt}{dt'} \approx (1 - \frac{\dot{x}w}{c^2})(1 - \frac{w^2}{2c^2})$ for \dot{q}_k is given by Eq. (2.22).

relativistic limit is given by the condition that the mass effectively becomes static and can thus be understood as a parameter $m = E_{rest}/c^2$. From the perspective of the group structure, the non-relativistic limit is obtained when the central element M is approximately *constant*. This condition is valid not only in classical mechanics—the quantum case is directly analogous. This sheds a new light on the physical meaning of the superselection rule for the mass in the non-relativistic quantum mechanics [3, 6, 7] and can be seen as its classical counterpart. These topics will be discussed in some more detail in the next Chapter.

2.2 Derivation of the Point-Particle Framework

2.2.1 Effective Dynamics of Relativistic N -Particle Systems

Consider a system comprising N particles with masses m_n , $n = 1, \dots, N$, charges e_n and coordinates $x_n^\mu(s)$, parametrised by a common parameter s and interacting via a four-potential A_μ . Lagrangian of such a system reads, [1]:

$$L_N = \sum_n -m_n c^2 \frac{d\tau_n}{ds} + e_n A_\mu(x_n) \frac{dx_n^\mu(s)}{ds} \quad (2.28)$$

where $c \frac{d\tau_n}{ds} = \sqrt{-g_{\mu\nu}(x_n) \frac{dx_n^\mu}{ds} \frac{dx_n^\nu}{ds}}$ and x_n denotes a four-vector, $x_n \equiv x_n^\nu$. The components x_n^0 can be chosen to be the same for all the particles and given by the common parameter s , which can be chosen to be time t as measured by a clock stationary and in the origin of the reference frame with respect to which the coordinates are defined. For all n one can thus set $x_n^0 = s \equiv ct$.

Consider a world line $Q^\mu(t)$ and coordinates where $\dot{Q}^i = 0$ and where Q^0 is chosen to be the proper time along this world line, $c\dot{\tau} = \sqrt{-g_{\mu\nu}(Q) \dot{Q}^\mu \dot{Q}^\nu}$. Since the quantities defining the Lagrangian are coordinate invariants, (i.e. $g_{\mu\nu} \frac{dx_n^\mu}{dt} \frac{dx_n^\nu}{dt} = g'_{\mu\nu} \frac{dx_n'^\mu}{dt} \frac{dx_n'^\nu}{dt}$ and $A_\mu \frac{dx_n^\mu(t)}{dt} = A'_\mu \frac{dx_n'^\mu(t)}{dt}$) changing the parametrisation in Eq. (2.28) into τ one can equivalently write the Lagrangian L_N as

$$L_N = \sum_n \left(-m_n c \sqrt{-g'_{\mu\nu} \frac{dx_n'^\mu}{d\tau} \frac{dx_n'^\nu}{d\tau}} + e_n A'_\mu \frac{dx_n'^\mu}{d\tau} \right) \frac{1}{c} \sqrt{-g_{\mu\nu}(Q) \dot{Q}^\mu \dot{Q}^\nu}. \quad (2.29)$$

No approximations were introduced thus far and Eq. (2.29) is fully equivalent to Eq. (2.28). Equation (2.29) has a general structure $L_N = f(x_n'^\nu, dx_n'^\nu/d\tau) \dot{\tau}$, however, this alone does not imply that it can be considered to describe a composed particle whose internal dynamics is given by $f(x_n'^\nu, dx_n'^\nu/d\tau)$. For such an interpretation to be consistent Q^μ shall represent the world line of the particle, e.g. its centre of mass,

and the coordinates where $Q^i = 0$ shall correspond to the centre of momentum frame, where the total momentum of the system vanishes. The canonical momentum conjugate to x_n is defined as

$$p_{ni} := \frac{\partial L_N}{\partial \dot{x}_n^i} \quad (2.30)$$

and reads $p_{ni}(x_n) = \frac{m_n \dot{x}_{in}}{\tau_n} + e_n A_i(x_n)$. In general the vectors p_{in} belong to different tangent spaces and there is no unique way to sum them up and define the total linear momentum. However, such a definition is possible in case where the metric components are approximately constant in the region occupied by the particles:

$$\forall_{n,m} g_{\mu\nu}(x_n) \approx g_{\mu\nu}(x_m), \quad (2.31)$$

which means that the region is approximately flat. For well-behaved metrics, the condition in Eq. (2.31) is satisfied if the particles are following sufficiently close-by⁵ world lines

$$\forall_{n,m} x_n \approx x_m. \quad (2.32)$$

The linear momenta are given by $P_{ni}(x_n) := \sum_n (p_{ni}(x_n) - e_n A_i(x_n))$ and the total linear momentum under the approximation (2.31) can meaningfully be defined as a sum of the individual linear momenta $P_i = \sum_n P_{ni}(x_n)$. The centre of mass frame is defined by the condition $P'_i = \sum_n P'_{ni}(x_n) = 0$, where $P'_{ni} = \frac{\partial x^\mu}{\partial x'^i} P_{nv}$. Note, that the validity of the requirement in Eq. (2.31) also guarantees that the condition $P'_i = 0$ (and P_i itself) is generally covariant. Indeed, with $P^i = \sum_n g^{ij}(x_n) P_{nj}$ one finds

$$P'^i = \sum_n \frac{\partial x'^i}{\partial x^\mu} g^{\mu\nu}(x_n) P_{nv} = \sum_n \frac{\partial x'^i}{\partial x^\mu} g^{\mu\nu}(x_n) \frac{\partial x'^\alpha}{\partial x^\nu} P_{n\alpha} = \sum_n g'^{ij}(x_n) P'_{nj}, \quad (2.33)$$

and if Eq. (2.31) holds:

$$P'^i \approx g'^{ij}(x_N) \sum_n P'_{nj} = 0. \quad (2.34)$$

More generally, the condition in Eq. (2.31) guarantees that a single coordinate chart can be used to cover all the region occupied by the particles, and in which the metric takes the Minkowski form. This allows defining trajectories on the space-time manifold for the parallel transport of the tangent vectors to some fixed point and or defining such quantities like the total momentum (without assuming Eq. (2.32)). Such a construction of the centroid for an N-particle system has been first given by Dixon [12] and leads to a generally covariant (and independent of the choice of the fixed point) notion of the centre of mass.

If the approximation in Eq. (2.32) holds, one can identify the world line $Q^\mu(t)$ in Eq. (2.29) with the world line of one of the constituent particles, say x_N , which

⁵Quantitative estimations will be discussed in more detail further in this section.

is done hereafter. $Q^\mu(t) \approx x_N$ thus represents the position of the composite system and the “primed” coordinates, defined by the condition $Q^i = 0$, can be identified with the centre of momentum frame. Condition in Eq. (2.32) also guarantees that the resulting description of the system is independent of which of the N world lines one choses to represent the system. Note, that this condition does not require that the particles follow exactly the same world lines and have exactly the same velocities—it is required to hold only to the extent that there is no considerable time-dilation between the different world lines. In such a case the quantity

$$L_{rest} = \sum_n \left(-m_n c \sqrt{-g'_{\mu\nu} \frac{dx_n'^{\mu}}{d\tau} \frac{dx_n'^{\nu}}{d\tau}} + e_n A'_\mu \frac{dx_n'^{\mu}}{d\tau} \right) \quad (2.35)$$

can consistently be used to represents internal Lagrangian of a composite system following the world line $Q^\mu(t)$. The total Lagrangian takes the form

$$L_N \approx L_{rest} \dot{\tau} =: L_{tot}, \quad (2.36)$$

with L_{rest} given by Eq. (2.35). Thus, a system comprising N relativistic particles moving along a narrow “world tube” approximates that of a composite point particle, discussed in the previous sections.

For completeness, derivation of the Hamiltonian corresponding to the Lagrangian L_{tot} , Eq. (2.36), is given below. The total Hamiltonian H_{tot} is obtained from the Legendre transform of L_{tot} and is a function of the momentum P —canonically conjugate to the external degree of freedom Q —and of the momenta w_n —conjugate to the internal degrees of freedom x_n' :

$$H_{tot}(Q, P; w_1, \dots, w_n) = P_i \dot{Q}^i + \sum_n w_{in} \dot{x}_n'^i - L_{tot}; \quad (2.37)$$

the canonical momentum of the external degree of freedom is defined as

$$P_i = \frac{\partial L_{tot}}{\partial \dot{Q}^i} = \frac{\partial L_{rest}}{\partial \dot{Q}^i} \dot{\tau} + L_{rest} \frac{d\dot{\tau}}{d\dot{Q}^i}$$

and the internal momenta:

$$w_{in} = \frac{\partial L_{tot}}{\partial \dot{x}_k'^i} = \frac{\partial L_{rest}}{\partial \frac{dx_k'^i}{d\tau}},$$

see also Sect. 2.1.4.

In order to compute $\frac{\partial L_{rest}}{\partial \dot{Q}^i}$ recall that quantities such as $\frac{dx^i}{d\tau}$ can equivalently be written as $\frac{\dot{x}^i}{\dot{\tau}}$ and thus $\frac{L_{rest}}{d\dot{Q}^i} = \sum_n \frac{\partial L_{rest}}{\partial \frac{dx_n'^i}{d\tau}} \dot{x}_n'^i \frac{-1}{\dot{\tau}^2} \frac{d\dot{\tau}}{d\dot{Q}^i}$, see also Sect. 2.1.3. The canonical momentum P_i of the composed particle thus reads

$$P_i = \left(\sum_n -\frac{\partial L_{rest}}{\partial \frac{x'_n}{d\tau}} \frac{dx'_n}{d\tau} + L_{rest} \right) \frac{d\dot{\tau}}{d\dot{Q}^i} = H_{rest} \frac{\dot{Q}_i}{c^2 \dot{\tau}}, \quad (2.38)$$

where the definition of the internal Hamiltonian given in Eq. (2.12) has been used.

First, the general structure of H_{tot} will be obtained. Substituting into Eq. (2.37) the expression for P_i from Eq. (2.38) and the definition of w_n above one finds

$$H_{tot} = H_{rest} \frac{\dot{Q}^i \dot{Q}_i}{c^2 \dot{\tau}} + H_{rest} \dot{\tau} = -H_{rest} \frac{g_{00} \dot{Q}^0 \dot{Q}^0}{c^2 \dot{\tau}} = -H_{rest} \frac{g_{00}}{\dot{\tau}}, \quad (2.39)$$

where the definition of H_{rest} as Legendre transform of L_{rest} has been used, as well as $c\dot{\tau} = \sqrt{-\dot{Q}^\mu \dot{Q}_\mu}$ and $Q^0 = ct$. Using again Eq. (2.38) one finds

$$c^2 P_i P^i = H_{rest}^2 \frac{\dot{Q}^i \dot{Q}_i}{c^2 \dot{\tau}^2} = H_{rest}^2 \left(-1 + \frac{-g_{00}}{\dot{\tau}^2} \right)$$

and after substitution into the Eq. (2.39) a final form of H_{tot} is found:

$$H_{tot} = \sqrt{-g_{00}(c^2 P_i P^i + H_{rest}^2)}, \quad (2.40)$$

and as expected the structure of H_{tot} above is that of the Hamiltonian in Eq. (2.2), describing an idealised point-like particle with internal degrees of freedom.

For the particular system defined by the Lagrangian L_{tot} in Eq. (2.36) with L_{rest} given by Eq. (2.35) the internal momenta explicitly read $w_n^i = m_n \frac{\dot{x}_{ni}}{\dot{\tau}_n} + e_n A'_i$. Analogous calculation to the one which led to the total Hamiltonian results in

$$H_{rest} = \sum_n \sqrt{-g'_{00}[(w_{ni} - e_n A'_i)(w_n^i - e_n A'^i) + m_n^2]} - e_n A'_0. \quad (2.41)$$

2.2.2 Quantitative Discussion of the Approximations

A relativistic N-particle system in the regime where Eq. (2.31) holds can be described as an effectively point-like, composed particle with a generally covariant external four-momentum vector P_i and with the internal energy H_{rest} . The latter is defined as the total energy in the zero-momentum frame, i.e. where $P'_i = 0$. The error made in describing an extended many particle system as a point-like “composed” particle on a world line $x^\mu(t)$ can be quantified e.g. by the difference between $P^\mu = \sum_n g^{\mu\nu}(x_n) P_{nv}(x_n)$ and $g^{\mu\nu}(x) P_v \equiv g^{\mu\nu}(x) \sum_n P_{nv}(x_n)$:

$$P^\mu - g^{\mu\nu}(x) P_v = \sum_n (g^{\mu\nu}(x_n) - g^{\mu\nu}(x)) P_{nv}. \quad (2.42)$$

Thus, the scale for the approximations is set by the variation of the metric across the distances between the constituent particles and by the total energy-momentum. Consider a region $\mathcal{U} := \bigcup_t \mathcal{U}_t$, with \mathcal{U}_t such that $\forall_n x_n(t) \in \mathcal{U}_t$. Assumption that the variation of the metric in \mathcal{U} is bounded can be expressed as

$$\exists_K \forall_{\mu\nu,n,m} |g^{\mu\nu}(x_n) - g^{\mu\nu}(x_m)| < K/(4N) \quad (2.43)$$

where $K > 0$ is a constant. Furthermore, if the energy scale of the particles in the region is bounded by some \tilde{P} , defined as

$$\tilde{P} := \max\{|P_{n\mu}(x_n)| : n \in \{1, \dots, N\}, x_n \in \mathcal{U}, \mu = 0, \dots, 3\}, \quad (2.44)$$

then, using Eqs. (2.43) and (2.44), the absolute value of the error, Eq. (2.42), satisfies

$$|P^\mu - g^{\mu\nu} P_\nu| = \left| \sum_{n,v} (g^{\mu\nu}(x_n) - g^{\mu\nu}(x)) P_{nv} \right| < K \tilde{P} \quad (2.45)$$

for any μ . An example of a metric with the required property is the Schwarzschild metric in isotropic coordinates: Its components restricted to any compact region of space-time with no singularity are Lipschitz functions.

On the other hand, Eq. (2.45) implies that given an energy bound and a finite measurement precision for any relativistic composite system on a well-behaved metric there exist a bound on the system's size, such that if the system is smaller than this bound, the error made by using the approximation (2.31) is below the resolution. The system can then be consistently treated as point-like particle with internal dynamical degrees of freedom, and is described by a Hamiltonian of a form $H = \sqrt{-g_{00}(c^2 p_j p^j + H_{rest}^2)}$, introduced in Sect. 2.1.1 or, equivalently, by a corresponding Lagrangian $L = L_{rest} \dot{\tau}$, Sect. 2.1.2, or a Routhian, $R = H_{rest} \dot{\tau}$, Sect. 2.1.4.

2.3 Relevance of the Framework for Experiments

The framework of point-like particles with internal dynamics naturally arises as a description of sufficiently well-localised (see Sect. 2.2.2) many-particle systems. This conclusion is important because the formalism can be interpreted as a theory of ideal clocks in relativity, see Sect. 2.1.4.

First, note that validity of such an effective description of composed systems underlies many experimental tests of special or general relativistic time-dilation. Such experiments are performed with various physical systems that are used to measure the elapsed time, such as Caesium atoms in the experiment of Hafele and Keating [13]. In this experiment one atomic clock was stationary on Earth and other were flown on board of a plane, east and westwards around the Earth. The experiment

was consistent with a prediction that clocks will show the proper time along their world line, and that these proper times will differ for the different trajectories—due to special relativistic and gravitational time dilation. Results of this and similar experiments are conveniently described as if the passage of time was directly compared between the different world lines—one speaks about the elapsed proper time along some path. Such an account of the time dilation experiments is only possible because the dynamics of physical systems used as clocks effectively takes the form $H_{rest} \int_{\gamma} d\tau$, where γ can be treated as the system’s world line. It is this universality of general relativistic description of composed systems, which allows us to abstract from the details of the systems’ dynamics and makes it meaningful to speak about the elapsed proper time $\tau_{\gamma} = \int_{\gamma} d\tau$ itself.

Another important feature of the regime of composite particles is that it shows how relativistic effects can be probed without the need for high centre of mass velocities. The systems can be slow or even stationary in the laboratory reference frame and are effectively described by the Eq. (2.19). The rest frame rate of their internal evolution v_{rest} according to Eq. (2.19) is time dilated by a factor $(1 - \frac{\vec{v}^2}{2c^2})$ if the system is moving with the centre of mass velocity \vec{v} (see also Sect. 2.1.4) with respect to the laboratory frame. In a recent experiment realised in the group of David Wineland [14] such an effect stemming from velocities as slow as few meters per second has been measured. This has been possible due to fast (of order 10^{15} Hz) and stable (up to 10^{-17}) internal dynamics of the utilised system—an Aluminium ion, and due to high precision of the measurement. Note, that the above effect is the regime described by H_{le} , formally equivalent to the framework of “Newtonian” particles with “dynamical mass”, which supports relativistic interpretation of that framework. In the experiment [14] also gravitational time dilation between two ion clocks was measured, with the clocks separated by ≈ 30 cm. Rate of internal dynamics of two identical systems stationary in a laboratory reference frame and located at different heights x_1 and $x_2 = x_1 + h$ reads: $v_{int} \left(1 + \frac{\Phi(x_1)}{c^2}\right)$ and $v_{int} \left(1 + \frac{\Phi(x_2)}{c^2}\right)$, respectively, see Eq. (2.19). Up to the linear terms in h the difference between these two rates is $v_{rest} \frac{gh}{c^2}$ with $g = GM/x_1^2$ denoting the gravitational acceleration on the surface of the earth, approximately 10 m/s^2 . For $h \approx 30 \text{ cm}$ the so-called redshift factor $\frac{gh}{c^2} \approx 10^{-17}$. Such a minute effect could be resolved on short time scales due to high rate and stability of internal dynamics. (For a single data point only about 2 hours of clocks comparison were sufficient, during which the clocks accrued about 10^{-14} s of a difference.) Similarly, redshift experiments—tests verifying the shift in internal energies due to the relativistic factors explained above—operate in a regime where centre of mass itself would not require relativistic description. For example, if the system’s internal Hamiltonian has some spectral line E_0 as measured in its rest frame, it will be measured to be $E = E_0(1 + \frac{\Phi(x_2)}{c^2})$, if the system is placed in a gravitational potential $\Phi(x)$. This effect has been probed by Pound and Rebka [15] in an experiment where the very narrow Mössbauer transition in iron was compared between an iron foil placed at the bottom and at the top of a 22.5 m high tower at Harvard University’s Jefferson laboratory. The experiment was consistent with the prediction that the Mössbauer transitions in identical iron foils placed at different

heights in the gravitational potential will differ by the gravitational redshift factor $\frac{gH}{c^2} \approx 10^{-15}$, for $H = 22.5$ m.

The above discussed features of the regime where composed relativistic systems can be described as point particles with internal structure are crucial for the design and analysis of time dilation experiments. Interestingly, the perspective taken here—that relativistic effects concerning properties of time and space stem from the specific form of interactions present in the relativistic dynamics of systems used as rods and clocks—has been mostly discussed in philosophy of physics, in the context of the “clock hypothesis” (which is the statement that clocks measure proper time along their world lines) see e.g. Ref. [16] for an interesting discussion. Considering explicitly this dynamical underpinning of time dilation will turn out to be particularly beneficial for studying time dilation effects in quantum theory, which is the main scope of this work.

References

1. S. Weinberg, *Gravitation and Cosmology: principle and Applications of General Theory of Relativity* (Wiley, New York, 1972)
2. M. Blau, *Lecture notes on General Relativity*. Albert Einstein Center for Fundamental Physics (2014)
3. D. Giulini, On galilei invariance in quantum mechanics and the bargmann superselection rule. *Ann. Phys.* **249**, 222–235 (1996)
4. E. Inönü, E. Wigner, Representations of the Galilei group. *Il Nuovo Cimento* **9**, 705–718 (1952)
5. S. Weinberg, *The quantum theory of fields*, vol. 2 (Cambridge University Press, 1996)
6. V. Bargmann, On unitary ray representations of continuous groups. *Ann. Math.* **59**, 1–46 (1954)
7. J.-M. Levy-Leblond, Galilei group and nonrelativistic quantum mechanics. *J. Math. Phys.* **4**, 776–788 (1963)
8. D.M. Greenberger, Inadequacy of the usual Galilean transformation in quantum mechanics. *Phys. Rev. Lett.* **87**, 100405 (2001)
9. D.M. Greenberger, Theory of particles with variable mass. I. Formalism. *J. Math. Phys.* **11**, 2329–2340 (1970)
10. D.M. Greenberger, Theory of particles with variable mass. II. Some physical consequences. *J. Math. Phys.* **11**, 2341–2347 (1970)
11. D.M. Greenberger, Some useful properties of a theory of variable mass particles. *J. Math. Phys.* **15**, 395–405 (1974)
12. W. Dixon, A covariant multipole formalism for extended test bodies in general relativity. *Il Nuovo Cimento* **34**, 317–339 (1964)
13. J.C. Hafele, R.E. Keating, Around-the-World Atomic Clocks: Observed Relativistic Time Gains. *Science* **177**, 168–170 (1972)
14. C.-W. Chou, D. Hume, T. Rosenband, D. Wineland, Optical clocks and relativity. *Science* **329**, 1630–1633 (2010)
15. R. Pound, G. Rebka, Apparent Weight of Photons. *Phys. Rev. Lett.* **4**, 337–341 (1960)
16. H.R. Brown, The behaviour of rods and clocks in general relativity, and the meaning of the metric field, in *Beyond Einstein: Essays on Geometry, Gravitation, and Cosmology*, D.E. Rowe, ed. Birkhäuser (Boston, 2009), [arXiv:0911.4440](https://arxiv.org/abs/0911.4440) [gr-qc]

Chapter 3

Quantum Clocks in General Relativity

This chapter derives and discusses quantisation of the relativistic “clock” Hamiltonian, providing dynamics of low energy quantum systems with internal degrees of freedom in a fixed background. The formalism applies in the limit of small systems under weak gravitational fields or accelerations, as discussed Sect. 2.2.1, where the systems can be approximated as point-like particles with internal dynamics. Interestingly, the present approach allows a novel perspective on the Bargmann’s mass-superselection rule—see Sect. 3.3.

3.1 Quantisation of the Composite Point-Particle Framework

For a derivation of a quantum “clock” Hamiltonian from quantum field theory in curved space-time, the reader is referred to Appendix A.1. Below some arguments supporting the resulting dynamics are given, based on established Hamiltonian approaches used in relativistic quantum mechanics.

Consider the Hamiltonian in Eq. (2.2), describing a point-like particle with internal energy H_{rest} : $H = \sqrt{-g_{00}(c^2 p_j p^j + H_{rest}^2)}$. This dispersion relation corresponds to the Klein-Gordon equation [1, 2]. For energies small compared to H_{rest} , such that the particle creation and other quantum-field effects are negligible, the Klein-Gordon field can be treated as a particle in first quantisation. The corresponding low-energy expansion of the Hamiltonian yields a Schrödinger equation with relativistic corrections. In particular for a point particle on a post-Newtonian background $g_{00} = -(1 + 2\Phi(x)/c^2 + 2\Phi^2(x)/c^4)$ and $g_{ij} = \delta_{ij}(1 - 2\Phi(x)/c^2)$, (with

Section 3.2 contains material from *Quantum formulation of the Einstein Equivalence Principle*, M. Zych and Č. Brukner, [arXiv:1502.00971](https://arxiv.org/abs/1502.00971) (2015).

$\Phi(x) = -Gm_e/x$ denoting the gravitational potential) the second-order expansion is given by the Hamiltonian operator [3]

$$H = Mc^2 + \frac{p^2}{2M} + M\Phi(x) - \frac{p^4}{8M^3c^2} + \frac{M\Phi^2(x)}{2c^2} + \frac{3}{2Mc^2} \left(\Phi(x)p^2 + [p\Phi(x)]p + \frac{1}{2}[p^2\Phi(x)] \right), \quad (3.1)$$

where $[p\Phi]$ acts only on the potential and where $M = H_{rest}/c^2$ is the total mass-energy of the particle. Equation (3.1) is applicable to systems like atoms whose total mass M is mostly given by the internal/binding energy of their constituents.¹

For an internal energy eigenstate with the energy eigenvalue E_j and thus $M_j = E_j/c^2$, Eq. (3.1) holds with $M \rightarrow M_j$. The linearity of quantum mechanics requires this to hold also for an arbitrary superposition of internal states: In quantum theory states are described by vectors $|E_j\rangle$ in a separable Hilbert space \mathcal{H}_{int} and the internal energy is described by a linear operator \hat{H}_{rest} on \mathcal{H}_{int} , such that $\hat{H}_{rest}|E_j\rangle = E_j|E_j\rangle$. This internal energy operator can be written in the form $\hat{H}_{rest} = mc^2\hat{I}_{int} + \hat{H}_{int}$, where the dynamical part for the internal energy is described by \hat{H}_{int} —quantised Hamiltonian describing internal dynamics—and \hat{I}_{int} is the identity operator on \mathcal{H}_{int} . The rest mass mc^2 can be seen as the energy of the ground state of \hat{H}_{rest} (in which case the lowest eigenvalue of \hat{H}_{int} is zero). This is in a full analogy to the classical case where the mass can be seen as the static part of the internal Hamiltonian. The Hamiltonian (3.1) thus describes the full quantum dynamics of the system, including internal and external degrees of freedom. The Hilbert space of the system is $\mathcal{H} = \mathcal{H}_{int} \otimes \mathcal{H}_{ext}$, where \mathcal{H}_{ext} is the state space of the external (centre of mass) degrees of freedom. To the first order in H_{int}/mc^2 (and skipping the “hats”, since all the operators are quantised and no confusion can arise) the Hamiltonian (3.1) reads

$$H = H_{cm} + H_{int} \left(1 + \frac{\Phi(x)}{c^2} - \frac{p^2}{2m^2c^2} \right), \quad (3.2)$$

where

$$H_{cm} = mc^2 + \frac{p^2}{2m} + m\Phi(x) - \frac{p^4}{8m^3c^2} + \frac{m\Phi^2(x)}{2c^2} + \frac{3}{2mc^2} \left(\Phi(x)p^2 + [p\Phi(x)]p + \frac{1}{2}[p^2\Phi(x)] \right) \quad (3.3)$$

acts on the centre of mass degrees of freedom. The following notation is used: $H_{cm} \equiv I_{int} \otimes H_{cm}$ and $H_{int}(1 + \dots) \equiv H_{int} \otimes (I_{ext} + \dots)$, where I_{ext} is the identity operator on \mathcal{H}_{ext} . In general, H_{cm} includes all terms acting on the centre of mass to

¹The mass energy equivalence—the change of the mass of the particle by $\delta E/c^2$ when its internal energy changes by δE —is currently verified up the precision of 10^{-7} [4].

this order of approximation and can thus have additional interactions, as in Sect. 2.2.1. The interaction terms between H_{int} and centre of mass operators are of the same form as in the fully classical case—and also describe time dilation and redshift effects. These interactions are entirely independent of the nature of the binding/internal energies which leads to the universality of the resulting time dilation (and redshift): they affect all systems (“clocks”) in the same way, irrespective of the latter specific composition.

The above dynamics is fully compatible with the understanding of the Hamiltonian as a generator of time translations and with general relativistic understanding of time. H_{rest} is a generator of time translations with respect to the proper time τ and describes the dynamics of internal states in the rest frame. This leads to the rest frame Schrödinger-like equation: $i\hbar \frac{\partial}{\partial \tau} = H_{rest}$. Changing coordinates to the laboratory frame, the evolution is given by $i\hbar \frac{\partial}{\partial t} = H_{rest} \dot{\tau}$, where $\dot{\tau} = \frac{d\tau}{dt}$ describes how fast the proper time flows with respect to the coordinate time. This form of dynamics is fully equivalent to a Schrödinger-like equation obtained with the full Hamiltonian and with the Hamiltonian in Eq. (3.2), in the low energy limit. To see this, note, that the above argument leads to dynamics expressed in terms of a Routhian (compare Eq. (2.15))—since $\dot{\tau}$ is given in terms of configuration space variables—which is fully equivalent to the Hamiltonian formulation, and the latter is obtained by expressing $\dot{\tau}$ in terms of phase space variables (see Eq. (2.8)).

3.2 Low-Energy and Non-relativistic Limits, and Symmetries of the Framework

All the crucial results concerning the non-relativistic limit and symmetry of the models are exactly the same as in the classical case, discussed in Sect. 2.1.5. In particular, also the quantised framework of point-particles with internal degrees of freedom admits as a symmetry a trivial central extension of the Poincaré group, with the internal mass-energy $M = H_{rest}/c^2$ as the center. Below only a brief commentary is presented with the main focus on the low energy limit, which is further relevant for Chap. 7.

In a full analogy to the classical case the non-relativistic limit of the system is given by

$$H_{nr} = mc^2 + H_{int} + \frac{p^2}{2m} + m\Phi(x). \quad (3.4)$$

It describes a system with internal Hamiltonian H_{int} and a mass parameter m . For example, for a spin \vec{S} in a magnetic field \vec{B} one finds $H_{int} \propto \vec{S}\vec{B}$. The symmetry group of this limit is a product of an internal symmetry group and the Galilei group. Representation of the Galilei group on the space of solutions of the Schrödinger equation (3.4) is shortly discussed below, see Refs. [5–8] for in-depth discussions of the various aspects of this subject. Generator of the Galilei boost in the representation of the Galilei group on the state-space of a non-relativistic particle with mass

parameter m is given by $\hat{K} = i\hbar t \frac{\partial}{\partial x} + mx$. Generator of spatial translations is the momentum operator \hat{P} and thus in quantum theory the two generators do not commute, $[\hat{K}, \hat{P}] = i\hbar m \hat{I}$. Consider again the sequence of the translations and boosts, Eq. (2.26). Recall, that in \mathcal{G} this sequence yields the identity $id_{\mathcal{G}}$

$$g_{-\vec{a}}g_{-\vec{w}}g_{\vec{a}}g_{\vec{w}} = id_{\mathcal{G}}. \quad (3.5)$$

However, the unitary representation² of the above transformations on the Hilbert space of the particle reads

$$U(g_{-\vec{a}})U(g_{-\vec{w}})U(g_{\vec{a}})U(g_{\vec{w}}) = e^{-im\vec{a}\vec{w}}I_{int}. \quad (3.6)$$

There is an additional, global, phase factor in the composition law for the representation of the Galilei group on the Hilbert space, not present in the group itself, Eq. (3.5)—such representations are called projective. Thus, the Galilei group admits a projective unitary representation on the state space of a massive particle (space of solutions to the Schrödinger equation (3.4)). Note, that this fact can be traced back to the canonical commutation relations for the position and momentum operators.

Recall, that in the algebra of *central extension of the Galilei group*, with central element given by the mass parameter m , the generators of spatial translations and boosts satisfy the same commutation relation (Eq. (2.27)) as the corresponding generators of the *representation of the Galilei group in Hilbert space*. Equation (2.26) entails that generators of the central extension of the Galilei group satisfy

$$\tilde{g}_{-\vec{a}}\tilde{g}_{-\vec{w}}\tilde{g}_{\vec{a}}\tilde{g}_{\vec{w}} = \tilde{g}_{\alpha=\vec{a}\vec{w}}, \quad (3.7)$$

where $\tilde{g}_{\alpha=\vec{a}\vec{w}}$ generates translation of the internal coordinate by $\alpha = \vec{a}\vec{w}$. Unitary representation of this group on the Hilbert space satisfies Eq. (3.6) with \tilde{g} instead of g . Thus, the Schrödinger equation describing a particle with a mass parameter m admits a faithful (non-projective) unitary representation of the central extension of the Galilei group. Therefore, also in quantum mechanics the dynamics of a particle with a mass parameter m can be described as invariant under a central extension of the Galilei group (with mass parameter as the centre) or—equivalently—as invariant under the Galilei group. Although the former has a faithful representation on the Hilbert space of the particle, whereas the latter has a projective representation, these two are physically equivalent—the mass-parameter as a generator only yields an unobservable, global, phase.³

²Recall that unitary representation of $g_{\alpha} \in \mathcal{G}$ (a transformation parametrised by α) generated by an operator G reads $U = e^{-i\alpha G/\hbar}$.

³Equivalence of the two pictures in classical physics was rooted in the fact that a constant generator does not induce any transformation. This is in full agreement with the quantum case, since the diagonal elements of a density operator of a quantum system can be seen as classical states.

From the Eq. (3.2), the low-energy limit reads

$$H_{le} = mc^2 + H_{int} + \frac{p^2}{2m} + m\Phi(x) + H_{int} \left(1 + \frac{\Phi(x)}{c^2} - \frac{p^2}{2m^2c^2} \right),$$

where the second order terms in the momenta and potential have been neglected as they are considered of lower order compared to $H_{int} \frac{\Phi(x)}{c^2}$ and $H_{int} \frac{p^2}{2m^2c^2}$. As in the classical case the above Hamiltonian is formally equivalent to a Hamiltonian of a particle with a “dynamical mass” $M = H_{rest}/c^2 = m I_{int} + H_{int}/c^2$:

$$H_{le} = M + \frac{p^2}{2M} + M\Phi(x) \quad (3.8)$$

The symmetry of the Hamiltonian in Eq. (3.8) is thus central extension of the Galilei group, with the central element given by the operator M or, equivalently, H_{rest} . Note, that a superposition of eigenstates of H_{int} with different eigenvalues corresponds also to different eigenvalues of M , which is just the total mass-energy. Such states are time-evolving⁴ and will exhibit time dilation effects due to the coupling to the kinetic and potential terms, in a full analogy to the classical case—see Sect. 2.1.5, e.g. Eq. (2.20). The internal energy eigenstates, on the other hand, are stationary and will not exhibit any time dilation effects. Thus not only in classical theory, but also in quantum mechanics central extensions of the Galilei group with a “dynamical mass” do not describe an operationally well-defined non-relativistic limit. For a consistent non-relativistic limit internal evolution needs to be slow (see Sect. 2.1.5) such that the effects of time dilation are effectively non-observable. In quantum physics this means that the maximal energy gap between internal energy eigenstates must be small compared to the centre of mass energies. Separating internal energy operator into a static part, proportional to the identity, and the remaining dynamical part, i.e. $H_{rest} = E_{stat}I_{int} + H_{dyn}$, the non-relativistic limit arises when the coupling terms between H_{dyn} and the potential and kinetic energies can be neglected (effects induced by these couplings are beyond resolution of any available measurement). The non-relativistic regime can thus be defined as the regime where effectively only the static part of the internal energy couples to the external degrees of freedom. Trivially, all internal states are eigenstates of $E_{stat}I_{int}$ with the same eigenvalue—these coupling terms do not induce any time dilation (nor red-shift) effects. The static part of the internal energy effectively becomes a parameter—as it is common to all physical states of the system. Thus, also in quantum theory such an operational understanding of the non-relativistic limit allows *defining* the mass parameter of a composite quantum system as a static part of its internal energy, $m \equiv E_{stat}/c^2$. Note, that the above does not preclude preparation of states with different internal energy H_{int} or their superpositions, but it guarantees that the dynamical H_{int} effectively only

⁴For example, an equal superposition of eigenstates with different energies, with an energy gap ΔE , evolves between mutually orthogonal states at a rate proportional to $\hbar/\Delta E$, [9–13], see also Chap. 4.

contributes to the rest energy term—and gives rise to an absolute time of Euclidean space-time, as required for a consistent non-relativistic theory. (The quantum case is fully analogous to the classical one and thus the reader is further referred to Sect. 2.1.5).

3.3 Mass Superselection Rule in the Context of Composite Particles

The observations in the section above are relevant for the discussion over the physical content of Bargmann’s superselection rule for the mass [5]. The original argument in Ref. [5] bases on the fact that the representation of the Galilei group is projective: applying combination of boosts and translations in Eq. (3.6) to a superposition state with masses m and m' would result in a relative phase $e^{i\vec{w}\vec{a}(m-m')}$ between the states, and therefore would yield a *different physical state*, unless $m = m'$. However, this operation shall represent identity transformation of the Galilei group, Eq. (3.5) and thus *cannot alter physical states*. Hence, it was concluded that the superposition of states with different masses cannot be a physical state in a theory with Galilei invariance—this is the Bargmann superselection rule. Such a derivation of the superselection rule has been later criticised as inconsistent [7]: in a theory with m being a parameter—with no corresponding degrees of freedom—there are simply no states of the system that could have different masses. For this reason theories of Newtonian particles with “dynamical mass” have been studied (see e.g. Ref. [7] for a thorough discussion). These theories, formally exactly equivalent to Eq. (3.8), admit as a symmetry the central extension of the Galilei group with the “dynamical mass” as the centre. Since the unitary representation of this group is faithful, no need for the superselection rule arises—this fact is still discussed in the literature on the topic and triggers questions [7]: what are the new degrees of freedom that correspond to this “dynamical mass” and if states with different masses indeed cannot be prepared, what is the origin of this impossibility? From the perspective introduced here the “dynamical mass” has a physical interpretation of the total internal energy of a composite system and the “new degrees of freedom” on which it acts are the internal states of the system. This interpretation provides also the dynamical origin, or rather context, of the “impossibility” of observing states with different masses in the non-relativistic physics. The discussion in the paragraph above shows that operationally well-defined non-relativistic physics arises in a regime where only the constant part of the “dynamical mass” is effectively observable (in the kinetic and potential terms of the Hamiltonian) and thus no states of the system are excluded—but the dynamics in an operationally defined non-relativistic regime is such, that all states have effectively the same eigenvalue of the “dynamical mass”.

There is no mathematical inconsistency in the framework of Newtonian particles with “dynamical mass”—no superselection rule is necessary in this sense. The tension arises only if one demands that this formalism describes non-relativistic physics,

in particular if one requires that internal evolution arising from such a theory is consistent with Euclidean space-time. Such a formalism, however, has a natural physical interpretation as a low-energy regime of composite systems whose internal evolution is affected by time dilation.

References

1. S. Weinberg, *The Quantum Theory of Fields*, vol. 2. (Cambridge University Press, 1996)
2. N.D. Birrell, P.C.W. Davies, *Quantum Fields in Curved Space*. No. 7. (Cambridge university press, 1984)
3. C. Laemmerzahl, A Hamilton operator for quantum optics in gravitational fields. *Phys. Lett. A* **203**, 12–17 (1995)
4. S. Rainville, J.K. Thompson, E.G. Myers, J.M. Brown, M.S. Dewey, E.G. Kessler, R.D. Deslattes, H.G. Borner, M. Jentschel, P. Mutti, D.E. Pritchard, World year of physics: a direct test of $E = mc^2$. *Nature* **438**, 1096–1097 (2005)
5. V. Bargmann, On unitary ray representations of continuous groups. *Ann. Math.* **59**, 1–46 (1954)
6. J.-M. Levy-Leblond, Galilei group and nonrelativistic quantum mechanics. *J. Math. Phys.* **4**, 776–788 (1963)
7. D. Giulini, On Galilei invariance in quantum mechanics and the Bargmann superselection rule. *Ann. Phys.* **249**, 222–235 (1996)
8. D.M. Greenberger, Inadequacy of the usual Galilean transformation in quantum mechanics. *Phys. Rev. Lett.* **87**, 100405 (2001)
9. L. Mandelstam, I. Tamm, The uncertainty relation between energy and time in non-relativistic quantum mechanics, in *Selected Papers* (Springer Berlin Heidelberg, 1991), pp. 115–123
10. G. Fleming, A unitarity bound on the evolution of nonstationary states. *Il Nuovo Cimento A* **16**, 232–240 (1973)
11. N. Margolus, L.B. Levitin, The maximum speed of dynamical evolution. *Phys. D: Nonlinear Phenom.* **120**, 188–195 (1998). Proceedings of the Fourth Workshop on Physics and Consumption
12. B. Zieliński, M. Zych, Generalization of the Margolus-Levitin bound. *Phys. Rev. A* **74**, 034301 (2006)
13. B.-G. Englert, Fringe visibility and which-way information: an inequality. *Phys. Rev. Lett.* **77**, 2154–2157 (1996)

Chapter 4

Quantum Complementarity and Time Dilation

This chapter explains the key conceptual features of the regime where time dilation affects internal dynamical of quantum clocks. The first section reviews the notion of quantum complementarity between the which-way information available in a two-way interferometer and the visibility (contrast) of the interference pattern. Next, a thought experiment is introduced with an interfering quantum clock under time dilation. Operational understanding of the proper time and of the quantum complementarity is then used to make a qualitative prediction of new physical effects that can arise in such experiments.

4.1 Quantum Complementarity—Interferometric Visibility Versus Which-Way Information

In quantum mechanics there is a strict trade-off in the predictability of physical properties that correspond to non-commuting observables. Such properties are therefore called complementary, as they cannot be simultaneously determined. For this work of particular relevance is the complementarity between the possibility to observe interference and the availability of which-way information—these aspects are mutually exclusive in any interference experiment like the double-slit or interferometry in a Mach-Zehnder setup. The short review below focuses on deriving a quantitative statement of the complementarity; key references for the subject are [1–3].

Consider a single, two-level system with Hilbert space \mathcal{H}_1 and orthonormal basis $\{|+\rangle, |-\rangle\}$. Without loss of generality these states can represent two paths of an

Section 4.2 contains material from: *Quantum interferometric visibility as a witness of general relativistic proper time*, M. Zych, F. Costa, I. Pikovski, and Č. Brukner, *Nature Commun.* **2**:505 doi:[10.1038/ncomms1498](https://doi.org/10.1038/ncomms1498) (2011).

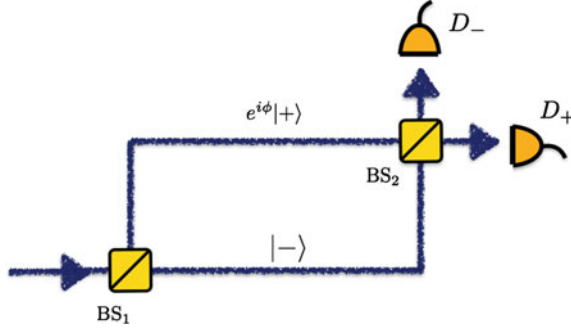


Fig. 4.1 A generic two-way interferometer: the setup consists of two beam splitters BS_1 , BS_2 and two detectors D_{\pm} . The interfering system is traversing the two paths of the interferometer in superposition. Path-modes are labelled $|\pm\rangle$ and the system can also acquire a relative phase ϕ between them, depending on the details of the setup. The two detectors D_{\pm} measure the system in a superposition of the path-modes: $|D_{\pm}\rangle \propto |+\rangle \pm |-\rangle$

interferometer, such as the Mach-Zehnder setup in the Fig. 4.1. The two detectors D_{\pm} in the setup depicted in the Fig. 4.1 can measure the observable

$$\hat{\sigma}_x := |+\rangle\langle-| + |-\rangle\langle+|,$$

when the detection of the system in D_{\pm} is assigned an outcome ± 1 . The detectors D_{\pm} thus correspond to normalised projectors onto $(|+\rangle \pm |-\rangle)$, respectively. Measurement of which path was taken is given by the observable

$$\hat{\sigma}_z := |+\rangle\langle+| - |-\rangle\langle-|,$$

which can be realised when the beam splitter BS_2 is removed.

A general pure state of a system inside the setup reads

$$|\phi\rangle = a|+\rangle + be^{i\phi}|-\rangle, \quad (4.1)$$

with $a, b \in \mathbb{R}$ such that $a^2 + b^2 = 1$ and where $\phi \in [0, 2\pi)$ denotes a relative phase between the amplitudes corresponding to the different paths.¹ Probability of detecting the system in D_{\pm} (probability of obtaining the outcome \pm in the measurement of $\hat{\sigma}_x$) exhibits interference when ϕ is varied:

$$p_{\hat{\sigma}_x=\pm 1}(\phi) = \frac{1}{2} \pm ab \cos \phi. \quad (4.2)$$

¹Depending on the physical implementations of the interferometer the relative phase can result from the difference in the dynamics of the system along the paths, the difference in the geometry (e.g. length) of the paths or other details of the setup.

Visibility \mathcal{V} of this interference pattern is defined as

$$\mathcal{V} := \frac{\max p_{\pm 1} - \min p_{\pm 1}}{\max p_{\pm 1} + \min p_{\pm 1}} = 2ab, \quad (4.3)$$

where the maximum/minimum is taken with respect to ϕ . On the other hand, for the observable $\hat{\sigma}_z$ and the state $|\phi\rangle$

$$p_{\hat{\sigma}_z=1}(\phi) = a^2 \text{ and } p_{\hat{\sigma}_z=-1}(\phi) = b^2. \quad (4.4)$$

The predictability \mathcal{P} of the measurement outcome of $\hat{\sigma}_z$ —the probability to guess the outcome correctly given the knowledge of the initial state—is expressed by

$$\mathcal{P} := |p_{\hat{\sigma}_z=1} - p_{\hat{\sigma}_z=-1}|. \quad (4.5)$$

Since the state $|\phi\rangle$ is normalised one immediately obtains

$$\mathcal{V}^2 + \mathcal{P}^2 = 1. \quad (4.6)$$

Equation (4.6) entails that non-zero predictability of the paths necessarily results in non-maximal visibility of the interference pattern, but also, that non-maximal predictability *guarantees* appearance of the interference pattern (and vice versa). Equation (4.6) can thus be seen as a statement of the limited information content of pure quantum states, which, on the other hand, are exactly those encoding maximal possible information about the system. For mixed states Eq. (4.6) generalises to an inequality:

$$\mathcal{V}^2 + \mathcal{P}^2 \leq 1, \quad (4.7)$$

consistent with the interpretation that mixed states express “lack of knowledge” about the state. Proof of the Eq. (4.7) is elementary: for a mixed state $\rho = a^2|+\rangle\langle+| + b^2|-\rangle\langle-| + c^*e^{-i\phi-i\alpha}|+\rangle\langle-| + ce^{i\phi+i\alpha}|-\rangle\langle+|$ the amplitude of the off-diagonal elements $|c|$ satisfies $|c| \leq ab$. The smaller is $|c|$ the more the state is mixed: $\text{Tr}\rho^2 = 1 - 2(a^2b^2 - |c|^4)$ defines the purity of the state. The probability to obtain $|\pm\rangle$ in $\hat{\sigma}_z$ measurement is independent of the off-diagonal elements and thus $\mathcal{P} = |a^2 - b^2|$. However, the probabilities for detecting the system in the state ρ in D_{\pm} reads $p_{\hat{\sigma}_x=\pm 1}(\rho) = \frac{1}{2} \pm |c| \cos \phi + \alpha_c$, where $c = |c|e^{i\alpha_c}$. The visibility of the interference in the outcomes of $\hat{\sigma}_x$ measurement reads $\mathcal{V} = 2|c|$ and thus $\mathcal{P}^2 + \mathcal{V}^2 = 1 - 4(a^2b^2 - |c|^4) \leq 1$ (by virtue of $|c| \leq ab$).

Measurement of the observable $\hat{\sigma}_x$ cannot be realised on the same degree of freedom and in the same experiment in which $\hat{\sigma}_z$ is measured. One could thus think that the complementarity does not apply when different degrees of freedom are used to encode the different properties, but this is not the case. Consider in addition to the interfering system a second one, which will be called a “which-way detector” (WW-D), see Fig. 4.2. The Hilbert space of the total system is $\mathcal{H} = \mathcal{H}_1 \otimes \mathcal{H}_2$, where \mathcal{H}_2 is the Hilbert space of WW-D. The “which-way detector” is initially in some

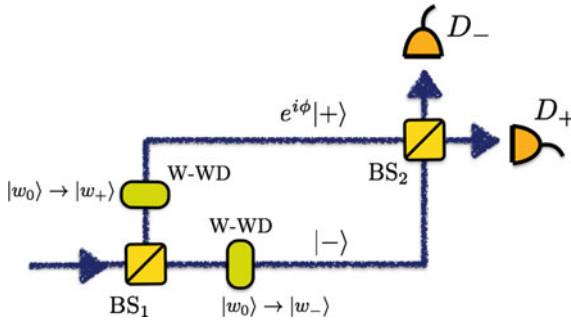


Fig. 4.2 Two-way interferometer with an additional degree of freedom for encoding the which-way information. The setup consist of two beam splitter BS_1 , BS_2 , two detectors D_{\pm} and a “which-way detector” W-WD—any degree of freedom initially uncorrelated with the interfering system that evolves into one of the two states $|w_{\pm}\rangle$, depending which of the paths $|\pm\rangle$ is taken by the interfering system. The system can in general acquire a relative phase ϕ between the path-modes and is finally registered in one of the D_{\pm} . In general, the interfering system and the WW-D become entangled, which allows obtaining which-way information from WW-D and renders the reduced state of the system mixed. This in turn results in a correspondingly reduced visibility of the interference in measurements of D_{\pm} —as required by the complementarity principle

state $|w_0\rangle$ uncorrelated with the system. Depending on which path the systems takes in the interferometer, WW-D makes a transition to one of the normalised states $|w_{\pm}\rangle$ and the joint state of the two systems reads

$$|\Phi\rangle = a|+\rangle|w_+\rangle + be^{i\phi}|-\rangle|w_-\rangle \quad (4.8)$$

It is now possible to simultaneously measure the two systems. In order to gain information about which path the system took one measures the “which-way observable”: $\hat{I}_1 \otimes \hat{\sigma}_z$ on WW-D, where \hat{I}_1 is identity operators on \mathcal{H}_1 . Detecting the interfering system in one of the two outputs D_{\pm} corresponds to the measurement of $\hat{\sigma}_x \otimes \hat{I}_2$ (\hat{I}_2 is identity on \mathcal{H}_2) on $|\Phi\rangle$. Probabilities associated to the outcomes ± 1 in this measurement read

$$p_{\hat{\sigma}_x=\pm 1}(\phi) = \frac{1}{2} \pm ab|\langle w_+|w_- \rangle| \cos(\phi + \alpha), \quad (4.9)$$

where α is defined from $\langle w_+|w_- \rangle = |\langle w_+|w_- \rangle|e^{i\alpha}$. The visibility of the interference is thus limited by the overlap between the states of the detector:

$$\mathcal{V} = 2ab|\langle w_+|w_- \rangle|. \quad (4.10)$$

If $|w_{\pm}\rangle$ are orthogonal, by measuring $\hat{I}_1 \otimes \hat{\sigma}_z$, one could learn with certainty which path the system took in the interferometer. It is important to notice that the reduction of the interferometric visibility does not depend on whether the detector states are measured or not. More generally, if the detector states are orthogonal (even if differ-

ent than the basis $|w_{\pm}\rangle$) there exists a measurement that could tell them apart with certainty, in such a case also $\langle w_+|w_- \rangle = 0$ and Eq. (4.10) entails that no interference can be observed. If the states $|w_{\pm}\rangle$ are not orthogonal, no measurement exists that can distinguish them with certainty and thus the two paths are not perfectly distinguishable even in principle. According to the Eq. (4.10), in this case the fringe visibility becomes non-zero.

A natural definition of the distinguishability of the paths provided by the detector is the trace norm distance² between the final states of the detector $\mathcal{D} = \frac{1}{2}\text{Tr}\{|w_+\rangle\langle w_+| - |w_+\rangle\langle w_+|\}$, which explicitly reads

$$\mathcal{D} = \sqrt{1 - |\langle w_+|w_- \rangle|^2} \quad (4.11)$$

Combining Eqs. (4.10) and (4.11) one obtains

$$\mathcal{V}^2 + \mathcal{D}^2 = 1 - (1 - \mathcal{D}^2)\mathcal{P}^2 \leq 1, \quad (4.12)$$

where it has been used that $1 - \mathcal{P}^2 = 4a^2b^2$. The above result has an intuitive interpretation—nonzero \mathcal{P} means that there is information about the path taken independent of the information contained in the detector’s state, thus even if $\mathcal{D} = 0$ the visibility has to be limited and one should recover Eq. (4.6), which is the case here. Moreover, for the case of $\mathcal{P} = 0$, the formula in Eq. (4.12) becomes an equality

$$\mathcal{V}^2 + \mathcal{D}^2 = 1. \quad (4.13)$$

This case will be the most important for the main results of this thesis.

Equation (4.13) applies to pure states of the joint system—for a mixed state one again obtains an inequality

$$\mathcal{V}^2 + \mathcal{D}^2 \leq 1, \quad (4.14)$$

see Ref. [3] for a proof in a general case. For this thesis the following spacial case is useful to keep in mind: consider an initial state of the WW-D $|w'_0\rangle$ for which it makes the transition to $|w_- \rangle$ if the path “+” was taken by the interfering system and to the $|w_+ \rangle$ for the path “−”, inversely as the state $|w_0\rangle$. From the Eq. (4.1) the total state of the system inside the setup with $|w'_0\rangle$ as the initial state and for $a = b$ reads

$$|\Phi'\rangle = \frac{1}{\sqrt{2}}(|+\rangle|w_- \rangle + e^{i\phi}|-\rangle|w_+ \rangle).$$

If $|w_{\pm}\rangle$ are orthogonal there is a perfect which way information for both initial preparations, $|w'_0\rangle$ and $|w_0\rangle$. Note, however, that the states which signals that the path “+” was taken are orthogonal for these two preparations. If $|w_{\pm}\rangle$ are orthogonal then also $|w'_0\rangle$ and $|w_0\rangle$ are (the whole “process” is unitary) and a state $\rho_w = \frac{1}{2}|w'_0\rangle\langle w'_0| +$

²Equivalent definition of \mathcal{D} —yielding the same formula—is the probability to correctly guess which path was taken upon making an optimal measurement on the states $|w_{\pm}\rangle$, see e.g. Ref. [3].

$\frac{1}{2}|w_0\rangle\langle w_0|$ is maximally mixed and remains unchanged, independently of the path taken. The which way information available from ρ_w is $\mathcal{D}_{\rho_w} = 0$ —this reflects that, if the initial preparation is not known, each of the states $|w_{\pm}\rangle$ signals with equal probability each of the two paths. Visibility of the interference pattern is, however, not restored if the initial preparation of the WW-D is ρ_w : For both initial preparations the visibility of the interference pattern vanishes, $\mathcal{V}_{w'_0} = \mathcal{V}_{w_0} = 0$. The interference pattern obtained in an experiment in which the state ρ_w is prepared will be an equally weighed average over the individual interference patterns³ and thus $\mathcal{V}_{\rho} = 0$. This is an extreme case of the inequality where $\mathcal{D} + \mathcal{V} = 0$.

It is also possible to refine the quantification of the which-way information: the formula $(1 - \mathcal{D}^2)(1 - \mathcal{P}^2)$ in Eq. (4.12) has an interpretation as the total probability to make a wrong guess about the path taken by the system, given the knowledge of the initial state (and thus of \mathcal{P}). The chance to guess correctly is therefore given by $\tilde{\mathcal{D}}^2 = 1 - (1 - \mathcal{D}^2)(1 - \mathcal{P}^2)$, which satisfies $\mathcal{V}^2 + \tilde{\mathcal{D}}^2 = 1$.

Finally, note that the state $|\Phi\rangle$ becomes entangled the more the states $|w_{\pm}\rangle$ are orthogonal. As a result, the reduced state of the interfering system, denoted ρ_1 —which is obtained by a partial trace over the states of the “which-way detector”: $\rho_1 := \text{Tr}_2\{|\Phi\rangle\langle\Phi|\}$ —becomes mixed:

$$\rho_1 = a^2|+\rangle\langle+| + b^2|-\rangle\langle-| + ab|w_+|w_-\rangle| (e^{-i\phi-i\alpha}|+\rangle\langle-| + e^{i\phi+i\alpha}|-\rangle\langle+|) . \quad (4.15)$$

Equation (4.7) entails that in general for a mixed state neither the visibility, nor the which way information are maximal. Note, that the visibility \mathcal{V} Eq. (4.10) is twice the amplitude of the off-diagonal elements, in a full analogy to the case of a single degree of freedom in a mixed state.⁴ In the case when $|w_{\pm}\rangle$ are indistinguishable, the total state of the system factors into the state of the which-way detector and of the system. Tracing away the detector states leaves the state of the system pure and maximal fringe visibility can be observed (for $a = b$). One can again interpret the complementarity as the statement about the limited information content of quantum states: Even if one encodes the information in correlations between different subsystems (degrees of freedom) of a pure state, these correlations in quantum mechanics necessary entail some degree of entanglement, which in turn, results in having mixed state of the subsystems—in which case \mathcal{V} in general cannot be maximal. Note that a pure state of subsystems (for a global pure state) signals that there is no entanglement between them—there are no correlations that could even in principle reveal which way information, thus maximal interferometric visibility is possible.

The amount of the which-way information that is potentially available from any degree of freedom sets an absolute upper bound on the fringe visibility in any inter-

³In the above discussion an interpretation of the mixed state as a classical mixture over the preparations of pure states is employed.

⁴In fact in quantum mechanics these two scenarios are formally exactly the same, since any mixed state can be obtained by considering the system to be a subsystem of a bigger system, which is in a pure state.

ferometric scenario. The loss of the visibility does not depend on whether the degrees of freedom which encode the path information are measured or not.

4.2 Which-Way Information from Time Dilation—Gedankenexperiment

Consider a quantum version of the time dilation scenario in Fig. 2.1—in which a single clock is following in superposition along two world lines which have different proper times, see Fig. 4.3. For a classical “clock”—a classical point-like system with evolving internal degrees of freedom—the final state of its internal degrees of freedom depends on the path taken, due to the time dilation (see Chap. 2).

Quantum theory allows to assign a quantum state to the external as well as the internal degrees of freedom of any system, also that used as a “clock”. Superposition principle of quantum theory and relativistic time dilation thus allow for conceptually novel situation—where a single “clock” runs two different proper times in superposition. What happens in an interference experiment with such a clock?

To answer this question consider the scenario depicted in Fig. 4.3, where the external state of the “clock” is put into a coherent superposition of following two

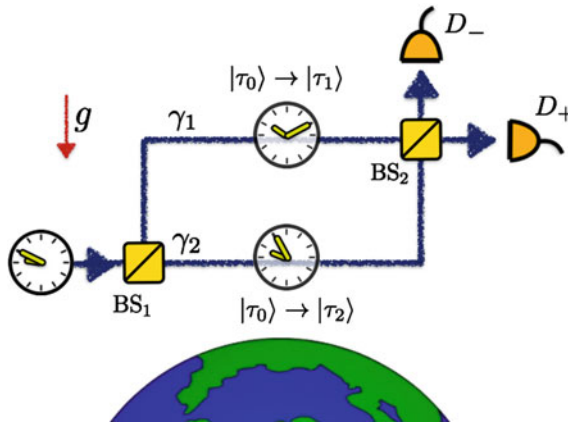


Fig. 4.3 Gedankenexperiment with a single “clock” following in superposition two paths γ_1, γ_2 with different proper times τ_1, τ_2 , respectively. The paths are the same as in Fig. 2.1 and likewise g denotes the gravitational field of earth. The “clock” is a system with internal time evolving degrees of freedom, which due to time dilation evolve into different final states $|\tau_1\rangle, |\tau_2\rangle$ depending on the path taken. These internal degrees of freedom serve as the “which-way detectors”—the setup is therefore also analogous to the one in Fig. 4.2. According to quantum complementarity the visibility of the interference pattern will be reduced to the extent to which the which-way information becomes accessible due to time dilation between the paths. This is a quantum version of the twin paradox—with a “quantum only child”, which sets up in superposition on two different voyages and due to time dilation ages in superposition, becoming older and younger than himself

arms of the interferometer, and the corresponding position amplitudes will be denoted $|r_i\rangle$, $i = 1, 2$. Denoting the internal state evolving along the corresponding path as $|\tau_i\rangle$ the state of the “clock” in the interferometer reads

$$|\Psi\rangle = \frac{1}{\sqrt{2}} \left(e^{-i\Phi_1} |r_1\rangle |\tau_1\rangle + e^{-i\Phi_2 + i\varphi} |r_2\rangle |\tau_2\rangle \right), \quad (4.16)$$

Φ_i denote trajectory dependent phases resulting from the dynamics of the “clocks” and φ is some additional controllable phase difference. The “clock” is finally detected in one of the two detectors D_{\pm} . If general relativity can be applied to a “clock” in superposition, the internal degrees of freedom will evolve at a different rate along each path and will thus store the path information—they act as the “which-way detector” (WW-D) discussed in the Sect. 4.1. Therefore, according to quantum complementarity, interference in the path degrees of freedom should correspondingly be diminished. The distinguishability of the paths \mathcal{D} for the state $|\Psi\rangle$ in Eq. (4.16) is given by the Eq. (4.11) where the internal states $|\tau_i\rangle$ play the role of the WW-D states $|w_{\pm}\rangle$; one finds

$$\mathcal{D} = \sqrt{1 - |\langle\tau_1|\tau_2\rangle|^2}. \quad (4.17)$$

The probabilities P_{\pm} of detecting the “clock” in state $|\Psi\rangle$ by detectors D_{\pm} now read

$$P_{\pm} = \frac{1}{2} \pm \frac{1}{2} |\langle\tau_1|\tau_2\rangle| \cos(\Delta\Phi + \alpha + \varphi), \quad (4.18)$$

where $\langle\tau_1|\tau_2\rangle = |\langle\tau_1|\tau_2\rangle| e^{i\alpha}$ and $\Delta\Phi := \Phi_1 - \Phi_2$. The visibility of the interference pattern obtained by varying φ , Eq. (4.3), for the case above reads

$$\mathcal{V} = |\langle\tau_1|\tau_2\rangle|. \quad (4.19)$$

The visibility of interference is thus indeed correspondingly limited and the quantitative statement of the complementarity between the which way information and the possibility to observe interference, derived in Eq. (4.13), is recovered $\mathcal{V}^2 + \mathcal{D}^2 = 1$. Note that if a “switched off clock”—a system in a stationary internal state—is taken instead, the which-way information is zero and the visibility of the interference pattern becomes maximal. Internal states would in this case remain the same along both paths and would factor out in Eq. (4.16), leaving pure state of the path-mode of the “clock”—which allows for maximal visibility of interference fringes. Observability of the time-dilation induced complementarity is only possible with a “switched on clock”. Note also, that in the non-relativistic case the rate of the time evolution of the “clock” would be the same along both paths and the final states would be the same, $|\tau_1\rangle = |\tau_2\rangle$. In the non-relativistic case, no which-way information is available from the time shown by the “clock” and the expected visibility is in principle always maximal—independently whether the “clock” is switched on or not.

In general, the distinguishability of the final states of the “clock” will depend on how $\Delta\tau$ compares with the precision t_{\perp} of the “clock”—i.e. the time that internal

states of the system need to evolve between the consecutive distinguishable states, in the context of quantum theory t_{\perp} is thus called orthogonalisation time [4, 5]. Thus, the expected visibility in Eq. (4.19) will generally take the form:

$$\mathcal{V} = F_{\odot}\left(\frac{\Delta\tau}{t_{\perp}}\right), \quad (4.20)$$

where the function F_{\odot} has the following properties: $F_{\odot}: R_+ \rightarrow [0, 1]$ is such that $F_{\odot}(0) = 1$ and $F_{\odot}(1) < 1$. This conclusion is not limited to any particular physical implementation of the clock. Time dilation necessary to cause a loss of quantum interference will only depend on the precision of the clock and not on its realisation—this is a consequence of the universality of general relativistic time dilation. Only the explicit form of the function F_{\odot} depends on the specific realisation of the clock. For example, a clock with a finite dimensional Hilbert space has a periodic time evolution and thus one expects periodic losses and *revivals* (when $\Delta\tau$ equals the period of the “clock”) of the visibility with increasing time dilation between the two arms of the interferometer. Note, that this allows already at this stage to infer that e.g. for a clock implemented in a two-level system (which evolves between two mutually orthogonal states) F_{\odot} will be a cosine function. The case of a periodic “clock” has an important advantage for experimental verification of the effect—unlike the observation of only the decrease in the interferometric visibility, the observation of its periodic modulations would allow for unambiguous discrimination between the time dilation effect and the visibility losses due to experimental imperfections. A different case, which also seems promising for an experimental verification, is a “clock” implemented in a position of photon on a path, where the function F_{\odot} becomes a Gaussian, for the photon with a Gaussian distribution of frequencies. These two cases are studied in details in Chap. 5.

If the paths γ_i are symmetrically split and overlapped—such that no considerable special relativistic time dilation between them is accrued—in order to explain the modulations in the interferometric visibility both quantum complementarity and the gravitational time dilation are necessary. Realisation of such a Gedanken experiment with interfering “clocks” in gravitational field—in which modulations of the interferometric visibility are measured—would allow probing the interplay between quantum theory and general relativity.

Finally, as discussed in Sect. 4.1 also mixed states of the which-way detectors cause loss of the visibility, and thus also mixed states of the “clocks” should result in loss of quantum interference. Note, that the visibility attainable with two initial states of the “clock” that differ by t_{\perp} is the same (as well any acquired phases)—the two states correspond just to a different choice of initial time. Thus, taking as initial state an equal mixture of these two “clocks” states, will yield the same visibility loss as each of the two states alone. By definition of t_{\perp} , these states are orthogonal and their mixture is a maximally mixed state (on the subspace spanned by the two states). Such a state is stationary and in particular provides no which way information. This is in agreement with the general relation between the visibility of the interference pattern and distinguishability of the paths for mixed states given in Eq. (4.14). Furthermore,

this shows that time dilation affects centre mass coherence of composite systems in a generic state of the internal degrees of freedom—such as a thermal state—and not just for specific, pure “clock” states. The resulting decoherence mechanism, induced by time dilation, is the subject of Chap. 6.

References

1. W.K. Wootters, W.H. Zurek, Complementarity in the double-slit experiment: quantum nonseparability and a quantitative statement of Bohr’s principle. *Phys. Rev. D* **19**, 473–484 (1979)
2. D.M. Greenberger, A. Yasin, Simultaneous wave and particle knowledge in a neutron interferometer. *Phys. Lett. A* **128**, 391–394 (1988)
3. B.-G. Englert, Fringe visibility and which-way information: an inequality. *Phys. Rev. Lett.* **77**, 2154–2157 (1996)
4. L. Mandelstam, I. Tamm, *The uncertainty relation between energy and time in non-relativistic quantum Mechanics*, in *Selected Papers* (Springer, Berlin, 1991), pp. 115–123
5. G. Fleming, A unitarity bound on the evolution of nonstationary states. *Il Nuovo Cimento A* **16**, 232–240 (1973)

Chapter 5

Interference of “Clocks”—Experimental Proposals

This chapter describes two proposals for practical realisation of the thought experiment from the previous chapter, with interfering “clocks” subject to time dilation. In the first one, the “clock” is implemented in the internal state of a massive particle. In the second—in a position of a photon. In the latter, gravitational time dilation arises from the Shapiro effect—the slow-down of light grazing a massive object as compared to the speed of light in a region further away from the mass (as measured by a fixed observer). It is shown how the experiment with a massive “clock” can lead to a conclusive test of theories which propose that proper time and mass are a pair of new conjugate degrees of freedom. For the massless case, it is shown how with a modified experimental setup one can rule out local realistic models of light in a post-Newtonian background. The last section discusses what aspects of the interplay between quantum mechanics and general relativity are probed by various effects in such experiments.

5.1 Massive Particle as a “Clock”

5.1.1 Time Dilation Effects for Massive Quantum Systems

The experimental proposal discussed below is aimed at earth-based, laboratory scale experiments with massive systems like atoms or molecules. In the considered real-

This chapter is based on and contains material from: *Quantum interferometric visibility as a witness of general relativistic proper time*, M. Zych, F. Costa, I. Pikovski, and Č. Brukner, *Nature Commun.* **2**:505 doi:[10.1038/ncomms1498](https://doi.org/10.1038/ncomms1498) (2011); and *General relativistic effects in quantum interference of photons*, M. Zych, F. Costa, I. Pikovski, T. C. Ralph, and Č. Brukner, *Class. Quant. Grav.* **29**, 224010 (2012).

isations the centre of mass energies are relatively low and thus the systems can be described by the Hamiltonian H_{Lab} derived in Chap. 3 (which includes up to second order relativistic corrections to the non-relativistic dynamics of a composite massive quantum particle). Since the internal Hamiltonian H_{int} in the present context describes the degrees of freedom in which the “clock” is implemented, it is denoted by a more telling H_{\odot} throughout this chapter. The laboratory reference Hamiltonian thus reads,

$$H_{Lab} \simeq mc^2 + H_{cm} + H_{\odot} \left(1 + \frac{\Phi(x)}{c^2} - \frac{p^2}{2m^2c^2} \right), \quad (5.1)$$

where the centre of mass Hamiltonian H_{cm} is given in Eq. (3.3) (up to a constant mc^2 term).

A semiclassical approximation of the particle’s motion in the interferometer is considered. All terms in H_{Lab} , apart from the internal Hamiltonian H_{\odot} , are thus considered to be already fixed functions along the interferometric paths as depicted in Fig. 5.1.

The particle follows in superposition two fixed non-geodesic paths γ_1, γ_2 in the homogeneous gravitational field.

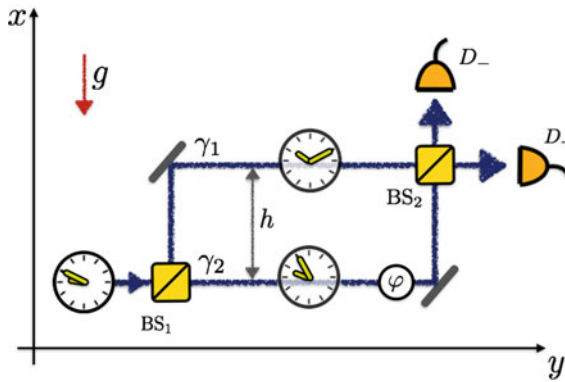


Fig. 5.1 Mach-Zehnder interferometer in a gravitational field. The setup consists of two beam splitters (BS), a phase shifter (PS) and two detectors D_{\pm} . The PS gives a controllable phase difference φ between the two trajectories γ_1 and γ_2 , which both lie in the $x - y$ plane. A homogeneous gravitational field (g) is oriented antiparallel to the x direction. The separation between the paths in the direction of the field is h . Interference of a particle following the paths which are not in a free fall is considered. If the particle has evolving internal degree of freedom which acts as a “clock”, general relativity predicts that due to the time dilation between the trajectories the internal degrees of freedom will evolve into different final states, depending on the path taken. Such an interference experiment will therefore not only display a phase shift, but also a reduced visibility of the interference pattern, to the extent to which the path information becomes available from the proper time of the “clock”

The particle inside the interferometer can be described by the superposition

$$|\Psi_{MZ}\rangle = \frac{1}{\sqrt{2}} (i|\Psi_1\rangle + e^{i\varphi}|\Psi_2\rangle), \quad (5.2)$$

where the states $|\Psi_i\rangle$ associated with the two paths γ_i are given by applying the Hamiltonian (5.1) to the initial state which is assumed to be factorisable¹ $|x^{in}\rangle|\tau^{in}\rangle$. Up to an overall phase these states read

$$|\Psi_i\rangle = e^{-\frac{i}{\hbar} \int_{\gamma_i} dt H_{cm} + H_{\odot} \left(1 - \frac{p^2}{2m^2 c^2} + \frac{\Phi(x)}{c^2}\right)} |x^{in}\rangle|\tau^{in}\rangle. \quad (5.3)$$

The coupling terms proportional to H_{\odot} result in a time evolution of internal state that depends on the state of the external degree of freedom

$$|\tau_i\rangle = e^{-\frac{i}{\hbar} \int_{\gamma_i} dt H_{\odot} \left(1 - \frac{p^2}{2m^2 c^2} + \frac{\Phi(x)}{c^2}\right)} |\tau^{in}\rangle \quad (5.4)$$

In particular, $\int_{\gamma_i} \left(1 - \frac{p^2}{2m^2 c^2} + \frac{\Phi(x)}{c^2}\right) dt = \tau_i$ is the proper time along the world line γ_i . Thus, equivalently, one can write the above as

$$|\tau_i\rangle = e^{-\frac{i}{\hbar} \int_{\gamma_i} d\tau H_{\odot}} |\tau^{in}\rangle, \quad (5.5)$$

the internal state of a quantum system evolves with respect to the proper time and along the system’s world line—also in quantum theory such systems can be seen as ideal “clocks”. Equations (5.4) and (5.5) also show how the clocks’s rate in the rest frame (with respect to the proper time τ) is related to the rate observed in the laboratory frame (with respect to the coordinate time t). Since the internal Hamiltonian is effectively “rescaled” by a factor $\left(1 - \frac{p^2}{2m^2 c^2} + \frac{\Phi(x)}{c^2}\right)$ when internal evolution is described with respect to the coordinate time t , also rest frame frequency of the “clock”,² denoted by ω_{rest} , in the laboratory frame reads

$$\omega^{lab} = \omega_{rest} \left(1 - \frac{p^2}{2m^2 c^2} + \frac{\Phi(x)}{c^2}\right) \quad (5.6)$$

and is modified by the special relativistic and gravitational time dilation—in exactly the same way as in the classical case. Time dilation of the system’s rate of evolution is the same whether the interactions between internal and external degrees of freedom are quantised or not.

¹In a typical interferometric scenario, e.g. in atomic fountains, this assumption is satisfied [1].

²Time evolution of any observable in quantum theory is given by the commutator of the observable with the Hamiltonian. Thus, rate of evolution of any internal observable will be modified by the same factor by which the rest frame Hamiltonian is rescaled.

With Eq. (5.5) it is elementary to find

$$\langle \tau_1 | \tau_2 \rangle = \langle \tau^{in} | e^{-\frac{i}{\hbar} H_{\odot} \Delta \tau} | \tau^{in} \rangle, \quad (5.7)$$

where $\Delta \tau = \int_{\gamma_2} d\tau - \int_{\gamma_1} d\tau$ is the proper time difference between path γ_2 and γ_1 . Visibility of the interference pattern \mathcal{V} for the state $|\Psi_{MZ}\rangle$ is given by the overlap between the internal states (c.f. Eqs. (4.16) and (4.19)) and reads

$$\mathcal{V} = |\langle \tau^{in} | e^{-\frac{i}{\hbar} H_{\odot} \Delta \tau} | \tau^{in} \rangle|. \quad (5.8)$$

In quantum mechanics the same interactions which cause the clock’s frequency shift and time dilation also result in entanglement between the internal and external degrees of freedom. Reduced visibility Eq. (5.8) is a direct consequence of this entanglement (if the path modes are orthogonal, which is the case here, \mathcal{V} is also a measure³ of this entanglement). The reduction in the coherence of a quantum superposition, described by \mathcal{V} is a genuine quantum effect, with no classical analogue.

5.1.2 Two-Level Quantum System as a Clock

Consider a particle in superposition of two internal states $|0\rangle, |1\rangle$ with corresponding energies E_0, E_1 . Such an effective description of internal atomic levels is applicable to typical matter-wave interferometry scenarios. Without loss of generality, the rest frame Hamiltonian of the internal degrees of freedom is

$$H_{\odot} = E_0 |0\rangle \langle 0| + E_1 |1\rangle \langle 1|. \quad (5.9)$$

For an initial state

$$|\tau^{in}\rangle = \frac{1}{\sqrt{2}}(|0\rangle + |1\rangle). \quad (5.10)$$

the Eq. (5.7) reads

$$\langle \tau_1 | \tau_2 \rangle = \cos\left(\frac{\Delta E \Delta \tau}{2\hbar}\right) e^{-i\langle H_{\odot} \rangle \Delta \tau / \hbar}, \quad (5.11)$$

where $\Delta E = |E_1 - E_0|$ and the expectation value $\langle H_{\odot} \rangle$ is taken with respect to $|\tau^{in}\rangle$.

The speed of the internal evolution for a given state and under a fixed Hamiltonian is conveniently quantified by the orthogonalisation time t_{\perp} —the minimal time after which the state evolves into an orthogonal one. t_{\perp} thus represents the precision of the “clock” in the present context. For the state $|\tau^{in}\rangle$ it reads $t_{\perp} = \frac{\pi\hbar}{\Delta E}$ and is also maximal for any state evolving under H_{\odot} [2–4] (therefore, $|\tau^{in}\rangle$ gives us the “clock”

³For a bipartite pure quantum state the purity of the reduced density matrix is a measure of entanglement and \mathcal{V} also quantifies the purity of the reduced state, see also Eq. (4.15).

with the highest precision for the given internal energy). The visibility, Eq. (5.8), can be written as

$$\mathcal{V} = \left| \cos \left(\frac{\Delta\tau}{t_\perp} \frac{\pi}{2} \right) \right|. \quad (5.12)$$

Visibility attainable in an interference experiment with a quantum system whose internal dynamics has a time scale t_\perp only depends on how t_\perp compares to the total time dilation $\Delta\tau$ between the superposed paths. Whenever $\Delta\tau$ is equal to t_\perp , there is a physically accessible which-way information stored in the internal states of the system, which results in a corresponding loss of the fringe contrast—this holds for any implementation of the “clock”. The cosine form of the visibility is due to the fact that the “clock” periodically evolves between two mutually orthogonal states.

Consider the trajectories γ_i , such that the acceleration and deceleration which the particle undergoes in the x direction, as well as velocity in the y direction, are the same for both trajectories. This assures that the trajectories have different proper lengths but in the final result there will be no time dilation stemming from special relativistic effects.

For this specific choice of γ_i the time dilation reads $\Delta\tau = \int_0^{\Delta T} dt \left(\frac{\Phi(r+h)}{c^2} - \frac{\Phi(r)}{c^2} \right) = \frac{gh\Delta T}{c^2}$, where the central gravitational potential $\Phi(x)$ has been approximated to linear terms in the distance h between the paths $\Phi(r+h) = \Phi(r) + gh + \mathcal{O}(h^2)$; $g = \frac{Gm_e}{r^2}$ denotes the value of the Earth’s gravitational acceleration in the origin of the laboratory frame (which is at a radial distance r from the centre of the earth); and ΔT is the time as measured in the laboratory frame for which the particle travels in superposition at constant heights. With the above, the probabilities of detection, Eq. (4.18), for a two level system with $t_\perp = \frac{\pi\hbar}{\Delta E}$ in the considered interference experiment read

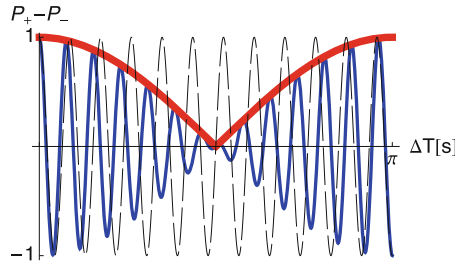
$$P_\pm = \frac{1}{2} \pm \frac{1}{2} \cos \left(\frac{\Delta E \Delta V \Delta T}{2\hbar c^2} \right) \cos \left(\left(m + \langle H_\odot \rangle / c^2 + \bar{E}_{corr}^{GR} \right) \frac{\Delta V \Delta T}{\hbar} + \varphi \right). \quad (5.13)$$

where $\Delta V := \Phi(r+h) - \Phi(r) \approx gh$ is the difference in the gravitational potential between the paths and \bar{E}_{corr}^{GR} is a mean value of the terms (present in H_{cm}) denoted as $E_{corr}^{GR} := \frac{m\phi(x)}{2c^2} + 3\frac{p^2}{2m^2c^2}$, which describe general relativistic corrections to the Newtonian dynamics of the centre of mass. The corresponding visibility thus reads

$$\mathcal{V} = \left| \cos \left(\frac{\Delta E \Delta V \Delta T}{2\hbar c^2} \right) \right|, \quad (5.14)$$

which is of course just the Eq. (5.12) for the particular paths considered here. The probabilities in Eq. (5.13) and the visibility are plotted in Fig. 5.2.

The term $m\Delta V \Delta T / \hbar$ in Eq. (5.13) is the non-relativistic gravitational phase shift, coming from the Newtonian gravitational potential, and is the effect measured in the COW experiment [6] (see also Chap. 2). It is the only effect of gravity in the non-relativistic limit in this setup. The detection probabilities Eq. (5.13) in this limit read



$$P_+ - P_- = \cos\left(\frac{\Delta E \Delta V \Delta T}{2\hbar c^2}\right) \cos\left((mc^2 + \langle H_{\odot} \rangle + \bar{E}_{corr}^{GR}) \frac{\Delta V \Delta T}{\hbar c^2} + \varphi\right)$$

Fig. 5.2 Plot of the difference between the probabilities P_{\pm} , Eq. (5.13), to find the particle in the detector D_{\pm} of the Mach-Zehnder interferometer as a function of the time ΔT for which the particle travels in a superposition of two trajectories at constant heights (this corresponds to changing the length of the interferometric arms). The term proportional to the particle’s mass is the phase originating from the Newtonian potential energy $m\Delta V$. General relativistic corrections stemming from external degrees of freedom are given by \bar{E}_{corr}^{GR} , see e.g. Ref. [5]. Without the “clock” degrees of freedom only these terms are present in the result (*dashed, black line* in the plot). In the situation with the “clock” (*thin blue line*) two additional effects arise: the change of the interferometric visibility given by the absolute value of the first cosine (*thick red line*) and an additional phase shift proportional to the average internal energy of the “clock”. The values for the energy gap ΔE and the gravitational potential difference ΔV between the interferometric paths are chosen such that $\frac{\Delta E \Delta V}{2\hbar c^2} = 1\text{Hz}$. While the phase shift alone can always be understood as an Aharonov-Bohm phase of an effective potential, the notion of general relativistic proper time is necessary to explain the decrease of the visibility

$$P_{nr\pm} = \frac{1}{2} \pm \frac{1}{2} \cos\left(\frac{m\Delta V \Delta T}{\hbar} + \varphi\right). \quad (5.15)$$

The presence of the “clock” degrees of freedom is irrelevant in the non-relativistic case—only a relative phase is acquired, which depends on the static part of the internal energy, i.e. on the system’s mass. The visibility of the resulting interference stays maximal independently of the internal state. More generally, the phase acquired by a state during its time evolution is proportional to the action along the trajectory γ_i on which the particle moves. In the presence of any position dependent potential $V(x)$ this phase becomes trajectory dependent: $\Phi_i = \propto \int_{\gamma_i} V(x(t))dt$ (assuming that contributions from the kinetic energy cancel out). Therefore, even in a homogeneous field the particle acquires a trajectory dependent phase although the force acting on it is the same at all points—the phase arises only due to the potential difference. For a homogeneous electric field such a relative phase is known as the electric (scalar) Aharonov-Bohm effect [7]. The case of Newtonian gravity is directly analogous—the role of the particle’s electric charge and of the Coulomb potential are taken by the particle’s mass and the Newtonian gravitational potential, respectively, [8].

The modulations in the interferometric visibility and the additional phase shift term—proportional to the average internal energy—depend on the state of the “clock” degrees of freedom and cannot be explained in the Newtonian limit. Note, that if the

internal degrees of freedom are in an energy eigenstate, say $|E_0\rangle$, Eq. (5.13), reads

$$P_{off\pm} = \frac{1}{2} \pm \frac{1}{2} \cos \left((m + E_0/c^2 + \bar{E}_{corr}^{GR}) \frac{\Delta V \Delta T}{\hbar} + \varphi \right)$$

and the visibility stays maximal. Interpretation of this result is straightforward—an energy eigenstate is stationary (it is a “switched off clock”) and will not provide any which-way information. It evolves into the same final state with only an additional phase difference on top of the Newtonian one. Note, that this correction to the Newtonian phase shift given generally by $\langle H_{\odot} \rangle$ can be obtained from a semiclassical mass-energy equivalence, i.e. considering that the total mass-energy of the system is $mc^2 + \langle H_{\odot} \rangle$ in the coupling to the external degrees of freedom. With such a coupling there is no time dilation in the time evolution of internal states. This means that probing only the phase shift is in principle consistent with the existence of global time—see Appendix C.1 for an explicit example. In contrast, the drop in the visibility is a consequence of a direct coupling of the particle’s internal Hamiltonian H_{\odot} to the potential in the Hamiltonian (5.1). Such a coupling is not found in Newtonian gravity and it is the mathematical expression of the prediction that the “clock” ticks at different rates when placed in different gravitational potentials. Testing this coupling is tantamount to testing the time dilation. To lowest order this coupling can directly be obtained from the Einstein equivalence hypothesis [9]. The latter postulates that accelerated reference frames are physically equivalent to those in the gravitational field of massive objects. When applied within special relativity this exactly results in the prediction that initially synchronised clocks subject to different gravitational potentials will show different times when brought together. The Einstein equivalence hypothesis is a corner stone of general relativity as it is crucial for the formulation of general relativity as a metric theory [9]. Thus, the modulations in the fringe contrast in the interference experiment with massive particle can be considered genuine quantum mechanical as well as genuine general relativistic effect, and in particular unambiguously probe the general relativistic notion of proper time.

5.1.3 Quantitative Predictions

Below a brief discussion is given of the various systems for the implementation of the interferometric setup. Interferometry with many different massive quantum systems has been achieved, e.g. with neutrons [6, 10], atoms [11, 12], electrons [13, 14], and molecules [15, 16]. In here presented framework, additional access to an internal degree of freedom is paramount, as to initialise the “clock” which “measures” the proper time along the interferometric path. Therefore, the experimental requirements are more challenging. To observe the full loss of the interferometric visibility, the proper time difference between the interferometric arms needs to be $\Delta\tau = t_{\perp}$. For a two-level system the revival of the visibility due to the indistinguishability of the proper time in the two arms occurs when $\Delta\tau = 2t_{\perp}$, Eq. (5.12).

Table 5.1 Comparison of different systems for the experimental observation of the reduced interferometric visibility. Several systems are compared on the basis of theoretically required and already experimentally achieved parameters, which are relevant for our proposed experiment. For a “clock” with a frequency $\omega = \frac{\Delta E}{\hbar}$, the required value of the parameter $\hbar \Delta T$ (\hbar being the separation between the interferometers arms and ΔT the time for which the particle travels in superposition at constant heights) for the full loss of the fringe visibility, see Eq. (5.14), is given in the rightmost column. In our estimations we assumed a constant gravitational acceleration $g = 10 \frac{m}{s^2}$

System	“Clock” (possible implementation)	ω (Hz)	$\hbar \Delta T$ (m · s) achieved	$\hbar \Delta T$ (m · s) required
Rb atoms [18]	Electronic states	10^{15}	0.5	10
Cs atoms [11, 12]	Electronic states	10^{15}	10^{-5}	10
Electrons [13, 14]	Spin precession	10^{13}	10^{-6}	10^3
Molecules [15, 16]	Vibrational modes	10^{12}	10^{-8}	10^4
Neutrons [6, 10]	Spin precession	10^{10}	10^{-6}	10^6

The best current atomic clocks operate at optical frequencies ω around 10^{15} Hz. For such systems $t_{\perp} = \frac{\pi}{\omega}$ and one would therefore require an atomic superposition with $\hbar \Delta T \approx 10$ ms in order to see full disappearance of the interferometric visibility. For example, the spatial separation would need to be of the order of 1 m, maintained for about 10 s. Achieving and maintaining such large superpositions of atoms still remains a challenge, but recent rapid experimental progress indicates that this interferometric setup could be conceivable in the near future. For neutrons, a separation of $\hbar \sim 10^{-2}$ m with a coherence time of $t \sim 10^{-4}$ s has been achieved [10]. To implement our “clock” in neutron interferometry one can use spin precession in a strong, homogeneous magnetic field. However, such a “clock” could reach frequencies up to $\omega \sim 10^9$ Hz (for a magnetic field strength of order of 10 T [17]), which is still a few orders of magnitude lower than necessary for the observation of full decoherence due to a proper time difference. Improvements in the coherence time and the size of the interferometer would still be necessary. Other systems, such as molecules, could be used as well and Table 5.1 summarizes the requirements for various setups (note again that the particles are assumed to travel at fixed height during the time ΔT).

The predicted effect can in principle be measured even without achieving full orthogonalisation of the “clocks”. Note that even for $\Delta\tau \ll t_{\perp}$ the small reduction of the visibility can already be sufficient to prove the accessibility of which-path information due to the proper time difference. With current parameters in atom interferometry, an accuracy of the measurement of the visibility of $\Delta\mathcal{V} = 10^{-6}$ would have to be achieved for the experimental confirmation of our predictions. A very good precision measurement of the interferometric visibility and a precise knowledge about other decoherence effects would make the requirements for the other parameters less stringent.

5.1.4 Discussion

Note, that the Newtonian interferometric phase shift can be equivalently expressed as $\frac{mc^2}{h} \Delta\tau$ where $\Delta\tau = \frac{\Delta V \Delta T}{c^2}$ is the proper time difference between the trajectories. Some authors interpret therefore the gravitational phase shift as the effect of gravitational time dilation [19]. Even though such an interpretation is consistent with general relativity, it cannot distinguish the Newtonian—non-metric—gravity from genuine general relativistic effects. An interpretation of the phase shifts experiments as measuring the time dilation can only be sustained if the very existence of the time dilation is pre-assumed, i.e. by pre-assuming that observed Newtonian effects are the low-energy limit of general relativistic effects. The phase shift measurements can be used to test possible deviations from general relativity in the Newtonian limit [20–22], but will always be compatible with an absolute time (flat space-time). In contrast, the drop in the interferometric visibility (only observable when using *physical* clocks), cannot be explained without the general relativistic notion of proper time.

To sustain the general relativistic viewpoint it has also been argued that, differently from classical free fall experiments, a massive quantum particle constitutes a “clock” ticking at the Compton frequency, mc^2/h , which causes the interference [19]. If any operational meaning was to be attributed to this clock, it would imply that which-way information is in principle accessible. The notion of such a “Compton clock” is, however, purely formal: no measurement on the particle within the interferometer can reveal the time of such a clock. In order to measure the frequency of the “Compton clock”, it would be necessary to measure the number of oscillations per unit time of the global phase of the wavefunction—in contradiction to the basic tenets of quantum mechanics. Reasoning that any (even just an abstract) frequency which can be ascribed to the particle allows considering proper time as a physical quantity would imply that interference should always be lost, as the which-path information is stored “somewhere”. One should then either assume that proper time is a quantum degree of freedom, in which case there should be a drop in the interferometric visibility, or that the quantum complementarity (between which-path information and interferometric visibility) ceases to apply when general relativistic effects become relevant.

The hypothesis that proper time is a degree of freedom has indeed been considered in various works [23–25] and the proposed interference experiment allows to test these possibilities. The idea that proper time and mass are canonically conjugate degrees of freedom like position and momentum was discussed e.g. in the context the equivalence principle in Refs. [23, 24] and of a mass—proper time uncertainty relation in Ref. [25]. The equations of motion for proper time treated dynamically as put forward in this references are in agreement with general relativity. Therefore, the predictions of Eq. (4.19) would also be valid, if the states $|\tau_i\rangle$, introduced in Eq. (4.16), stand for this new degree of freedom. Already performed experiments, like in Refs. [6, 19], which measured a gravitational phase shift, immediately rule out the possibility that the state of proper time was sharply defined in those tests, in the sense of $\langle \tau_1 | \tau_2 \rangle = \delta(\tau_1 - \tau_2)$. However, such experiments can put a bound on the possible

Table 5.2 Discussion of what the different outcomes of the proposed experiment entail for the hypothesis that proper time is an independent degree of freedom (d.o.f). The measured visibility \mathcal{V}_m is compared with the quantum mechanical prediction \mathcal{V}_{QM} , Eq. (5.14). Assuming that the distribution of such a proper time d.o.f is a Gaussian of the width σ_τ , current interferometric experiments give bounds on σ_τ in terms of the proper time difference $\Delta\tau$ between the paths and the experimental error $\Delta\mathcal{V}$ of the visibility measurement

Experimental visibility	Possible explanation	Experimental status
$\mathcal{V}_m = 0$	Proper time: quantum d.o.f., sharply defined	Disproved in e.g. Refs. [6, 11]
$0 < \mathcal{V}_m < \mathcal{V}_{QM}$	Proper time: quantum d.o.f with uncertainty σ_τ	Consistent with current data for $\sigma_\tau > \frac{ \Delta\tau }{\sqrt{-8 \ln(1-\Delta\mathcal{V})}}$
$\mathcal{V}_m = \mathcal{V}_{QM}$	Proper time: not a quantum d.o.f. or has a very broad uncertainty	Consistent with current data
$\mathcal{V}_m > \mathcal{V}_{QM}$	Quantum complementarity does not apply when general relativity becomes relevant	Not tested

uncertainty in the state of proper time. The phase shift measured in those experiments can be phrased in terms of the difference in the proper time $\Delta\tau$ between the paths. Denote by $\Delta\mathcal{V}$ the experimental error with which the visibility of the interference pattern was measured in those tests. As a result, a Gaussian state of the proper time degree of freedom with the width σ_τ such that $\sigma_\tau > \frac{|\Delta\tau|}{\sqrt{-8 \ln(1-\Delta\mathcal{V})}}$, is consistent with the experimental data. An estimate of the proper time uncertainty can be based on the Heisenberg uncertainty principle for canonical variables and the equation of motion for the proper time. In such an analysis one assumes canonical commutation relation between mass and proper time $[\tau, mc^2] = i\hbar$ [23–25]. Table 5.2 shows what can be inferred about proper time as a quantum degree of freedom from an experiment in which the measured visibility is \mathcal{V}_m and where \mathcal{V}_{QM} is the visibility predicted by quantum mechanics as given by Eq. (5.14).

5.2 Photons as Clocks

Gravitational time dilation results in decrease of the speed of light passing near a massive object: Consider two paths with common endpoints and with the same proper lengths (locally measured lengths). If there is a difference in gravitational potential between the paths, two identical light pulses simultaneously fed each into one path will not meet at the end point—they will take different times to traverse the paths. Such an effect has been predicted and measured by Irwin I. Shapiro [26] and named the “fourth test of general relativity”. Here it is discussed how the Shapiro delay could be used in a quantum optics realisation of the “clock” interference experiment. The photon travelling in superposition along two paths in an interferometer is considered,

with each arm experiencing a different gravitational time dilation. If the difference in the time dilations is comparable with the photon's coherence time, the visibility of the quantum interference is predicted to drop, while for shorter time dilations the effect of gravity will result only in a relative phase shift between the two arms—in a full agreement with quantum complementarity, which is of course not limited to massive quantum systems. It is discussed what aspects of the interplay between quantum mechanics and general relativity are probed in such an experiment and the experimental feasibility is analysed.

5.2.1 Gravitational Time Dilation for Light—Shapiro Delay

Interferometric setup considered in this section is the same as in Fig. 5.1—i.e. with the same geometry – but with single photons used as “clocks”. In this case, the “clock” is implemented in the position degree of freedom of the photon on the path, which has an infinite dimensional Hilbert space, as opposed to the two-dimensional state space of the massive “clock” discussed in the previous section.

First, the light-like geodesics within the interferometer are discussed and the results are then applied to a single photon travelling in superposition along these paths. The interferometer is placed, vertically oriented, on the surface of the earth and the space-time is modelled by the Schwarzschild metric. For a small size of the interferometer as compared to its radial coordinate r , all points on each of the horizontal paths are approximately at the same radial distance and the vertical distance h can be adjusted whilst keeping the horizontal path length l constant. The attention can thus be restricted to horizontal propagation in the x direction and the motion can be described in a $2D$ metric of a general form

$$ds^2 = g_{00}c^2dt^2 + g_{xx}dx^2, \quad (5.16)$$

Since the trajectory in this case is light-like, i.e. $ds^2 = 0$, the velocity of light with respect to the coordinate length and time $v_c = \frac{dx}{dt}$ reads

$$v_c = c\sqrt{-\frac{g_{00}}{g_{xx}}}. \quad (5.17)$$

Note, that v_c is also the velocity of light on the considered path as measured by a far away observer⁴ (and thus the propagation of light in general relativistic space time is formally analogous to the propagation of light in a non-dispersive material with

⁴By a faraway observer is here considered an observer at a large enough radial distance from the mass, such that locally measured times and distances are arbitrary close to the coordinate time and distance—for the Schwarzschild space-time considered in this work $|g_{\mu\nu}| \rightarrow 1$ for $r \rightarrow \infty$.

index of refraction $n_{gr} = c/v_c = \sqrt{-\frac{g_{xx}}{g_{00}}}$.) The velocity v_c in isotropic coordinates $g_{00} = -\left(1 + \frac{2\Phi(r)}{c^2}\right) + \mathcal{O}(c^{-4})$ and $g_{xx} = \left(1 - \frac{2\Phi(r)}{c^2}\right) + \mathcal{O}(c^{-4})$ reads

$$v_c = c \left(1 + \frac{2\Phi(r)}{c^2}\right), \quad (5.18)$$

where only up to second order terms in general relativistic corrections to the Minkowski metric were kept. This slow down of light depending on where the light-like geodesic passes with respect to the massive object is the Shapiro delay. The Shapiro effect is of course not limited to the “horizontal” propagation of light. In any coordinates and for a general metric, the i th component of the coordinate three-velocity of light (v_c^1, v_c^2, v_c^3) is given by $v_c^i = c \sqrt{-\frac{g_{00}}{g_{ii}}}$ and thus generally differs from c

Note, however, that a local observer—using local space and time coordinates given by

$$d\tau_r^2 = g_{00}dt^2, \quad dx_r^2 = g_{xx}dx^2 \quad (5.19)$$

effectively sees the Minkowski metric $ds^2 = -c^2d\tau_r^2 + dx_r^2$ and in particular measures the speed of light to be c .

Consider now a horizontal path which has the length l as measured by a local observer, that is $l = \int \sqrt{g_{xx}}dx$. The coordinate time, as measured by a far away observer, which light takes to traverse this path is $t_r = l/v_c = \frac{l}{c\sqrt{-\frac{g_{00}}{g_{xx}}}}$. By definition of the metric:

$$t_r = \frac{l}{c\sqrt{1 + \frac{2\Phi(r)}{c^2}}}. \quad (5.20)$$

According to Eq. (5.20), the time of the photon’s flight along the horizontal path can be seen as a clock, which is subject to the gravitational time dilation as predicted by general relativity (which is the Shapiro effect). The definition of the horizontal path length as the locally measured distance corresponds to the definition of the rest frame Hamiltonian as the Hamiltonian seen by a local, rest frame observer. It will be thus considered that both arms of the interferometer measured locally have length l . (Note that this corresponds to a natural alignment procedure for the interferometer—such that the paths have equal length when the setup is horizontal, or when brought together—which is possible for a fiber-based interferometer.) Thus, depending on the radial distance r of the path from the earth, the photon will arrive at the second beam splitter in the Mach-Zehnder setup Fig. 5.1 at different coordinate times, as given by Eq. (5.20). From the symmetry of the setup the coordinate time of the photon’s flight in the radial direction is the same for both trajectories γ_i . The total difference in photon arrival times as measured by the far away observer is therefore $t_r - t_{r+h}$. For the local observer at the upper path (at the radial distance $r + h$) this time dilation is given by

$$\Delta\tau = \sqrt{1 + \frac{2\Phi(r+h)}{c^2}} (t_r - t_{r+h}) \approx \frac{lg h}{c^3}, \quad (5.21)$$

with $g = \frac{GM}{r^2}$. The approximation in Eq. (5.21) is valid for a small size of the interferometer, i.e. $h \ll r$, and when second order terms in the potential can be neglected. (Moreover, the result is independent of the specific coordinates used in the derivation).

5.2.2 Gaussian Photon Wave-Packet as a Clock

To probe quantum mechanics in the presence of time dilation, consider the above effect on a single photon following in superposition along the paths γ_1, γ_2 . The state of a photon moving in the $+x$ direction at the radial distance r in the space-time given by the metric (5.16) in terms of local coordinates τ_r and x_r , Eq. (5.19) can be written as [27]

$$|1\rangle_f = a_f^\dagger |0\rangle = \int d\nu f(\nu) e^{i\frac{\nu}{c}(x_r - c\tau_r)} a_\nu^\dagger |0\rangle, \quad (5.22)$$

where $f(\nu)$ is the mode function with ν the angular frequency defined with respect to a local observer at radial distance r and a_ν^\dagger —a single frequency bosonic creation operator. According to Eq. (5.21) the wave packet moves along each of the trajectories with a different group velocity with respect to a fixed observer. Therefore, the superposition states reaching the two detectors D_\pm take the form

$$|1\rangle_{f\pm} \propto \int d\nu f(\nu) \left(e^{i\frac{\nu}{c}(x_r - c\tau_r)} \pm e^{i\frac{\nu}{c}(x_r - c(\tau_r + \Delta\tau))} \right) a_\nu^\dagger |0\rangle,$$

with $\Delta\tau$ as given by Eq. (5.21). The probabilities of detecting the particle in D_\pm read (see Appendix B.1 for a supplementary calculation)

$$P_{f\pm} = \frac{1}{2} \left(1 \pm \int d\nu |f(\nu)|^2 \cos(\nu \Delta\tau) \right). \quad (5.23)$$

The mode function is normalised such that $\int d\nu |f(\nu)|^2 = 1$. Two limits of this expression can be identified, which in turn correspond to tests of two different physical effects:

- (i) For $\Delta\tau$ small with respect to the frequency-width of the mode function $f(\nu)$ the cosine term will be approximately constant over the relevant range of ν and so can be taken outside the integral giving a phase shift term $\cos(\nu_0 \Delta\tau)$, (where ν_0 denotes central frequency of the mode function) and the visibility remains maximal. Note that such a phase shift can be explained as arising from the coupling of the average energy of the photon to the Newtonian gravitational potential in the

Euclidean space-time, where the time is absolute and no time dilation occurs— analogously to the case of a massive particle. The gravitational phase shift for a photon is also of the same form as the phase shift for a massive particle, Eq. (5.15), with the photon’s energy (divided by c^2) substituting the particle’s mass. Observation of such a phase shift for photons—a photonic version of the COW experiment—would be a test of the mass-energy equivalence and the resulting coupling to gravity, one of the conceptual pillars of general relativity. Although the measurement of a gravitational phase shift cannot be considered as a test of the time dilation, its observation with a single photon differs from a corresponding test for a massive particle because in the Newtonian limit of gravity no effect on a massless particle would be expected (see also Fig. 5.5). In this sense in such an experiment both quantum and general relativistic effects could simultaneously be tested. Furthermore, probing such an effect seems feasible with current technology.⁵

- (ii) In the other limit, when the time dilation dominates over the photon width, the oscillatory cosine term averages out the whole integrand, resulting in no interference. More precisely, the amplitude of the phase shift term is given by the overlap between the modes associated with the two paths. For $\Delta\tau$ much larger than the coherence time of the photon wave packet (the pulse width) the interferometric visibility is lost as the two modes arrive at the second beam splitter at distinctly different times. Note that the slow-down of light is a direct consequence of the gravitational time dilation, and is absent in the non-metric Newtonian theory (see Sect. 5.2.4 and Appendix C.1 for further discussion). The drop in the interferometric visibility is therefore probing a regime beyond the Newtonian limit. In this parameter regime the experiment directly tests the gravitational time dilation for superpositions of single photons.

The two limits can be clearly seen when considering the specific case of a gaussian wave packet $f_{\sigma}^{\nu_0}(\nu) = (\frac{\sigma}{\pi})^{1/4} \exp[-\frac{\sigma}{2}(\nu - \nu_0)^2]$:

$$P_{f_{\sigma}^{\nu_0} \pm} = \frac{1}{2} \left(1 \pm e^{-(\Delta\tau/2\sqrt{\sigma})^2} \cos(\nu_0 \Delta\tau) \right). \quad (5.24)$$

The width σ of the gaussian mode function gives the precision t_{\perp} of the photon-clock. In particular, defining as distinguishable the wave packets whose overlap is not larger than e^{-1} , for the gaussian packets one finds $t_{\perp} = 2\sqrt{\sigma}$, and the visibility of the interference in Eq. (5.24) reads

$$\mathcal{V} = e^{-\left(\frac{\Delta\tau}{t_{\perp}}\right)^2}. \quad (5.25)$$

The clock implemented in the position degree of freedom of a photon is analogous to the clock implemented in an internal degree of freedom of a massive particle,

⁵Proposal to probe gravitationally induced phase shift of classical light in a laboratory experiment was first formulated in Ref. [28], but has not yet been realised.

Eq. (5.12). The interferometric visibility depends on the ratio of the time dilation to the precision of the used clock⁶ which for photon is given by the width of the frequency distribution, whereas the phase shift depends on the average energy of the clock, which is the mean frequency for the case of a photon. (The specific form of the visibility function can be traced back to the fact, that the clock is here given by a gaussian wave packet, which is not periodic.)

5.2.3 Quantitative Predictions

For a single photon in superposition, a full loss of the visibility can be obtained in a sufficiently large interferometer, such that $\Delta\tau > t_\perp$. Assuming the gravitational field to be homogeneous the corresponding area of the interferometer obtained from the Eq. (5.21) reads

$$A_\perp \approx t_\perp \frac{c^3}{g}. \quad (5.26)$$

For a clock of the same frequency but moving at a subluminal velocity v , the corresponding area of the interferometer necessary to observe the loss of the interferometric visibility is by v/c smaller than the area needed for the clock moving at velocity c . Thus, the size of the interferometer necessary for realizing the proposed experiment with the clock implemented in a photon is orders of magnitude larger than the setup needed for a massive clock. However, such an implementation can still be a feasible route for the observation of time dilation in a quantum system as an implementation with photons may provide some advantages. For example, the control over the exact length and separation between the interferometric paths would be easier with a photon clock since it could be confined in an optical fiber. Moreover, experiments were already performed confirming the high-fidelity transmission of polarization-encoded qubits from entangled photon pair sources over 100 km in a fiber [29]. For the preparation of a clock with a fixed precision one needs to control only the width of the photon's wave packet. The preparation of light pulses with duration on the order of 10 fs has already been achieved [30] and recent rapid progress in the preparation of attosecond optical pulses may provide a feasible route to such high-precision clocks [31, 32]. Finally, using slow light materials (e.g. with a suitable frequency dependent index of refraction) may allow reducing the necessary size of the interferometer.

The experimental parameters necessary to measure the gravitational phase shift for single photons are much less demanding than those required for full orthogonalization—see Table 5.3 for a comparison of the experimental parameters necessary to observe those effects and Fig. 5.3 for a plot of the detection probability P_- , Eq. (5.24), as a function of the interferometer's area. For a photon with a central frequency ν_0 , the

⁶Defining two wave packets to be distinguishable when the absolute value of the amplitude between them is $1/n$ yields $\mathcal{V}_n = n^{-(\Delta\tau/t_{n\perp})^2}$ where $t_{n\perp} = 2 \log(n) \sqrt{\sigma}$ is the corresponding clock's precision.

Table 5.3 The size of the interferometer necessary to observe a loss of visibility due to the gravitational time dilation and to observe the gravitational phase shift. For the realization of the clock in the position degree of freedom of a photon the precision is given by the coherence time of the photon’s wave packet. For the clock implemented in the internal degree of freedom of a massive particle—by the orthogonalization time (the shortest time after which the final state becomes orthogonal to the initial one). In both cases only the average internal energy of the system is relevant for the observation of the gravitational phase shift

Time dilation	System	Clock	t_{\perp} (s)	A_{\perp} (km ²)
	Photon	Position	10^{-15}	10^3
	Atom	Hyperfine states	10^{-15}	10^{-7}
Phase shift	Photon frequency (Hz)			A_{ps} (km ²)
	10^{15}			10^{-3}

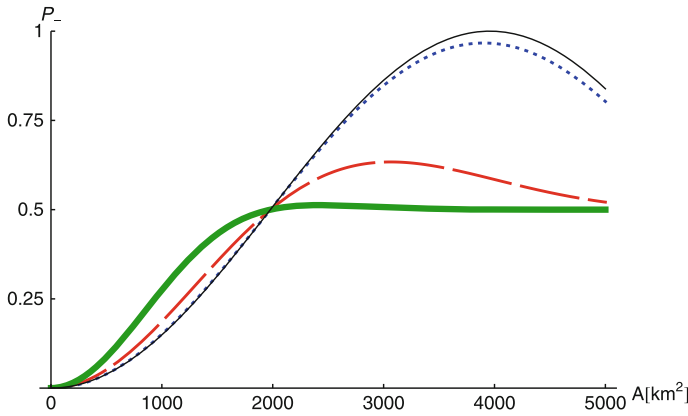


Fig. 5.3 Probing the general relativistic slowdown of light in the proposed single photon interference experiment. The probabilities $P_{f\nu_0-}$ (Eq. (5.24)) to find the photon in the detector D_- are shown as a function of the area A (km²) of the interferometer in the *vertical* plane. The single-photon pulse has mean angular frequency $\nu_0 \approx 4 \times 10^{15}$ Hz. The four graphs correspond to different widths σ of the wave packet and thus to different coherence times $t_{\perp} = 2\sqrt{\sigma}$: $t_{\perp} = 0.05$ fs (thick green line), $t_{\perp} = 1$ fs (red dashed line), $t_{\perp} = 5$ fs (blue dotted line) and $t_{\perp} = \infty$ fs (thin black line), which is a limiting case of an infinitely long pulse (and thus with the clock effectively switched off). Observing a gravitational phase shift of a photon is within reach of current experimental capabilities

gravitational phase shift in the considered interferometer is $\Delta\Phi \approx \nu_0 \frac{lg\hbar}{c^3}$. For the angular frequency $\nu_0 = 10^{15}$ Hz, and the time dilation as above ($\Delta\tau = 10^{-15}$ s) the phase shift is of order of one radian. Since phase shifts that are at least six orders of magnitude smaller can be experimentally resolved [33], the area enclosed by the interferometer that would suffice to result in the measurable phase shift effect is correspondingly smaller: $A_{ps} = 10^3$ m². Such a size is feasible with current technology. One could also introduce some improvements to the proposed realisation of the experiment. For example, by using multi-photon states or different interfer-

ence schemes [34, 35] not only would it be possible to enhance the precision of the measured phase but, by observing an interference with no classical analogue, the interpretation of the experiment as testing the mass-energy equivalence in conjunction with quantum mechanics would be unambiguous.

5.2.4 Discussion

In the absence of relativistic effects, clocks run at the same rate independently of their position with respect to a gravitational field. In the experiment where the clock is implemented in the position of the photon in the direction parallel to the earth's surface, since the gravitational field is constant in that direction, Newtonian gravity would not provide any measurable effect on the time evolution of the “clock”, i.e. on the displacement of the photon. A difference in the arrival time for the two superposed wave packets of the photon is inconsistent with such a non-relativistic model and can therefore be considered as a genuine general-relativistic effect. Since in the above proposal the difference in the arrival time is measured by the drop in the interferometric visibility, the experiment needs to be able to discriminate between this effect and other sources of decoherence, which could also lead to the loss of interference. This can be done by rotating the interferometer from a vertical to a horizontal position, which should lead to a corresponding recovery of the interference; a correlation between the rotation angle and the visibility would imply that gravity is responsible for the effect. Another possibility is to use wave packets with a modulated profile in the time domain (e.g. with a double or multiple peak): by increasing the time delay the visibility should be partially recovered, as the two superposed wave packets start overlapping again. Since a revival of visibility cannot be attributed to decoherence, this possibility would be ruled out by the experiment.

The proposed quantum optics experiment may also allow testing some non-standard theories of quantum fields [36] in curved background. Some of these alternative models predict a difference in the time evolution of entangled states in the presence of gravitational potential as compared to predictions of standard quantum field theory in the same space-time (for the Minkowski space-time, such models reduce to the standard quantum field theory). For example, the model proposed in Ref. [36] predicts a decorrelation of entangled photons, which can have a measurable effect on the expected visibility in our setup.

In order to qualify as a genuine test of quantum mechanics, the results of the experiment should be incompatible with a classical model of light. It is not sufficient that an arbitrary part of the experiment shows some quantum property (in fact, quantum mechanics is necessary to explain the atomic transitions of the clocks used in already performed tests of GR). What should be stressed is that the experiments performed so far are still compatible with models where classical, localised degrees of freedom “keep track of time” (see also Appendix C.1). Accessing the “quantum domain” means showing experimentally that the degree of freedom keeping track of time was in a genuine quantum superposition, with each part of the superposition

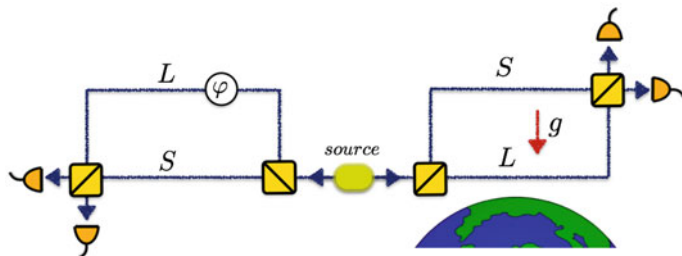


Fig. 5.4 A Franson-type interferometer modified to test a local realistic description of photons undergoing gravitational time dilation. It consists of a source of photon pairs and two Mach-Zehnder setups with arms of different optical lengths S , L . On the *right-hand side* this difference is due to the general relativistic time dilation. This can be realized by utilizing a Mach-Zehnder setup as in Fig. 5.1, where the two paths of equal length are at different gravitational potentials, so that there will be a time dilation $\Delta\tau$ between them. The Mach Zehnder interferometer on the *left-hand side* is placed such that both arms are at the same gravitational potential and the difference in their lengths is $L - S = c\Delta\tau$. In each of the interferometers a controllable phase shift φ_1 , φ_2 is induced in the optically longer arm. By varying those phases it is possible to violate Bell’s inequalities on a subsample of coincident photons

evolving at a different rate due to GR. In the case of photons an analogous interference with a modulation in the visibility could also be observed in the intensity of classical electromagnetic wave packets following the paths of the interferometer. However, within such a picture the phase at each point of the electromagnetic wave is a classical degree of freedom that keeps track of time. An interference experiment in which a single photon source is utilised and single photons are detected is incompatible with this picture and thus would rule out an explanation of the experiment in terms of classical electromagnetic waves. The observation of quantum interference also rules out the model of photons as classical particles. As already noted, in the current proposal the signature of the general-relativistic time dilation is *the loss* of interference. Implementation of an additional, controllable delay in the upper arm compensating the general relativistic time dilation would result in a recovery of the interference, which would prove the quantum nature of the photons affected by general-relativistic time dilation.

Disproving local-realistic description of the experiment The experimental scheme discussed so far can rule out models where light is described by classical electromagnetic waves or by classical particles evolving on a curved space-time.⁷ However, as any single photon experiment, it can still be described with a local realistic model.

In order to rule out all local realistic models of photons in a curved background, a modified version of the experiment can be used. The idea is to use a Franson-type interferometer [37], where the difference in the optical length between the two arms on one side of the interferometer is produced by the general relativistic time dilation (see Fig. 5.4).

⁷Note, that classical models of light have already been extensively disproved experimentally, but only in regimes where no effect of GR is present.

In this version of the experiment, pairs of time-correlated photons are emitted by a source and fed into two separated Mach-Zehnder interferometers. The right-hand side interferometer has arms of equal length and is positioned vertically with respect to the surface of the earth, thus the arrival time of the lower arm is delayed by an amount $\Delta\tau$, as given by Eq. (5.21). The left-hand side interferometer is horizontal, thus insensitive to gravity, but the two arms differ in their optical lengths by an amount $\Delta l = c\Delta\tau$; in this way both interferometers effectively consist of a shorter and a longer arm, labelled by L and S respectively, which pairwise have the same optical length. Two additional, controllable phases, φ_1 and φ_2 , are added to the longer arms of the right and left interferometer, respectively. The emission time of the two photons is correlated (to within their coherence time), but the specific emission time is unknown. For the coherence time of photons shorter than the time delay $\Delta\tau$, coincident photons will have the same time of flight. As a result, the state of the post-selected fraction of coincident photons (just before the second beam splitter) is entangled:

$$|\psi\rangle = \frac{1}{\sqrt{2}} (e^{i(\varphi_1+\varphi_2)} |L\rangle_1 |L\rangle_2 + |S\rangle_1 |S\rangle_2). \quad (5.27)$$

By varying the phases φ_1 and φ_2 , it is possible to violate Bell's inequalities (even when taking into account the post-selection procedure [38]). Thus, the scheme can provide a conclusive refutation of any model in which photons are described by local-realistic variables. At the same time, the violation of the inequalities is only possible if a photon travelling in the lower arm of the right-hand side interferometer is delayed by a time $\Delta\tau = \Delta l/c$. Since Δl (the length difference in the left arm) can be controlled independently, it can be used to measure the time dilation on the right-hand side and verify the prediction of general relativity.

5.3 General Relativistic and Quantum Aspects of the Proposals

The aim of the proposed experiments is to access a physical regime where the effects stemming from both quantum mechanics and general relativity (GR) cannot be neglected. To this end, experimental results should simultaneously falsify a model of quantum fields or particles evolving in a Newtonian potential *and* a model of classical fields or particles in curved space-time (see Fig. 5.5). Below it is analysed in which sense and how this can be achieved.

The effect of gravity can also be detected by observing a shift in the relative phase between the superposed amplitudes travelling along the two arms, in both massive, Sect. 5.1.2, and massless, Sect. 5.2.2, case. The observation of the phase shift alone could not be directly interpreted as a test of the time dilation, since it can be understood in terms of a coupling between the mass and a potential in a flat space-time, which would yield the same phase shift *without* the time dilation. There is a formal analogy between a massive particle in the Newtonian limit of

gravity and a charged particle in a Coulomb electrostatic potential. In the latter, the notion of proper time unquestionably never enters, which suggests that only those gravitational effects which have no electrostatic analogues can be seen as genuinely general relativistic, in the present interferometric context. The gravitational phase shift effect does have an electrostatic analogue experimentally verified with electrons in a Coulomb potential, see e.g. [13]. Thus measurements of the gravitational phase—such alone, such as those of Refs. [6, 11], do not contradict non-metric, Newtonian gravity and cannot be seen as tests of general relativity. The interaction of *photons* with the Newton potential, however, requires an additional ingredient: it is necessary to assign an effective gravitational mass to the photon, whereas massless particles, or electromagnetic waves, do not interact with gravity in the non-relativistic mechanics. Such an interaction is a direct consequence of the mass-energy equivalence.

More precisely, the interaction necessary to obtain the gravitational phase shift follows from postulating the equivalence between the system’s mass and its average total energy, i.e. that internal energy contributes to the system’s rest mass: $mc^2 \rightarrow mc^2 + \langle \hat{H}_s \rangle$, where \hat{H}_s is the non-gravitational Hamiltonian of the system. This yields a gravitational energy term

$$\hat{H}_{phase} = \langle \hat{H}_s \rangle \frac{V(\hat{r})}{c^2}, \quad (5.28)$$

which reduces to the Newtonian gravitational potential energy, $mV(\hat{r})$, in the non-relativistic limit. In this sense, observation of a gravitationally induced phase shift for a photon ($m = 0$) can already be considered as a test of general relativity. In particular, it probes a *semi-classical* version of the mass-energy equivalence, which endows photons with an effective gravitational mass *parameter*⁸: $\frac{\langle \hat{H}_s \rangle}{c^2} = \frac{\hbar\nu}{c^2}$.

The interaction (5.28) results in a relative phase between the amplitudes of a wave function at different gravitational potentials, but it predicts no drop in the interferometric visibility (see Appendix C.1). The latter effect is only present if the total Hamiltonian includes a direct coupling between the energy operator and the potential, a term of the form

$$\hat{H}_{vis} = \hat{H}_s \frac{V(\hat{r})}{c^2}. \quad (5.29)$$

Such a term follows from postulating the equivalence between mass and the energy *operator* $mc^2 \rightarrow mc^2 + \hat{H}_s$, which can be seen as a full *quantum* implementation of the mass-energy equivalence.

⁸Note that the Pound-Rebka experiment [39] probed the same aspect of GR: the redshift can be explained as each photon having a gravitational potential energy of ghE/c^2 , with $E = \hbar\nu$. The redshift is then a consequence of the (semi-classical) mass-energy equivalence and energy conservation. However, the quantum nature of the photons was not probed directly in the Pound-Rebka experiment, which is thus still consistent with a classical description of light (more precisely, the experiment is consistent with classical waves on a curved background *or* with classical particles in a Newtonian potential, see Fig. 5.5 and Chap. 1). Measuring the gravitational phase shift in single photon interference would allow probing this aspect of GR in a quantum regime. In simple terms, it would provide a quantum extension of the Pound-Rebka experiment in the same way as the COW experiment [6] was a quantum extension of Galilei’s free fall experiments.

		gravity		
		non-metric, Newtonian	non-metric, Newtonian + semi-classical mass-energy equivalence	general relativity (time dilation)
mechanics	classical	wave	<i>well-tested</i>	<i>Pound-Rebka [20], Shapiro delay [21-22]</i>
		particle	<i>well-tested</i>	<i>Pound-Rebka [20]</i> <i>Shapiro delay [21-22]</i>
	quantum	<i>phase-shift of a matter wave [14-17]</i> <i>(probes: $mV(\hat{r})$)</i>	<i>phase-shift of a single photon</i> <i>[not yet tested]</i> <i>(probes: $\langle \hat{H}_s \rangle \frac{V(\hat{r})}{c^2}$)</i>	<i>quantum interference of clocks</i> <i>[not yet tested]</i> <i>(probes: $\hat{H}_s \frac{V(\hat{r})}{c^2}$)</i>

Fig. 5.5 Summary of the key interpretational aspects of the proposed here—and of the already performed—experiments. In order to test the overlap between quantum mechanics and general relativity, the observed effect cannot be compatible with classical mechanics nor with the Newtonian limit of gravity. An experiment in a given entry of the table (and the indicated coupling) are compatible with both theories that label the entry’s row and column. The coupling of the gravitational potential $V(\hat{r})$ to: mass m , average energy $\langle H_s \rangle$, and the energy operator \hat{H}_s can be interpreted as testing the gravitational coupling due to: Newton gravity, the semi-classical extension of the mass-energy equivalence, and the full quantum extension of the latter, respectively. Some of the experiments have more than one possible interpretation, and thus fit in several different slots of the table. In contrast, the clock interferometry experiment can only be placed in the slot of the table at the intersection of general relativity and quantum mechanics. Its successful realisation would thus probe general relativity and quantum mechanics in a hitherto untested regime

In fact, not only phase-shift tests but all current observations are in agreement with effective theories, in which gravitational interactions of quantum particles do not include \hat{H}_{vis} : Appendix C.1 shows a toy model that does not include \hat{H}_{vis} and which correctly predicts *so far tested* general relativistic effects in the classical limit and quantum effects in the Newtonian limit. Physical motivation to introduce—and test—the distinction between couplings (5.28) and (5.29) is to answer the question: How does the mass-energy equivalence extend to quantum mechanics, in particular, how does it apply to superpositions of different energy eigenstates?

References

1. A. Peters, K.Y. Chung, S. Chu, High-precision gravity measurements using atom interferometry. *Metrologia* **38**, 25 (2001)

2. N. Margolus, L.B. Levitin, The maximum speed of dynamical evolution. *Phys. D: Nonlinear Phenom.* **120**, 188–195 (1998). Proceedings of the Fourth Workshop on Physics and Consumption

3. P. Kosiński, M. Zych, Elementary proof of the bound on the speed of quantum evolution. *Phys. Rev. A* **73**, 024303 (2006)

4. B. Ziałyński, M. Zych, Generalization of the Margolus-Levitin bound. *Phys. Rev. A* **74**, 034301 (2006)

5. S. Wajima, M. Kasai, T. Futamase, Post-Newtonian effects of gravity on quantum interferometry. *Phys. Rev. D* **55**, 1964 (1997)
6. R. Colella, A. Overhauser, S. Werner, Observation of gravitationally induced quantum interference. *Phys. Rev. Lett.* **34**, 1472–1474 (1975)
7. Y. Aharonov, D. Bohm, Significance of electromagnetic potentials in the quantum theory. *Phys. Rev.* **115**, 485–491 (1959)
8. V.B. Ho, M.J. Morgan, An experiment to test the gravitational Aharonov-Bohm effect. *Aust. J. Phys.* **47**, 245–252
9. C.M. Will, *Theory and Experiment in Gravitational Physics* (Cambridge University Press, 1993)
10. M. Zawisky, M. Baron, R. Loidl, H. Rauch, Testing the world’s largest monolithic perfect crystal neutron interferometer. *Nucl. Instrum. Meth. Phys. Res., Sect. A* **481**, 406–413 (2002)
11. A. Peters, K.Y. Chung, S. Chu, Measurement of gravitational acceleration by dropping atoms. *Nature* **400**, 849–852 (1999)
12. H. Müller, S.-W. Chiow, S. Herrmann, S. Chu, Atom interferometers with scalable enclosed area. *Phys. Rev. Lett.* **102**, 240403 (2009)
13. I. Neder, M. Heiblum, D. Mahalu, V. Umansky, Entanglement, dephasing, and phase recovery via cross-correlation measurements of electrons. *Phys. Rev. Lett.* **98**, 036803 (2007)
14. Y. Ji, Y. Chung, D. Sprinzak, M. Heiblum, D. Mahalu, H. Shtrikman, An electronic Mach-Zehnder interferometer. *Nature* **422**, 415–418 (2003)
15. M. Arndt, O. Nairz, J. Vos-Andreae, C. Keller, G. Van der Zouw, A. Zeilinger, Wave-particle duality of C60 molecules. *Nature* **401**, 680–682 (1999)
16. S. Gerlich, S. Eibenberger, M. Tomandl, S. Nimmrichter, K. Hornberger, P.J. Fagan, J. Tüxen, M. Mayor, M. Arndt, Quantum interference of large organic molecules. *Nat. Commun.* **2**, 263 (2011)
17. J.R. Miller, The NHMFL 45-T hybrid magnet system: past, present, and future. *IEEE Trans. Appl. Supercond.* **13**, 1385–1390 (2003)
18. T. Kovachy, P. Asenbaum, C. Overstreet, C. Donnelly, S. Dickerson, A. Sugarbaker, J. Hogan, M. Kasevich, Quantum superposition at the half-metre scale. *Nature* **528**, 530–533 (2015)
19. H. Müller, A. Peters, S. Chu, A precision measurement of the gravitational redshift by the interference of matter waves. *Nature* **463**, 926–929 (2010)
20. S. Dimopoulos, P.W. Graham, J.M. Hogan, M.A. Kasevich, General relativistic effects in atom interferometry. *Phys. Rev. D* **78**, 042003 (2008)
21. S. Fray, C.A. Diez, T.W. Hänsch, M. Weitz, Atomic interferometer with amplitude gratings of light and its applications to atom based tests of the equivalence principle. *Phys. Rev. Lett.* **93**, 240404 (2004)
22. H. Müller, S.-W. Chiow, S. Herrmann, S. Chu, K.-Y. Chung, Atom-interferometry tests of the isotropy of post-Newtonian gravity. *Phys. Rev. Lett.* **100**, 031101 (2008)
23. D.M. Greenberger, Theory of particles with variable mass. I. Formalism. *J. Math. Phys.* **11**, 2329–2340 (1970)
24. D.M. Greenberger, Theory of particles with variable mass. II. Some physical consequences. *J. Math. Phys.* **11**, 2341–2347 (1970)
25. S. Kudaka, S. Matsumoto, Uncertainty principle for proper time and mass. *J. Math. Phys.* **40**, 1237–1245 (1999)
26. I.I. Shapiro, Fourth test of general relativity. *Phys. Rev. Lett.* **13**, 789–791 (1964)
27. N.D. Birrell, P.C.W. Davies, *Quantum Fields in Curved Space*, no. 7 (Cambridge university press, 1984)
28. K. Tanaka, How to detect the gravitationally induced phase shift of electromagnetic waves by optical-fiber interferometry. *Phys. Rev. Lett.* **51**, 378 (1983)
29. H. Hřřbel, M. R. Vanner, T. Lederer, B. Blauensteiner, T. Lorřřnser, A. Poppe, A. Zeilinger, High-fidelity transmission of polarization encoded qubits from an entangled source over 100 km of fiber. *Opt. Express* **15**, 7853–7862 (2007)
30. P.J. Mosley, J.S. Lundeen, B.J. Smith, P. Wasylczyk, A.B. U’Ren, C. Silberhorn, I.A. Walmsley, Herald generation of ultrafast single photons in pure quantum states. *Phys. Rev. Lett.* **100**, 133601 (2008)

31. G. Sansone, L. Poletto, M. Nisoli, High-energy attosecond light sources. *Nat. Photonics* **5**, 655–663 (2011)
32. L. Gallmann, C. Cirelli, U. Keller, Attosecond science: recent highlights and future trends. *Ann. Rev. Phys. Chem.* **63**, 447–469 (2012)
33. N. Matsuda, R. Shimizu, Y. Mitsumori, H. Kosaka, K. Edamatsu, Observation of optical-fibre Kerr nonlinearity at the single-photon level. *Nat. Photonics* **3**, 95–98 (2009)
34. G.-Y. Xiang, B.L. Higgins, D. Berry, H.M. Wiseman, G. Pryde, Entanglement-enhanced measurement of a completely unknown optical phase. *Nat. Photonics* **5**, 43–47 (2011)
35. R. Ghosh, C. Hong, Z. Ou, L. Mandel, Interference of two photons in parametric down conversion. *Phys. Rev. A* **34**, 3962 (1986)
36. T. Ralph, G. Milburn, T. Downes, Quantum connectivity of space-time and gravitationally induced decorrelation of entanglement. *Phys. Rev. A* **79**, 022121 (2009)
37. J. Franson, Bell inequality for position and time. *Phys. Rev. Lett.* **62**, 2205 (1989)
38. S. Aerts, P. Kwiat, J.-A. Larsson, M. Zukowski, Two-photon Franson-type experiments and local realism. *Phys. Rev. Lett.* **83**, 2872 (1999)
39. R. Pound, G. Rebka, Apparent weight of photons. *Phys. Rev. Lett.* **4**, 337–341 (1960)

Chapter 6

Decoherence from Time Dilation

This chapter generalises the discussion of time dilation effects on “clocks”—quantum systems whose internal states are pure and time evolving (Chap. 5)—to systems in an arbitrary internal state. The coupling terms in the relativistic Hamiltonian of a composite system, which are tantamount to time dilation, result in entanglement between external and internal degrees of freedom. This entanglement causes loss of coherence of the centre of mass of a generic system with internal degrees of freedom, not only of the specific pure “clock” states. This chapter derives the general formula for the visibility and discussed in what sense the fully unitary evolution of the system nevertheless results in an effective decoherence mechanism.

6.1 Visibility for General Internal States

Consider again a massive particle with internal degrees of freedom described by the Hamiltonian H_{Lab} , Eq. (3.2). The centre of mass degrees of freedom are assumed to evolve in superposition along predefined paths γ_i , $i = 1, 2$. At time $t = 0$ the state of the centre of mass reads $|\psi_{cm}(0)\rangle = \frac{1}{\sqrt{2}}(|\gamma_1(0)\rangle + |\gamma_2(0)\rangle)$, but the internal degrees of freedom are considered to be in a general mixed state $\rho_{int}(0)$. An initial state of the joint system is taken to be a product

$$\rho(0) = \rho_{cm}(0) \otimes \rho_{int}(0) \quad (6.1)$$

with $\rho_{cm}(0) = |\psi_{cm}(0)\rangle\langle\psi_{cm}(0)|$. After time t the systems evolves into $\rho(t) = e^{-\frac{i}{\hbar} \int H_{Lab} dt} \rho(0) e^{\frac{i}{\hbar} \int H_{Lab} dt}$, which explicitly reads

This chapter builds upon and Sects. 6.3, 6.4 contain material from *Universal decoherence due to gravitational time dilation*, I. Pikovski, M. Zych, F. Costa, and Č. Brukner, *Nat. Phys.* **8**, 668–672 (2015).

$$\begin{aligned} \rho(t) = & \frac{1}{2} |\gamma_1(t)\rangle \langle \gamma_1(t)| \otimes \rho_{int, \gamma_1}(t) + \frac{1}{2} |\gamma_2(t)\rangle \langle \gamma_2(t)| \otimes \rho_{int, \gamma_2}(t) \\ & + \frac{1}{2} \{ |\gamma_2(t)\rangle \langle \gamma_1(t)| \otimes e^{-\frac{i}{\hbar} \int_{\gamma_2} H_{int} d\tau} \rho_{int}(0) e^{\frac{i}{\hbar} \int_{\gamma_1} H_{int} d\tau} + h.c. \}, \end{aligned} \quad (6.2)$$

where $\rho_{int, \gamma_i}(t) := e^{-\frac{i}{\hbar} \int_{\gamma_i} H_{int} d\tau} \rho_{int}(0) e^{\frac{i}{\hbar} \int_{\gamma_i} H_{int} d\tau}$ and the Eq. (5.5) has been used to write down the time evolution of the internal states with respect to the proper time τ along the centre of mass path γ_i . Due to the coupling between internal and external degrees of freedom, which is tantamount to the time dilation and creates entanglement between internal and external degrees of freedom, the joint state in general does not remain factorisable. The magnitude of the off-diagonal elements $\langle \gamma_2(t) | \rho(t) | \gamma_1(t) \rangle$ quantifies the coherence of the centre of mass superposition. In particular, $\mathcal{V}(t) = |\langle \gamma_2 | \text{Tr}_{int} \{ \rho(t) \} | \gamma_1 \rangle|$ where the trace is performed over the internal degrees of freedom, is the visibility of the interference fringes in any interference experiment where the external amplitudes γ_i are coherently superposed and the output modes are detected, see Sect. 4.1. For the state in Eq. (6.2) the visibility explicitly reads

$$\mathcal{V} = \left| \langle e^{-\frac{i}{\hbar} H_{int} \Delta\tau} \rangle \right|, \quad (6.3)$$

(with $\langle O \rangle \equiv \text{Tr}_{int} \{ O \rho_{int} \}$), which is generalisation of the result for pure states in Eq. (5.8). The above result is valid for any internal state ρ and quantifies coherence between external modes that followed in superposition arbitrary paths with the total proper time difference $\Delta\tau$. Note, that the only internal states which do not lead to the loss of coherence of the centre of mass degree of freedom are the exact eigenstates of the internal Hamiltonian. The effect is therefore as universal as the time dilation itself—all composite quantum systems are affected, independently of the nature and kind of their internal energy, unless all the internal degrees of freedom are frozen out. Decoherence caused by the time dilation comes from a unitary dynamics and is in principle always reversible. However, in order to avoid this effect experimentally one must ascertain that the chosen paths have vanishing proper time difference or that all internal degrees of freedom are prepared in eigenstate of the internal Hamiltonian.

Equation (6.3) can be equivalently written in the form

$$\mathcal{V} = \left| \sum_{n=0}^{\infty} \left(\frac{-i \Delta\tau}{\hbar} \right)^n \langle H_{int}^n \rangle \right|$$

and thus the decoherence effect is fully described by the moments of the internal energy distribution, $\langle H_{int}^n \rangle$, and the time dilation $\Delta\tau$ between the centre of mass amplitudes. Keeping only up to second moments gives the lowest order approximation to the visibility

$$\mathcal{V} \approx \left| 1 - \frac{i \Delta\tau}{\hbar} \langle H_{int} \rangle - \frac{1}{2} \left(\frac{\Delta\tau}{\hbar} \right)^2 \langle H_{int}^2 \rangle \right| = \sqrt{1 - \left(\frac{\Delta\tau \Delta H_{int}}{\hbar} \right)^2}, \quad (6.4)$$

where $\Delta H_{int} = \sqrt{\langle H_{int}^2 \rangle - \langle H_{int} \rangle^2}$ is the internal energy variance. This approximation is valid for $\Delta\tau\Delta H_{int}/\hbar \ll 1$, in particular, expanded to lowest order in this parameter

$$\mathcal{V} \approx 1 - \frac{1}{2} \left(\frac{\Delta\tau\Delta H_{int}}{\hbar} \right)^2,$$

which agrees with the corresponding limit of the expression Eq. (5.12) obtained for a particular pure state of a two-level system. Moreover, the orthogonalisation time t_\perp of any state is universally bounded by its energy variance ΔH_{rest} : $t_\perp \geq \frac{\pi\hbar}{2\Delta H_{rest}}$ [1–4] or, more generally, by higher moments of the energy distribution [5]:

$$\frac{1}{t_\perp} \leq \frac{2^{\frac{1}{n}}}{\pi\hbar} \langle (H_{rest} - E_0)^n \rangle^{\frac{1}{n}}, \quad n > 0, \quad (6.5)$$

where E_0 is the lowest eigenvalue of H_{rest} . This expression is valid also for mixed states, provided the state belongs to the domain of $(H_{rest} - E_0)^n$. Thus, for an estimation of the decoherence effect the relevant quantities are the time dilation between external amplitudes and internal energy distribution. For time evolving states, the moments of the internal energy distribution give the rate of the states' evolution and the effect can be interpreted in terms of time dilation of quantum “clocks”. For stationary mixed states (such as any thermal state) the decoherence in general occurs as well (they have non-vanishing ΔH_{rest} , unless H_{rest} is fully degenerate), however, such states cannot be directly interpreted as clocks. For mixed states the decoherence effect has two equivalent interpretations: in terms of time dilation of internal dynamics or in terms of redshift of internal energy values. The latter interpretation arises when the state is expressed as a mixture of energy eigenstates. The former—when the mixture is expressed in a basis constructed from superpositions of internal energy eigenstates, which are time evolving. See Appendix D.1 for further discussion.

6.2 Visibility and Decoherence Time for Thermal States

Consider a system with N internal modes described by the Hamiltonians h_i , i.e. $H_{int} = \sum_i h_i$. If each of the modes is in a thermal state at temperature T the joint state is

$$\rho_T = \Pi_{i=1}^N \rho_i = \Pi_{i=1}^N \frac{e^{-\beta h_i}}{\mathcal{Z}_i(\beta)}, \quad (6.6)$$

where $\beta = 1/k_B T$, k_B is the Boltzmann constant and the partition functions read

$$\mathcal{Z}_i(\beta) = \text{Tr}_i \{ e^{-\beta h_i} \}, \quad (6.7)$$

where Tr_i denotes that trace is performed over the i th mode. Substituting ρ_T into the visibility formula, Eq. (6.3), one finds $\mathcal{V} = \prod_{i=1}^N \left| \frac{\text{Tr}_i \left\{ e^{-(\beta + \frac{i\Delta\tau}{\hbar})h_i} \right\}}{\mathcal{Z}_i(\beta)} \right|$. Note, that the visibility can formally be expressed through partition functions of thermal states at a complex temperature $\beta + i\Delta\tau/\hbar$:

$$\mathcal{V} = \prod_{i=1}^N \left| \frac{\mathcal{Z}_i(\beta + \frac{i\Delta\tau}{\hbar})}{\mathcal{Z}_i(\beta)} \right|. \quad (6.8)$$

Particularly physically relevant is the case when the internal Hamiltonians h_i , $i = 1, \dots, N$, describe harmonic oscillators, as this can be used to model phononic modes of e.g. a molecule consisting of $N/3 + 2$ atoms (and in which case independent harmonic modes correspond to the normal modes of the molecule). Internal Hamiltonians in this case read

$$h_i = (n_i + \frac{1}{2})\hbar\omega_i \quad (6.9)$$

where n_i are number operators, ω_i —the mode frequencies, and the partition functions (6.7) are

$$\mathcal{Z}_i(\beta) = \frac{e^{-\frac{1}{2}\beta\hbar\omega_i}}{1 - e^{-\beta\hbar\omega_i}}.$$

Analytic expression for the visibility can be found for this case:

$$\mathcal{V} = \prod_{i=1}^N \left| \frac{1 - e^{-\beta\hbar\omega_i}}{1 - e^{-(\beta + \frac{i\Delta\tau}{\hbar})\hbar\omega_i}} \right|. \quad (6.10)$$

Expression (6.10) describes the visibility for a system of N harmonic modes in a thermal state, at a temperature T , in a scenario where the centre of mass followed arbitrary prepared paths with a proper time difference $\Delta\tau$, for initially uncorrelated state of the internal and external degrees of freedom.

The effect depends exponentially on the number of the thermalised internal modes, which is important for the scaling of the effect and its magnitude in the macroscopic limit. For example, consider a system at a temperature $T = 300$ K and with the frequencies $\omega_i = 10^{13}$ Hz, which is the typical magnitude for molecular vibrational modes. For a single-mode, the visibility drops to $\frac{1}{2}$ for the time dilation $\Delta\tau \approx 10^{-12}$ s. For the time dilation caused dominantly by the gravitational potential difference gh , which reads $\Delta\tau = \frac{gh}{c^2}$ with $g \approx 10$ m/s² and $h = 1$ mm, the laboratory time t_{dec} necessary to observe such a visibility drop is $t_{dec} = 10^7$ s (116 days). For one of the largest molecules with which interference has been observed which has the number of normal modes $N = 2424$ [6] one finds $t_{dec} \approx 3.5 \times 10^4$ s (less than 10 h). However, already for a system with $N = 10^{18}$, the decoherence time becomes very short $t_{dec} \approx 1.7 \times 10^{-5}$ s. Macroscopic object with $N = 10^{23}$ constituents have decoherence time of order of few microseconds.

In order to obtain an explicit expression for the decoherence time scale consider again the expression in (6.8), which in a regime $\beta > \Delta\tau/\hbar$ can be approximated as

$$\mathcal{V}_i = \left| 1 + \frac{i\Delta\tau}{\hbar} \frac{1}{\mathcal{Z}_i(\beta)} \frac{\partial \mathcal{Z}_i(\beta)}{\partial \beta} - \frac{1}{2} \left(\frac{\Delta\tau}{\hbar} \right)^2 \frac{1}{\mathcal{Z}_i(\beta)} \frac{\partial^2 \mathcal{Z}_i(\beta)}{\partial \beta^2} + \mathcal{O} \left(\frac{\Delta\tau}{\hbar} \right)^4 \right|. \quad (6.11)$$

(Note, that from $\frac{1}{\mathcal{Z}_i(\beta)} \frac{\partial^n \mathcal{Z}_i(\beta)}{\partial \beta^n} = (-1)^n \text{Tr}_i \{h_i^n \rho_T\} \equiv (-1)^n \langle h_i^n \rangle$ it is immediate to see that the above expression for any i th mode is the same as Eq. (6.4).)

In a high temperature limit $k_B T \gg \hbar\omega_i$, for each harmonic mode $\langle h_i \rangle = k_B T$ and $\langle h_i^2 \rangle = (k_B T)^2$. Thus in this limit

$$\mathcal{V}_i \approx \sqrt{1 - \left(\frac{k_B T \Delta\tau}{\hbar} \right)^2}.$$

For the paths γ_i as specified in the previous chapter, for which $\Delta\tau \approx \frac{gh t}{c^2}$ (i.e. the paths remaining for time t at fixed heights x_1 and $x_2 = x_1 + h$ above the earth, and arranged such that kinetic contributions to the proper time cancel out), the visibility for the N -mode system becomes

$$\mathcal{V}(t) \approx \left(1 - \left(\frac{k_B T g h t}{\hbar c^2} \right)^2 \right)^{\frac{N}{2}} \approx e^{-(t/t_{dec})^2}, \quad (6.12)$$

where the last approximation is valid for large N . Decoherence time t_{dec} can be defined as

$$t_{dec} = \sqrt{\frac{2}{N}} \frac{\hbar c^2}{k_B T g h}. \quad (6.13)$$

The above provides an estimate of the decoherence time which very well agrees with the decoherence time obtained from the exact expression in Eq. (6.10). The decoherence rate scales linearly with the superposition size h , while other decoherence mechanisms typically show a quadratic scaling [7]. Note, that in the high temperature limit the energy variance of a thermal state and thus also the decoherence rate do not depend of the individual frequencies of the internal modes.

6.3 Ideas for Experimental Verification

In order to directly verify the decoherence due to time dilation it is necessary to bring relatively complex systems into superposition. This can in principle be achieved with molecule interferometry [6, 8], trapped microspheres [9–12] or with micro-mechanical mirrors [13–15]. The latter, however, is expected to be limited to very small separations only [14–16] (on the order of 1 pm) and is therefore less suitable.

To see decoherence caused by time dilation, other decoherence mechanisms will need to be suppressed: The scattering with surrounding molecules and with thermal radiation requires such an experiment to be performed at liquid Helium temperatures and in ultra-high vacuum [17], which has no direct effect on the decoherence due to time dilation. However, the emission of thermal radiation by the system [18] will be a directly competing decoherence source. In order to probe the effects of proper time on quantum coherence, the decoherence due to emission of radiation shall be weaker than that due to time dilation, which could be achieved at cryogenic temperatures with sapphire microspheres, see Ref. [19] for further details. Further study of decoherence mechanisms due to both time dilation and photon emission in this temperature regime will be required for finding the optimal parameter regime for experiments. Note, that the emission of radiation can be further suppressed if the mode density is reduced, which can ease the restrictions on the temperature.

6.4 Discussion

The universal coupling between internal degrees of freedom and the centre-of-mass of a composite system which causes time dilation and entanglement, for sufficiently complex quantum systems results in a genuine decoherence mechanism for the centre of mass. For particles with few modes or in the “clock” states (as discussed in Chap. 5) the time evolution has a short period, which results in loss and revivals of centre of mass coherence on a short time scale. For example, for a particle with finite number N of internal states and in a thermal state, Eq. (6.10) shows that: (a) revivals of the visibility depend on the lowest frequency mode; (b) the more modes the system comprises, the faster the visibility becomes negligible with increasing the superposition size h or time t ; (c) the shorter is the duration of the revival peaks. For a system with $N \sim 10^{23}$ internal modes and for $h \sim 1$ mm, the visibility is below 0.01 already after 2 s. Note also, that for bulk matter the frequency of the lowest phonon mode decreases with the linear dimension of the system and the revival time thus becomes increasingly long for larger systems. For the above system with all harmonic modes at a frequency ~ 500 rad/s, revival time estimated from Eq. (6.10) is 10^{17} s—the approximate age of the Universe. The above shows that for large systems time dilation generically causes loss of the centre of mass coherence on short time scales, the revivals of coherence are scarce and short—It is in this sense that time dilation results in an effective decoherence mechanism

The centre of mass coherence can in principle be restored by a suitable operation on the internal state—this, however, would require a precise control over 10^{23} internal modes of the macroscopic system. Other way to ensure coherence in the centre of mass would be to arrange the external degrees of freedom to follow paths with exactly vanishing time dilation. However, for a system of that size already time dilation as small as 10^{-24} s causes the visibility to be practically lost ($\mathcal{V} \approx 0.08$). In order to control time dilation to such a precision, the path separation and the time spent in the interferometer would have to be controlled down to the precision of 10^{-9} ms. Turning the

argument around: with increasing size of systems utilised in quantum interference experiments, the experimental setups will have to be controlled with a great precision in order to avoid this decoherence mechanism.

Decoherence due to time dilation can be collated with two lines of research: on the emergence of classical physical laws from quantum mechanics, and with studies of general relativistic models of decoherence. The first research program is motivated by the fact that although interference experiments can demonstrate coherent quantum effects for ever increasing systems: from neutrons [20, 21], through atoms [22, 23] up to large molecules reaching 10000 atomic mass units [6, 8, 24], quantum superpositions are not part of our everyday experience. The origin of this quantum-to-classical transition is an active field of research. A prominent role in this transition is commonly attributed to interaction of particle with some environment [25–27], such as phonons [28–31], photons [17, 18, 32], spins [33–35] and gravitational waves [36–39]. A different approach in explaining classicality is taken in the so-called “collapse models” [40–43]—often inspired by general relativity but based on a postulated breakdown of the quantum superposition principle. In contrast, decoherence due to relativistic time dilation arises without any modification of quantum mechanics and no external environment is necessary—the role of environment is taken by the internal degrees of freedom while time dilation provides the universal coupling of the centre of mass to this “internal environment”. Moreover, even as weak time dilation as on earth suffices to suppress spatial coherence—already classical general relativity in its weak-field limit can thus play a significant role in the emergence of classicality.

Previously considered models of gravitationally induced decoherence described the effect due to interactions with quantised gravitational waves (e.g. a thermal bath of gravitons) [36, 38, 39] which causes decoherence into the energy basis. An effect of a stochastic classical gravitational wave background has also been investigated in the context of matter wave interferometry, e.g. in Ref. [37]. Decoherence due to quantum fluctuations of the space-time was investigated in Ref. [44]. The above models are within the framework of quantum mechanics, however, there are also models postulating break down of unitarity of quantum theory due to gravity, such as the spontaneous collapse models mentioned above [42, 43] or collapse due to postulated gravitational self-interactions, such as in Refs. [40, 41, 45]. In contrast to all previous approaches, the time-dilation-induced decoherence arises already in classical and static space time—no gravitational wave or graviton background is necessary. The effect discussed here is conceptually also entirely different from collapse models—it is fully within quantum theory, no break down of unitarity or self-interactions are required—yet it predicts that “for all practical purposes” superpositions of macroscopic systems lose quantum coherence on short time scales.

In the context of research on the quantum-to-classical transition, time dilation thus provides an ideal decoherence mechanism: it universally affects all systems and is present in any general relativistic background.

References

1. L. Mandelstam, I. Tamm, The uncertainty relation between energy and time in non-relativistic quantum mechanics, in *Selected Papers* (Springer, Berlin, Heidelberg, 1991), pp. 115–123
2. G. Fleming, A unitarity bound on the evolution of nonstationary states. *Il Nuovo Cimento A* **16**, 232–240 (1973)
3. N. Margolus, L.B. Levitin, The maximum speed of dynamical evolution. *Phys. D: Nonlinear Phenom.* **120**, 188–195 (1998). Proceedings of the Fourth Workshop on Physics and Consumption
4. P. Kosiński, M. Zych, Elementary proof of the bound on the speed of quantum evolution. *Phys. Rev. A* **73**, 024303 (2006)
5. B. Zia, M. Zych, Generalization of the Margolus-Levitin bound. *Phys. Rev. A* **74**, 034301 (2006)
6. S. Eibenberger, S. Gerlich, M. Arndt, M. Mayor, J. Tüxen, Matter-wave interference of particles selected from a molecular library with masses exceeding 10000 amu. *Phys. Chem. Chem. Phys.* **15**, 14696–14700 (2013)
7. H.-P. Breuer, F. Petruccione, *The Theory of Open Quantum Systems* (Oxford Univ. Press, 2002)
8. M. Arndt, O. Nairz, J. Vos-Andreae, C. Keller, G. Van der Zouw, A. Zeilinger, Wave-particle duality of C60 molecules. *Nature* **401**, 680–682 (1999)
9. T. Li, S. Kheifets, M.G. Raizen, Millikelvin cooling of an optically trapped microsphere in vacuum. *Nat. Phys.* **7**, 527–530 (2011)
10. J. Gieseler, B. Deusch, R. Quidant, L. Novotny, Subkelvin parametric feedback cooling of a laser-trapped nanoparticle. *Phys. Rev. Lett.* **109**, 103603 (2012)
11. N. Kiesel, F. Blaser, U. Delić, D. Grass, R. Kaltenbaek, M. Aspelmeyer, Cavity cooling of an optically levitated submicron particle. *Proc. Natl. Acad. Sci.* **110**, 14180–14185 (2013)
12. P. Asenbaum, S. Kuhn, S. Nimmrichter, U. Sezer, M. Arndt, Cavity cooling of free silicon nanoparticles in high vacuum. *Nat. Commun.* **4**, 2743 (2013)
13. W. Marshall, C. Simon, R. Penrose, D. Bouwmeester, Towards quantum superpositions of a mirror. *Phys. Rev. Lett.* **91**, 130401 (2003)
14. D. Kleckner, I. Pikovski, E. Jeffrey, L. Ament, E. Eliel, J. Van Den Brink, D. Bouwmeester, Creating and verifying a quantum superposition in a micro-optomechanical system. *New J. Phys.* **10**, 095020 (2008)
15. B. Pepper, R. Ghobadi, E. Jeffrey, C. Simon, D. Bouwmeester, Optomechanical superpositions via nested interferometry. *Phys. Rev. Lett.* **109**, 023601 (2012)
16. I. Pikovski, *On Quantum Superpositions in an Optomechanical System*. Diploma Thesis (Freie Universität Berlin, 2009)
17. E. Joos, H.D. Zeh, The emergence of classical properties through interaction with the environment. *Zeitschrift für Physik B Condens. Matter* **59**, 223–243 (1985)
18. L. Hackermüller, K. Hornberger, B. Brezger, A. Zeilinger, M. Arndt, Decoherence of matter waves by thermal emission of radiation. *Nature* **427**, 711–714 (2004)
19. I. Pikovski, M. Zych, F. Costa, Č. Brukner, Universal decoherence due to gravitational time dilation. *Nat. Phys.* **11**, 668–672 (2015)
20. R. Colella, A. Overhauser, S. Werner, Observation of Gravitationally Induced Quantum Interference. *Phys. Rev. Lett.* **34**, 1472–1474 (1975)
21. M. Zawisky, M. Baron, R. Loidl, H. Rauch, Testing the world's largest monolithic perfect crystal neutron interferometer. *Nucl. Instrum. Methods Phys. Res., Sect. A* **481**, 406–413 (2002)
22. S. Chu, Laser manipulation of atoms and particles. *Science* **253**, 861–866 (1991)
23. T. Kovachy, P. Asenbaum, C. Overstreet, C. Donnelly, S. Dickerson, A. Sugarbaker, J. Hogan, M. Kasevich, Quantum superposition at the half-metre scale. *Nature* **528**, 530–533 (2015)
24. S. Gerlich, S. Eibenberger, M. Tomandl, S. Nimmrichter, K. Hornberger, P.J. Fagan, J. Tüxen, M. Mayor, M. Arndt, Quantum interference of large organic molecules. *Nat. Commun.* **2**, 263 (2011)
25. E. Joos, H. Zeh, C. Kiefer, D. Giulini, J. Kupsch, I. Stamatescu, *Decoherence and the Appearance of a Classical World in Quantum Theory* (Springer, Berlin, Heidelberg, 2010)

26. W.H. Zurek, Decoherence, einselection, and the quantum origins of the classical. *Rev. Mod. Phys.* **75**, 715 (2003)
27. M.A. Schlosshauer, *Decoherence and the Quantum-to-Classical Transition* (Springer, 2007)
28. A.O. Caldeira, A.J. Leggett, Path integral approach to quantum Brownian motion. *Phys. A: Stat. Mech. Appl.* **121**, 587–616 (1983)
29. A.J. Leggett, S. Chakravarty, A. Dorsey, M.P. Fisher, A. Garg, W. Zwerger, Dynamics of the dissipative two-state system. *Rev. Mod. Phys.* **59**, 1 (1987)
30. T. Yu, J. Eberly, Phonon decoherence of quantum entanglement: robust and fragile states. *Phys. Rev. B* **66**, 193306 (2002)
31. S. Takahashi, I. Tupitsyn, J. Van Tol, C. Beedle, D. Hendrickson, P. Stamp, Decoherence in crystals of quantum molecular magnets. *Nature* **476**, 76–79 (2011)
32. M.R. Gallis, G.N. Fleming, Environmental and spontaneous localization. *Phys. Rev. A* **42**, 38 (1990)
33. N. Prokof'ev, P. Stamp, Theory of the spin bath. *Rep. Prog. Phys.* **63**, 669 (2000)
34. R. Hanson, V. Dobrovitski, A. Feiguin, O. Gywat, D. Awschalom, Coherent dynamics of a single spin interacting with an adjustable spin bath. *Science* **320**, 352–355 (2008)
35. T. Carle, H. Briegel, B. Kraus, Decoherence of many-body systems due to many-body interactions. *Phys. Rev. A* **84**, 012105 (2011)
36. C. Anastopoulos, Quantum theory of nonrelativistic particles interacting with gravity. *Phys. Rev. D* **54**, 1600 (1996)
37. B. Lamine, R. Hervé, A. Lambrecht, S. Reynaud, Ultimate decoherence border for matter-wave interferometry. *Phys. Rev. Lett.* **96**, 050405 (2006)
38. M. Blencowe, Effective field theory approach to gravitationally induced decoherence. *Phys. Rev. Lett.* **111**, 021302 (2013)
39. C. Anastopoulos, B. Hu, A master equation for gravitational decoherence: probing the textures of spacetime. *Class. Quantum Gravity* **30**, 165007 (2013)
40. R. Penrose, On gravity's role in quantum state reduction. *Gen. Relativ. Gravit.* **28**, 581–600 (1996)
41. L. Diósi, Models for universal reduction of macroscopic quantum fluctuations. *Phys. Rev. A* **40**, 1165 (1989)
42. P. Pearle, Combining stochastic dynamical state-vector reduction with spontaneous localization. *Phys. Rev. A* **39**, 2277 (1989)
43. G.C. Ghirardi, P. Pearle, A. Rimini, Markov processes in Hilbert space and continuous spontaneous localization of systems of identical particles. *Phys. Rev. A* **42**, 78–89 (1990)
44. F. Karolyhazy, Gravitation and quantum mechanics of macroscopic objects. *Il Nuovo Cimento A* **42**, 390–402 (1966)
45. P.C.E. Stamp, Environmental decoherence versus intrinsic decoherence. *Phil. Trans. R. Soc. A* **370**, 4429–4453 (2012)

Chapter 7

Quantum Formulation of the Einstein Equivalence Principle

Results of the previous chapters rely on the validity of both quantum theory and classical general relativity. However, in order to ensure that gravity indeed can be described in terms of a space-time metric, as in general relativity, dynamics of physical systems has to satisfy certain conditions. These conditions comprise the Einstein Equivalence Principle (EEP). This chapter analyses the EEP for quantum systems. The results show that validity of the metric picture of gravity in classical physics does not imply its validity in quantum mechanics. Very generally, quantised interactions bring in new physical effects, not present in the classical limit, which in turn implies that testing the structure of quantised dynamics is more requiring—conceptually new test are necessary and more parameters need to be constrained.

7.1 Motivation

General relativity describes a field, whose dynamics on the one hand depends on the mass-energy of matter and which, on the other hand, universally governs the dynamics of all types of matter. Whereas the former aspect renders general relativity a theory of gravity, the universality of the field's interactions with matter allows identifying it with the space-time itself, more precisely, with the space-time metric. The importance of the equivalence principle is that it provides conditions, independent of the mathematical framework of general relativity, which all physical interactions have to satisfy in order that such a metric description of gravity is viable.

These conditions can be elucidated following the hypothesis introduced by Einstein [1], which posits strict equivalence with respect to physical laws between a coordinate system subject to a constant acceleration and a stationary one in a homogeneous gravitational field. Requiring the equivalence to hold only for the laws of

This chapter is based on and contains material from the publication *Quantum formulation of the Einstein Equivalence Principle*, M. Zych and Č. Brukner, [arXiv:1502.00971](https://arxiv.org/abs/1502.00971) (2015).

non-relativistic physics still retains the description of gravity as a force, but already predicts universal acceleration of free-fall. (While universality of free-fall has been known as an empirical fact at least since the VIth century [2], it remained a “neglected clue” prior to Einstein’s work). Extending the validity of the equivalence hypothesis to all laws of physics allows us to fully equate gravitational and fictitious forces, as they cannot even in principle be distinguished. This further identifies inertial reference frames as the free-falling ones. Free-fall can thus be understood as an inertial motion, along a “straight line” albeit in space-time that, in general, is not flat.

Applied to special relativity, the equivalence hypothesis establishes that the space-time is a Lorentzian manifold. Requirements of the validity of the equivalence hypothesis and of special relativity together comprise the Einstein Equivalence Principle (EEP). In a modern formulation EEP is organised into three conditions [3]:

1. Equivalence between the system’s inertia and weight—the Weak Equivalence Principle, (WEP);
2. Independence of outcomes of local non-gravitational experiments of the velocity of a freely-falling reference frame in which they are performed (or: validity of special relativity)—Local Lorentz Invariance (LLI);
3. Independence of outcomes of local non-gravitational experiments of their location—Local Position Invariance (LPI).

The role of the EEP is to constrain the dynamical formulation of physical theories—so that they are compatible with the metric description of gravity. In particular, so that coordinates established by physical systems used as rods and clocks give rise to the Lorentzian space-time manifold, and the action of a system can be expressed as the length of the corresponding curve on the manifold. (Trajectories of free particles—given by least action principle—are then the geodesics of the manifold—minimising the length functional of the curve.) The EEP establishes that mass-energy of a system is a universal physical quantity: inertia and weight have to be equal in order to guarantee universality of free fall in the non-relativistic limit; validity of special relativity requires that internal energy contributes equally to the rest mass and to inertia; and for gravitational phenomena to be equivalent to those in non-inertial frames, internal energy must contribute equally to the weight and to inertia. For these reasons, current tests of the equivalence hypothesis focus on probing the equivalence between the inertia and weight for particles of different composition, as well as the contributions of the binding energies to the mass.

From the perspective of quantum physics current EEP tests focus on violations that would modify only the spectra of internal energies of test systems. The state space of a quantum system, however, contains also their arbitrary superpositions, and the internal energy is described by a Hamiltonian operator, governing the internal dynamics of the system. Testing EEP for the eigenstates alone constrains only the diagonal elements of the internal energy operators, whereas to conclude about its validity it is necessary to constrain the off-diagonal elements as well. A tacit assumption has been made so far: that internal energy operators must necessarily commute and EEP violations can only modify their eigenvalues. For this reason a quantum expression of the EEP is put forward in this chapter and a corresponding test theory is

constructed that lift this assumption—and incorporate quantised, rather than simply discretised, mass-energy operators.

There is a growing interest in experiments probing the EEP with quantum metrology techniques [4–7] as they allow for tests with smaller masses and at shorter distance scales than classical techniques [8]. Motivation for these tests is a general expectation, that the metric picture of gravity must be violated at some scale as low-energy effect of quantum gravity [9–11]. In thus far realised quantum tests the mass-energies of the involved systems were still compatible with classical description. These tests thus probed the same concepts as the classical ones—the equivalence of inertial and gravitational mass-energy values—albeit in combination with the superposition principle for the centre of mass. Such tests are not sufficient to conclude about validity of the EEP in quantum theory, as argued in this chapter. Results of the present work will thus become relevant in the future high precision experiments aimed at testing fundamental physics in space—where both quantum and general relativistic effects will have to be included, such as the space missions proposed in Refs. [12–15].

7.2 Quantum Formulation and Test Theory of the EEP

The analysis below focuses on the regime where only the lowest order relativistic corrections to the internal dynamics are relevant—since this regime already features all the conceptual and quantitative aspects crucial for the quantum formulation of the equivalence hypothesis. These relativistic corrections are derived from quantum field theory in Appendix E.1, but can also simply be obtained from the mass-energy equivalence extended to quantum theory—which is briefly shown below.

Hamiltonian of a non-relativistic quantum system with mass m subject to a gravitational potential ϕ reads: $\hat{H}_{nr} = mc^2 + \frac{\hat{p}^2}{2m} + m\phi(\hat{Q})$, where \hat{Q} , \hat{P} are centre of mass position and momentum operators (and mc^2 is included just for convenience of the following arguments). Mass-energy equivalence derived from special relativity entails that increasing body's internal energy by E increases also its mass by E/c^2 [16]. As a result, dynamics of the system with additional internal energy E is described by a Hamiltonian as above but with $m \rightarrow M := m + E/c^2$ (currently verified up the precision of 10^{-7} [17]). Mass-energy equivalence holds for any internal energy state, both in classical and quantum theory. However, in quantum theory one requires the equivalence to hold also for arbitrary superpositions of different internal energies, due to the linear structure of the state-space of the theory. This leads to a quantum formulation of the mass-energy equivalence principle:

$$\hat{M} = m\hat{I}_{int} + \frac{\hat{H}_{int}}{c^2}, \quad (7.1)$$

where I_{int} is the identity operator on the space of internal degrees of freedom, \hat{H}_{int} is the internal Hamiltonian of the system and the rest mass mc^2 can be defined as the ground state of the total mass-energy (i.e the lowest eigenvalue of \hat{H}_{int} is zero). The dynamics of the system is described again by the Hamiltonian as above but with the mass-energy operator instead of the mass-energy parameter: $m \rightarrow \hat{M}$ and thus $\hat{H}_{nr} \rightarrow \hat{H} = \hat{M}c^2 + \frac{\hat{P}^2}{2\hat{M}} + \hat{M}\phi(\hat{Q})$. Hamiltonian \hat{H} is valid up to first order corrections in \hat{H}_{int}/mc^2 , and can be expanded as

$$\hat{H} = mc^2 + \hat{H}_{int} + \frac{\hat{P}^2}{2m} + m\phi(\hat{Q}) - \hat{H}_{int} \frac{\hat{P}^2}{2m^2c^2} + \hat{H}_{int} \frac{\phi(\hat{Q})}{c^2}. \quad (7.2)$$

Hamiltonian (7.2) is an effective description of a low-energy massive system with quantised internal dynamics, and subject to weak gravitational field. It describes the system from the laboratory reference frame. In a full analogy to classical physics, also in quantum theory mass-energy equivalence introduces the lowest order time-dilation effects, described by the interaction terms: $\hat{H}_{int} \frac{\hat{P}^2}{2m^2c^2}$ and $\hat{H}_{int} \frac{\phi(\hat{Q})}{c^2}$. The first comes from considering the inertia and the second—from considering the weight of the quantised internal energy.

A test model for analysing the validity of the EEP in quantum theory is constructed below. It reduces to Eq. (7.2) if the principle is valid. In a standard approach to constructing such test theories one introduces possibly different inertial and gravitational mass parameters m_i and m_g and internal energy values. In order to generalise this approach to quantum theory consider that the entire mass-energy operators can have distinct gravitational \hat{M}_g and inertial \hat{M}_i form, and that both can differ from the rest mass-energy operator, \hat{M}_r . This introduces a modified quantum formulation of the mass-energy equivalence Eq. (7.1):

$$\hat{M}_\alpha := m_\alpha \hat{I}_{int} + \frac{\hat{H}_{int,\alpha}}{c^2} \quad \alpha = r, i, g, \quad (7.3)$$

where $\hat{H}_{int,r}$ is the rest energy operator (operationally defined as the Hamiltonian of the system in a reference frame in which it is at rest and in a region with vanishing gravitational field), $\hat{H}_{int,i}$ and $\hat{H}_{int,g}$ are the contributions of the internal energy to m_i and m_g , respectively. Rest mass parameter m_r is not observable in the present context and can be assigned an arbitrary value without changing predictions of the model (it acquires physical meaning of active gravitational mass when gravitational field generated by the system is considered). With the mass-energy operators of Eq. (7.3) we obtain the following test Hamiltonian: $\hat{H}_{test} = \hat{M}_r + \frac{\hat{P}^2}{2\hat{M}_i} + \hat{M}_g\phi(Q)$ which is valid to the lowest order in relativistic corrections:

$$\hat{H}_{test}^Q = m_rc^2 + \hat{H}_{int,r} + \frac{\hat{P}^2}{2m_i} + m_g\phi(\hat{Q}) - \hat{H}_{int,i} \frac{\hat{P}^2}{2m_i^2c^2} + \hat{H}_{int,g} \frac{\phi(\hat{Q})}{c^2}. \quad (7.4)$$

Hamiltonian \hat{H}_{test}^Q constitutes a new model for analysing the the EEP in a regime where the relevant degrees of freedom—internal mass-energies—are quantised. It incorporates non-trivial expression of all the three conditions into which the EEP is organised. Validity of the WEP requires equivalence between inertia and weight and its quantitative expression in our model reads $\hat{M}_i = \hat{M}_g$. As all the relativistic effects in the considered regime are derived from the mass-energy equivalence, the validity of special relativity, LLI, is to lowest order expressed by requiring that internal energy contributes equally to the rest mass and to inertia: $\hat{H}_{int,r} = \hat{H}_{int,i}$, analogously, LPI is expressed by requiring that rest energy equally contributes to weight: $\hat{H}_{int,r} = \hat{H}_{int,g}$. Keeping in mind that m_r can be assigned arbitrary value without changing the physics of the model, the validity of the EEP (to lowest order) is in quantum theory expressed by $\hat{M}_r = \hat{M}_i = \hat{M}_g$. For n -level quantum system testing validity of the EEP thus requires measuring $2n^2 - 1$ real parameters (comparing elements of hermitian operators M_α , where one parameter, m_r , is free).

In Appendix E.2 the test theory \hat{H}_{test}^Q and the conditions for the validity of the EEP are re-derived, directly from imposing validity of the Einstein's hypothesis of equivalence on the dynamics of a low-energy relativistic quantum system with internal degrees of freedom, showing that the two approaches are fully equivalent.

In a model with internal energy incorporated as classical parameters the conditions expressing validity of the EEP are just a special case of the quantum conditions derived above. See Fig. 7.1 for a summary. Such model can be described by

$$H_{test}^C = M_r + \frac{\hat{P}^2}{2M_i} + M_g \phi(\hat{Q}) \approx m_r c^2 + E_r + \frac{\hat{P}^2}{2m_i} + m_g \phi(\hat{Q}) - E_i \frac{\hat{P}^2}{2m_i c^2} + E_g \frac{\phi(\hat{Q})}{c^2}. \quad (7.5)$$

where $M_\alpha := m_\alpha + E_\alpha/c^2$ denote the total mass-energies with E_r the value of internal energy contributing to the rest mass; E_i —to the inertial mass, and E_g —to

		EEP			
		WEP	LLI	LPI	# param.
Newtonian	classical & quantum	$m_i = m_g$	—	—	1
Newtonian +	classical	$m_i c^2 + E_i = m_g c^2 + E_g$	$E_r = E_i$	$E_r = E_g$	$2n - 1$
mass-energy equiv.	quantum	$m_i c^2 \hat{I} + \hat{H}_i = m_g c^2 \hat{I} + \hat{H}_g$	$\hat{H}_r = \hat{H}_i$	$\hat{H}_r = \hat{H}_g$	$2n^2 - 1$

Fig. 7.1 Conditions for the validity of the EEP in the classical and in the quantum theory and number of parameters to test it (to lowest order) for a system with n internal states. In the non-relativistic limit the EEP reduces to the Weak Equivalence Principle (WEP), and only requires equivalence of the inertial m_i and the gravitational m_g mass parameters. Validity of the Local Lorentz Invariance (LLI) and of the Local Position Invariance (LPI) guarantees universality of special and general relativistic time dilation of the internal dynamics, respectively. In quantum mechanics their validity requires equivalence of the rest, inertial and gravitational internal energy operators \hat{H}_α , $\alpha = r, i, g$. In the classical case, it suffices that the values E_α of the corresponding internal energies are equal. Quantities E_α can be seen as the diagonal elements of $\hat{H}_{int,\alpha}$ and thus, beyond the Newtonian limit, validity of the EEP in classical mechanics does not guarantee its validity in quantum theory

the weight. In the test model H_{test}^C WEP is expressed by requiring $M_i = M_g$, LLI—by requiring $E_r = E_i$ and LPI—by $E_r = E_g$, for each internal state. These conditions are the same for a fully classical theory (see also Appendix E.3). Although H_{test}^C incorporates quantised centre of mass degrees of freedom it incorporates only the classical formulation of the EEP, from this perspective is equivalent to a classical test theory. The classical conditions above can be seen as a restriction of the quantum requirements to the diagonal elements of the internal energy operators (or only to the operators' eigenvalues). The quantum conditions reduce to the classical ones only if an additional assumption is made—that operators $\hat{H}_{int,\alpha}$ mutually commute. For a system with n internal classical states testing validity of the EEP requires measuring only $2n - 1$ parameters. Therefore, validity of the EEP in quantum physics is not guaranteed by its validity in classical theory and requires conducting independent experiments. (Only in the non-relativistic limit quantum and classical formulations of the EEP coincide, as both reduce to the requirement $m_g = m_i$, which is the non-relativistic expression of the WEP).

Modern quantum tests of the EEP are performed with composed systems, like atoms, in interferometric experiments where internal energy levels are used to manipulate external degrees of freedom of the system [4–7]. In these tests internal atomic energy can consistently be treated semi-classically (as discretised energy levels, with possibly different, EEP-violating eigenvalues) and they thus remain probing the same aspects of the EEP as the classical tests. But such tests are not sufficient to verify the validity of the EEP. Experiments with systems in superpositions of internal energy states will be required and for a meaningful analysis of such experiments test theory incorporating quantised internal energy, like \hat{H}_{test}^Q , is necessary.

Quantised¹ internal energy has not been previously incorporated into theoretical frameworks for analysing the EEP in quantum mechanics. Models studied thus far introduce a modified Lagrangian (or action) like e.g.: the $TH\epsilon\mu$ -formalism [18], Standard Model Extensions (SME) [19] or a modified Pauli equation [20]. Possibility of violations of the EEP is incorporated by introducing distinct inertial and gravitational mass parameters, (spatial) mass-tensors [21] or spin-coupled masses [20] for elementary particles or fields. In these approaches, for describing bound systems one derives from the elementary model an effective one, with EEP-violating parameters which describe shifts in values of the binding energies, see e.g. [22], but the dynamics of the degrees of freedom associated to the binding energy has not been considered. Note, however, that if the fundamental interactions are modified, not only the eigenvalues but also the eigenstates of the effective internal Hamiltonians of composed systems will be different. This shows that here discussed features of the quantum formulation of the EEP are generic in theories incorporating EEP violations at the level of fundamental interactions. For a direct comparison between our Hamiltonian approach and the Lagrangian-based frameworks we derive the Lagrangian formulation of our test theory in the Appendix E.4.

¹EEP violations affecting internal energy levels were considered thus far, but such an approach tacitly assumes that internal operators commute—and thus only incorporates *discretised* internal states—which is not the same as the *quantisation*.

Internal energy described as a quantum operator was thus far considered only in the context of the WEP for neutrinos [23, 24]. It has been studied how neutrino oscillations would be affected if the neutrinos' weak interaction eigenstates would be different from the states with a well-defined value of the gravitational mass. (For massless neutrinos such effects are excluded with a precision of 10^{-11} [23] and for models of massive neutrinos are ruled out by the existing experimental data [24]).

Understanding the (in)dependence relations between the three tenets of the EEP is important not only for counting the number of parameters to test. For the field of precision tests of the EEP particularly important is the question: under what assumptions tests of the WEP impose constraints on the violations of LPI? First, note that no single principle implies the others—see e.g. Fig. 7.1. Second, test theory \hat{H}_{test}^Q is based on three assumptions: (1) energy is conserved, (2) in the non-relativistic limit standard quantum theory is recovered when inertial and gravitational mass parameters are equal, (3) mass-energy equivalence extends to quantum mechanics as in Eq. (7.3). With these assumptions alone validity of the WEP ($\hat{M}_g = \hat{M}_i$) does not imply validity of LPI ($\hat{H}_{int,r} = \hat{H}_{int,g}$). Additional assumption has to be made: (4) LLI is valid ($\hat{H}_{int,r} = \hat{H}_{int,i}$). Only under all four assumptions constraints on the violations of the WEP can in principle give some constraints on the violations of the LPI. Note, that all the four assumptions are in fact made also in the well-known Nordtvedt's Gedankenexperiment [25], which is often invoked as a proof that energy conservation alone yields tests of the WEP to be equivalent to tests of LPI. We stress that the three tenets of the EEP concern very different aspects of the theory, which itself merits their independent experimental verification.

7.3 Testing the Quantum Formulation of the EEP

Within the present approach one can introduce an unambiguous distinction between tests of the classical and of the quantum formulation of the EEP: As tests of the classical formulation of the EEP qualify experiments whose potentially non-null results (indicating violations of the EEP) can still be explained by a diagonal test theory—i.e. test theory where internal energy operators are assumed to commute. (E.g. by a model like H_{test}^C which can be seen as a diagonal element of \hat{H}_{test}^Q in a special case when all $\hat{H}_{int,\alpha}$ commute). In contrast, experiments which non-null results cannot be explained by a diagonal model, can be seen as tests of the quantum formulation of the EEP. Below we discuss some experimental scenarios for testing various parts of the EEP and show which aspects of such experiments test the quantum and which test the classical formulation of the EEP.

In order to use experimental results to put quantitative constraints on the violations of the quantum formulation of the EEP, it is convenient to introduce a suitable parameterisation of the violations. Violations of the quantum formulation of the WEP will be described by a parameter-matrix $\hat{\eta} := \hat{I}_{int} - \hat{M}_g \hat{M}_i^{-1}$; of the LLI by $\hat{\beta} := \hat{I}_{int} - \hat{H}_{int,i} \hat{H}_{int,r}^{-1}$; and of the LPI by $\hat{\alpha} := \hat{I}_{int} - \hat{H}_{int,g} \hat{H}_{int,r}^{-1}$. In order to para-

metrise violations of the classical formulation of the EEP one needs: for the WEP—a real parameter $\eta_{class} := 1 - M_g/M_i$ for each internal state; for LLI and LPI we need one parameter $\beta_{class} := 1 - E_i/E_r$ and one $\alpha_{class} := 1 - E_g/E_r$, for each internal state (apart from, say, the ground state which can be set arbitrarily through a free parameter m_r). The classical parameters $\eta_{class}, \alpha_{class}, \beta_{class}$ can again be seen as the diagonal elements of the quantum parameter-matrices: $\hat{\eta}, \hat{\alpha}, \hat{\beta}$. Note, that there is a total of $2n^2 - 1$ independent real parameters for testing the quantum and $2n - 1$ for the classical formulation of the EEP as explained in Sect. 7.2.

7.3.1 Testing the Quantum Formulation of the WEP

The physical meaning of the validity of the WEP in classical theory is the universality of free fall—which is also how WEP is usually tested. In quantum theory, universality of free fall can be generalised to the requirement that the “acceleration” of the position operator for the centre of mass is independent of the internal degrees of freedom. This is best seen in the Heisenberg picture, where time evolution of an observable \hat{A} under a Hamiltonian \hat{H} is given by $d\hat{A}/dt = -i/\hbar[\hat{A}, \hat{H}]$. Under \hat{H}_{test}^Q the acceleration of the centre of mass $\hat{a}_{\hat{H}_{test}^Q} := d^2\hat{Q}/dt^2 = -\frac{1}{\hbar^2}[[\hat{Q}, \hat{H}_{test}^Q], \hat{H}_{test}^Q]$ is given by

$$\hat{a}_{\hat{H}_{test}^Q} = -\hat{M}_g \hat{M}_i^{-1} \nabla \phi(\hat{Q}) + \frac{i}{\hbar} [\hat{H}_{int,i}, \hat{H}_{int,r}] \frac{\hat{P}}{m_i c^2} + \mathcal{O}(1/c^4). \quad (7.6)$$

Note, that the commutator in Eq. (7.6) is present even in a vanishing gravitational potential $\phi(Q)$ and expresses a violation of LLI. Under the Hamiltonian H_{test}^C the centre of mass “acceleration” $\hat{a}_{H_{test}^C}$ reads

$$\hat{a}_{H_{test}^C} = -M_g M_i^{-1} \nabla \phi(\hat{Q}) \quad (7.7)$$

(as expected, it can be obtained from Eq. (7.6) as a special case of commuting internal energy operators). From Eqs. (7.6) and (7.7) follows that also in quantum theory probing the WEP is tantamount to probing whether the time evolution of the centre of mass degree of freedom is universal, does not depend on the internal state of the system.

Classical WEP violations, effects derivable from $\hat{M}_i \neq \hat{M}_g$ but with $[\hat{H}_{int,i}, \hat{H}_{int,g}] = 0$, would result in different accelerations for different internal states. Violations stemming from $[\hat{H}_{int,i}, \hat{H}_{int,g}] \neq 0$ result in additional effects. Assume that LLI holds. Equation (7.6) and a relation $\hat{M}_g \hat{M}_i^{-1} = \hat{I}_{int} - \hat{\eta}$ entail that only eigenstates of the parameter-matrix $\hat{\eta}$, which explicitly reads $\hat{\eta} \approx m_g/m_i (\hat{I} + \hat{H}_{int,g}/m_g c^2 - \hat{H}_{int,i}/m_i c^2)$, have a well defined free fall acceleration (of the centre of mass degree of freedom). Hence, for a given internal energy eigenstate the external degree of freedom will in general be in a superposition of states each falling with a different accelera-

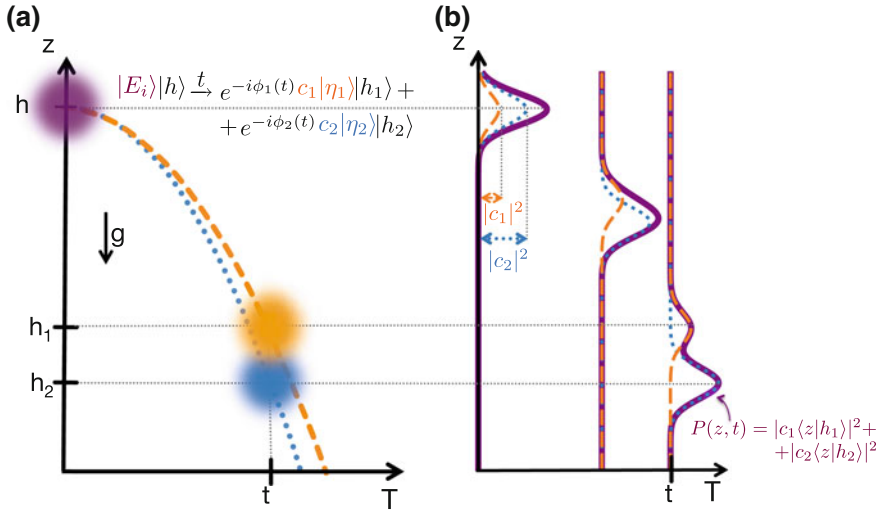


Fig. 7.2 Free evolution of the centre of mass (c.m.) degree of freedom (d.o.f.) of a quantum system in a gravitational field g in a presence of the Weak Equivalence Principle (WEP) violations. Initially state of the system is a product of an internal state $|E_i\rangle$ and c.m. position $|h\rangle$ given by a gaussian distribution centred at height h . If the quantum formulation of the WEP is violated the system is in superposition of c.m. states each falling with different accelerations. **a** Dashed orange and dotted blue lines represent semi-classical trajectories of the c.m. correlated with the internal states $|\eta_1\rangle$, $|\eta_2\rangle$, for which acceleration is well defined $\eta_1 g, \eta_2 g$. **b** Probability distribution $P(z, t)$ of finding the system at height z at time t (see main text) is marked by a thick purple line. Dashed orange and dotted blue lines represent the probability conditioned on the internal state $|\eta_1\rangle$ and $|\eta_2\rangle$, respectively. Modulations in $P(z, t)$ indicate violation of the quantum formulation of the WEP under the assumption that linearity of quantum theory is not violated. Probing entanglement between internal and c.m. d.o.f. generated in the above scenario, would constitute a direct test of the quantum formulation of the WEP

tion, see Fig. 7.2a. Consider an eigenstate of $\hat{H}_{int,i}$ initially semi-classically localised at some height $|h\rangle$: $|\Phi(0)\rangle = |E_i\rangle|h\rangle$. (An eigenstate of $\hat{H}_{int,i}$ can be prepared e.g. with a precise mass-spectroscopy, as it selects states of a given inertial mass-energy.) Under free fall the state generally evolves into $|\Phi(t)\rangle = \sum_i e^{-i\phi_i(t)} c_i |\eta_i\rangle |h_i\rangle$, where $|\eta_i\rangle$ are eigenstates of $\hat{\eta}$, c_i are normalised amplitudes such that: $|E_i\rangle = \sum_i c_i |\eta_i\rangle$, and $\phi_i(t)$ are the phases acquired during the evolution. When $|h_i - h_j|$ for different i, j become larger than the system's coherence length, the position amplitudes become distinguishable, $\langle h_j | h_i \rangle = \delta_{ij}$, and the state $|\Phi(t)\rangle$ becomes entangled: with the centre of mass position entangled to the internal degree of freedom. Probing this entanglement would constitute a direct test of the quantum formulation of the WEP, since under a “diagonal test model” (model in which internal energy operators commute) initially separable state $|\Phi(0)\rangle$ cannot evolve into an entangled one.

As a result of the above described entanglement, the probability of finding the system at time t as a function of the height z , $P(z, t) = |\langle z | \Phi(t) \rangle|^2$, develops distinguished spatial modulations, see Fig. 7.2b. In the opposite limit, when the coherence

length dominates over $|h_i - h_j|$, the spatial probability distribution just broadens in the direction of gravity gradient. For an initial eigenstate of $\hat{H}_{int,i}$ such modulations or broadening would not appear if $[\hat{H}_{int,i}, \hat{H}_{int,g}] = 0$, unless it allows that a pure state $|\Phi(0)\rangle$ evolves into a mixed one $\hat{\rho}(t) := \sum_i |c_i|^2 |\eta_i\rangle\langle\eta_i| \otimes |h_i\rangle\langle h_i|$. Such a model does not violate the quantum formulation of the WEP, but it violates unitarity of quantum theory. It can explain the broadening or the spatial modulations of the probability distribution, since $|\langle z|\hat{\rho}(t)|z\rangle|^2 \equiv P(z, t)$, but cannot account for the entanglement as $\hat{\rho}(t)$ is separable. Thus, probing such broadening or modulations can be considered a test of the quantum WEP under an additional assumption that linear structure of quantum theory is retained. Note however, that such additional broadening would be very difficult to measure precisely and to distinguish from the standard quantum mechanical effects causing spreading of the particles' wave-packets.

A recent experiment realised in a drop tower in Bremen with Bose Einstein Condensate (BEC) of ^{87}Rb in extended free fall [26] can be used to put some bounds on the strength of such modulations and constrain some of the new parameters of \hat{H}_{test}^Q . A small, but non-zero variance of the parameter-matrix $\hat{\eta}$, denoted by $\Delta\eta$, would lead to an anomalous spreading of the free falling BEC cloud by $\Delta S \approx \Delta\eta g T^2/2$, where $T \approx 0.5$ s denotes the free-fall time and $g \approx 10\text{m/s}^2$. As no anomalous spreading or modulations of the BEC cloud has been reported we assume that ΔS can be bounded by the size of the BEC cloud, which we estimate to be $L \approx 10^{-4}\text{m}$; as a result $\Delta\eta < 8 \times 10^{-5}$. Under the assumption that the initial state of the atoms was an eigenstate of $\hat{H}_{int,i}$ and that unitarity of quantum theory is not violated, a non-zero $\Delta\eta$ could only arise from $[\hat{H}_{int,i}, \hat{H}_{int,g}] \neq 0$.

7.3.2 Testing the Quantum Formulation of the LPI and LLI

Validity of LLI and LPI can be tested in experiments probing the special relativistic and the gravitational time dilation, respectively: Allowing for different internal Hamiltonians $\hat{H}_{int,\alpha}$ in general results in a different speed of the internal evolution. Denoting the internal degree of freedom by \hat{q} the Hamiltonian \hat{H}_{test}^Q yields

$$\hat{q}(\hat{Q}, \hat{P}) = \hat{q}_r \hat{I}_{ext} - \hat{q}_i \frac{\hat{P}^2}{2m_i^2 c^2} + \hat{q}_g \frac{\phi(\hat{Q})}{c^2}, \quad (7.8)$$

where $\hat{q}_\alpha := -i/\hbar[\hat{q}, \hat{H}_{int,\alpha}]$ and \hat{I}_{ext} is the identity operator on the space of external degrees of freedom (\hat{Q}, \hat{P}) . In terms of the velocity \hat{Q} canonically conjugate to the momentum \hat{P} (see also Appendix E.4) we can write Eq. (7.8) in the form $\hat{q}(\hat{Q}, \hat{Q}) = \hat{q}_r \hat{I}_{ext} - \hat{q}_i \frac{\hat{Q}}{2c^2} + \hat{q}_g \frac{\phi(\hat{Q})}{c^2}$. If internal energy is coupled universally, $\hat{H}_{int,\alpha} = \hat{H}_{int}$ for $\alpha = i, r, g$, we have $\hat{q}_\alpha = \hat{q}$ and thus: $\hat{q}(\hat{Q}, \hat{P}) = \hat{q}(\hat{I}_{ext} - \frac{\hat{P}^2}{2m_i^2 c^2} + \frac{\phi(\hat{Q})}{c^2})$ —i.e. we recover universal special relativistic and gravitational time dilation of the internal dynamics (up to lowest order in c^{-2}). (Note, that since the constant mass parameters

m_α are irrelevant for the rate of the internal evolution, in the non-relativistic limit there is no time dilation and the internal evolution is just given by the rest energy operator). The condition for the gravitational time dilation to be universal reads $\hat{H}_{int,g} = \hat{H}_{int,r}$ and analogously for the special relativistic time dilation: $\hat{H}_{int,i} = \hat{H}_{int,r}$. Testing universality of the time dilation effects is therefore equivalent to probing LPI and LLI (to lowest order), see also Appendix E.2.

In any test-theory incorporating classical internal energy one can at most consider special relativistic and gravitational redshifts of the internal energy values. Analogously to the above discussed case, in the theory described by H_{test}^C special relativistic redshift is universal once $E_r = E_i$ and the gravitational redshift is universal if $E_r = E_g$. These conditions also hold in a fully classical theory, see the also Appendix E.3. In turn, this entails that an experiment measuring only the redshift of atomic spectra or only the time dilation of clocks following classical paths, can always be explained via LLI or LPI violations which are compatible with $[\hat{H}_{int,r}, \hat{H}_{int,i}] = 0$ or $[\hat{H}_{int,r}, \hat{H}_{int,g}] = 0$, respectively. Without additional assumptions or measurements of additional effects, such experiments can only be seen as tests of the classical formulation of the equivalence principle.

Violations of the quantum formulation of the LLI (LPI) coming from $[\hat{H}_{int,r}, \hat{H}_{int,i}] \neq 0$ ($[\hat{H}_{int,r}, \hat{H}_{int,g}] \neq 0$) lead to conceptually different effects, since the non-commuting operators generally have different stationary and time-evolving states—an eigenstate of, say, $\hat{H}_{int,r}$ will generally not be an eigenstate of $\hat{H}_{int,i}$ ($\hat{H}_{int,g}$). Consider an interference experiment where a particle follows in superpositions two different semi-classical trajectories γ_1, γ_2 which are then coherently overlapped and the resulting interference pattern is observed, see Fig. 7.3a for a sketch of the setup. If the centre of mass degrees of freedom are constrained to follow a semi-classical path $\gamma_j, j = 1, 2$ the total Hamiltonian describes the dynamics of the internal degrees of freedom along this path; which will be denoted by $\hat{H}_{test}^Q(\gamma_j)$. If the initial internal state is an eigenstate $|E(\gamma_1)\rangle$ of $\hat{H}_{test}^Q(\gamma_1)$ it remains stationary along path γ_1 like a “rock”. However, it will generally non-trivially evolve in time along γ_2 , like a “clock”, if $[\hat{H}_{test}^Q(\gamma_1), \hat{H}_{test}^Q(\gamma_2)] \neq 0$. As a result, the internal state of the particle entangles to the centre of mass and the coherence of the centre of mass superposition decreases. This loss of coherence is given by the overlap between the two internal amplitudes evolving along different paths.

For a quantitative analysis assume that gravitational potential is approximately homogeneous $\phi(x) = gx$ and paths γ_j are defined such that the particle remains at rest in a laboratory frame at fixed height h_j for time T ; so that $\hat{H}_{test}^Q(\gamma_j) = \hat{H}_{int,r} + (m_g c^2 + \hat{H}_{int,g}) \frac{gh_j}{c^2}$ and the contributions from the vertical parts of γ_j , are the same. For such a case the coherence of the centre of mass superposition reads $\mathcal{V} \approx |\cos(\Delta H_{int,g} \frac{ghT}{\hbar c^2})|$, where $h \equiv h_2, h_1 = 0$ and with $\Delta H_{int,g} := \sqrt{\langle \hat{H}_{int,g}^2 \rangle - \langle \hat{H}_{int,g} \rangle^2}$, where expectation values are taken with respect to the initial state $|E(\gamma_1)\rangle$, i.e. the eigenstate of $\hat{H}_{int,r}$. Quantity \mathcal{V} is also the visibility of the interference pattern observed in such an experiment:

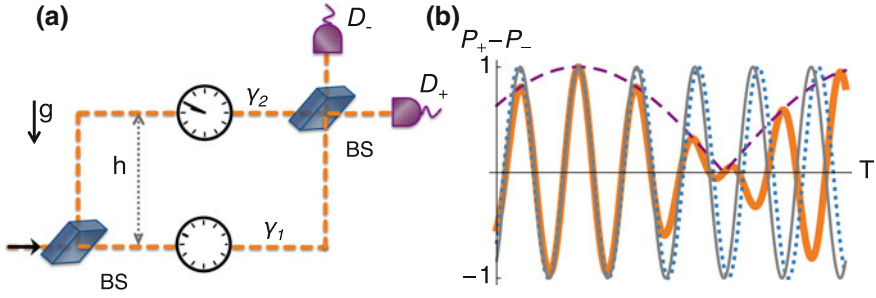


Fig. 7.3 **a** Mach-Zehnder interferometer for probing the quantum formulation of the Local Position Invariance (LPI) and **b** detection probabilities in different scenarios. The setup consists of two beam splitters (BS) and two detectors D_{\pm} , is stationary in the laboratory reference frame subject to gravitational field g . The setup permits two fixed trajectories γ_1, γ_2 with separation h in the direction of the field. Initial internal state of the system is stationary along γ_1 . If LPI is respected, gravitationally induced phase shift of the interference pattern will be observed—*thin, grey line*—with in principle maximal visibility. Observing a different phase shift—*dotted blue line*—indicates a violation, but it can always be explained by a diagonal test theory. Modulations of the visibility—*purple, dashed line*—cannot be explained with a diagonal model (for here chosen initial state) and arise directly from the non-commutativity of the internal energy operators. *Thick, orange line* represents detection probabilities in this case. Internal d.o.fs stationary along γ_1 will generally not be stationary along γ_2 and the system is therefore represented as a “ticking clock” only along γ_2 . The resulting entanglement between internal and external d.o.fs leads to the modulation in the fringe contrast. Measurements of the visibility of the gravitationally induced interference pattern can thus probe the quantum formulation of the LPI, whereas measurements of the phase shift alone can always be seen as probing only the classical formulation

the probabilities P_{\pm} to detect the particle in the detector D_{\pm} read in this case $P_{\pm} \approx \frac{1}{2} \left(1 \pm \cos \left(\Delta H_{int,g} \frac{ghT}{\hbar c^2} \right) \cos \left(\langle \hat{M}_g \rangle \frac{ghT}{\hbar} \right) \right)$ see Fig. 7.3b. The first term is the overlap between the amplitudes that were evolving along different paths, the second comes from the relative phase-shift between them. In a general case of arbitrary paths γ_j and arbitrary initial state, the detection probabilities read $P_{\pm} = \frac{1}{2} \left(1 \pm \text{Re} \{ \langle e^{\frac{i}{\hbar} \int_{\gamma_1} ds \hat{H}_{test}^Q(\gamma_1(s))} e^{-\frac{i}{\hbar} \int_{\gamma_2} ds \hat{H}_{test}^Q(\gamma_2(s))} \rangle \} \right)$ and the visibility reads $\mathcal{V} = |\langle e^{\frac{i}{\hbar} \int_{\gamma_1} ds \hat{H}_{test}^Q(\gamma_1(s))} e^{-\frac{i}{\hbar} \int_{\gamma_2} ds \hat{H}_{test}^Q(\gamma_2(s))} \rangle|$, where the expectation values are taken with respect to the initial state of the system.

If the EEP is valid, modulations in the visibility in such an interference experiment only occur if an initial state has a non-vanishing internal energy variance and if there is time dilation between the paths γ_j , see e.g. Chap. 6 or Refs. [27, 28]. An internal energy eigenstate remains an eigenstate in the standard theory, independently of the path taken by the centre of mass and only results in a phase shift term, with in principle maximal visibility $\mathcal{V} = 1$. In a diagonal test theory the initial state would also remain an eigenstate along both paths, with at most different eigenvalues of the different internal energies. This would result in modifications of the observed phase shift, but would also allow for a maximal visibility. Modulations in the visibility

of the inference pattern in the experiment with a system prepared in the internal eigenstate can thus probe the quantum formulation of the EEP.

It is convenient to write the probabilities P_{\pm} in terms of the parameters quantifying violations of the quantum and of the classical formulation of the EEP. What aspects of the EEP are tested in a given experiment, depends on which parameters are independently measured and which are actually inferred from the test. In the considered scenario the system is prepared in an eigenstate of $\hat{H}_{int,r}$. One can thus rewrite $\Delta H_{int,g} \equiv E_r \Delta\alpha$ where $\Delta\alpha$ is a variance of a parameter-matrix $\hat{\alpha} := \hat{I}_{int} - \hat{H}_{int,g} \hat{H}_{int,r}^{-1}$. In many atom interference experiments the separation between the paths is not measured directly but is given by a momentum transfer from a laser. In such a case $h = \hbar k t_s / \langle \hat{M}_i \rangle$, where k is a wave-vector of the light and t_s is the time after which, in our scenario, the amplitudes remain at fixed heights. Note, that $\langle \hat{M}_g \rangle / \langle \hat{M}_i \rangle \neq 1$ can always be explained by commuting \hat{M}_g , \hat{M}_i with only different eigenvalues; one can identify $\eta_{class} = 1 - \langle \hat{M}_g \rangle / \langle \hat{M}_i \rangle$. Without further assumptions

$$P_{\pm} = \frac{1}{2} \left(1 \pm \cos \left(\Delta\alpha \frac{E_r}{\langle \hat{M}_i \rangle c^2} g k t_s T \right) \cos ((1 - \eta_{class}) g k t_s T) \right).$$

The term proportional to $(1 - \eta_{class})$ describes the gravitational phase shift and its possible modifications due to the violations of the classical formulation of the WEP. Moreover, the above entails that any modification to the phase shift in such an interference test can be fully explained by a model that only violates the non-relativistic limit of the the WEP (i.e. a test theory with $m_i \neq m_g$ and $\hat{H}_{int,i} = \hat{H}_{int,r} = \hat{H}_{int,g}$). The visibility of this interference pattern (the first cosine term) allows probing the quantum formulation of the LPI as it depends on the variance of the quantum parameter-matrix $\hat{\alpha}$.

No experiment has yet succeeded to probe jointly general relativistic and quantum effects required for the above test. No direct bound thus exist on the quantum violations of the LPI. By assuming validity of the LLI some constraints can be inferred e.g. from an interferometric experiment realised in the group of T. Hänsch [4] measuring gravitational phase shift for two Rubidium isotopes ^{85}Rb and ^{87}Rb , and for two different hyperfine states of ^{85}Rb . For the quantitative analysis we take $\langle \hat{M}_r \rangle = \langle \hat{M}_i \rangle \approx 2.5 \times 10^{-25} \text{ kg}$ for the mass of Rubidium and $E_r = \hbar\omega$ with $\omega \approx 10^{15} \text{ Hz}$. The wave vector of the light grating used in the experiment was $k \approx 7.5 \times 10^6 \text{ m}^{-1}$ and to obtain the interference pattern the time T was varied between 40.207 and 40.209 ms. We can set $T = T_0 \pm \delta T$ with $T_0 = 40$ and $\delta T = 10^{-3} \text{ ms}$. The height difference achieved with this interferometric technique was $h \approx \hbar k T_0 / \langle \hat{M}_r \rangle$. Experimentally measured visibility remains constant over the interrogation times $T_0 \pm \delta T$ and was equal $\mathcal{V} = 0.09$. Any variations of the visibility must therefore be of order 10^{-3} or smaller, which allows us to obtain a bound $\Delta\alpha < 9 \times 10^6$.

For testing LLI an interferometric experiment analogous to the one in the Fig. 7.3 can be used: with a horizontal setup where the two interferometric paths remain at

the same gravitational potential. One amplitude, γ'_1 , is kept at rest with respect to the laboratory frame whereas the other, γ'_2 , is given some velocity and after reflection is overlapped with the first one. If $[\hat{H}_{int,r}, \hat{H}_{int,i}] \neq 0$ even if the internal state of the interfering system is stationary along γ'_1 , it will generally not be stationary along γ'_2 . In a full analogy to the above discussed test of the LPI, violations of the quantum formulation of the LLI will result in a modulation of the contrast of the interference pattern. Violations of the classical formulation of the LLI will only modify the relative phase acquired by the amplitudes.

It is worth stressing that test theory including quantised internal energy of the test-systems and the quantum formulation of the EEP are relevant even when internal energy operators are assumed to commute. For example, in order to describe entanglement created between centre of mass and internal degrees of freedom, which would arise in an experiment probing WEP for a superposition of two different internal eigenstates having different accelerations of free fall due to classical violations of the WEP (see Appendix E.5 for more details of such a Gedankenexperiment).

7.4 Discussion

Equivalence principle in quantum theory is an active research topic in experimental [4, 7, 13–15] and theoretical physics [6, 29–38]. While uncontroversial in classical theory, in quantum mechanics the EEP still appears to be contentious. Nearly any claim about it can find support in the scientific literature: that the EEP is violated in quantum mechanics [34, 35]; that there is a tension between the very formulation of the EEP and quantum theory—and therefore EEP has to be suitably reformulated before its validity can be discussed in quantum mechanics [20]—but also that there is no difference between testing validity of the EEP in classical and quantum physics [38]. (The latter view is motivated by the fact that so far proposed reformulations still gave rise to the same quantitative conditions in the quantum and in the classical case. In the light of our results, this comes from the fact that such reformulations were analysed for systems with quantised only external degrees of freedom.) Below we address some of the concerns regarding the very possibility of formulating the EEP in quantum theory that are being raised.

Some authors express concerns that WEP is by construction violated in quantum theory, since mass does not cancel from the description of a quantum system. Note, however, that mass appears as a dimensional proportionality factor in the action of a system even in the absence of any gravitational field. Moreover, it plays a physical role in quantum theory—it describes how fast the phase is accumulated along the system's path and can be measured in principle even for a free particle in flat space-time (as a relative phase or via wave-packet spreading). Requiring that mass should not enter the description of a quantum system subject to gravity is from such a perspective in contradiction with the equivalence hypothesis, and thus with the rationale of the EEP. Such a requirement is tenable only in the classical limit, where no interference

can be observed between different paths and only diagonal elements of the state of the system are accessible—from which the phase, and thus also the mass, cancels.

It is also often argued that for the formulation of the EEP one needs exactly point test systems and since a strict locality is fundamentally irreconcilable with the tenets of quantum theory (e.g. the uncertainty principle), EEP cannot be formulated in quantum mechanics. The same argument could, however, apply also in classical statistical physics—e.g. to a situation in which only the probability distribution for finding a classical particle in a certain region is known—and hence has nothing to do with quantum physics. In practice, given a finite measurement accuracy, the relevant description of a quantum (or classical) experiment can always be restricted to a finite region. Homogeneity of gravity in such a region is then also required to hold only up to a finite experimental precision. One can thus introduce a single correspondingly accelerated reference frame and meaningfully ask whether the two situations are physically equivalent. A pair of neutron experiments in which the phase shift of the interference pattern caused by gravity [39] and inertial acceleration [40] was measured serve as just one example of successful quantum tests, in which the above conditions were met. (These two experiments together can be regarded as a test of the non-relativistic limit of the WEP in quantum theory).

It should be stressed that the equivalence hypothesis can be incorporated into any physical theory, since any theory can be written in arbitrary coordinates and one can further postulate that the effects stemming from accelerated coordinates are equivalent to the effects of the corresponding gravitational field. In this sense the equivalence hypothesis can be incorporated into classical and quantum theories alike—an example of the latter is relativistic quantum field theory in curved space-time [41]. Concerns regarding the formulation of the EEP in quantum mechanics in fact can be seen as originating from a question—what do we need to test (and how) in order to verify whether physics in the regime where quantum effects are relevant complies with the equivalence hypothesis, with a metric picture of gravity? Approach developed here stresses, that the very phrasing of the EEP, here cited after Ref. [3], is applicable to classical as well as to quantum theory, but the quantitative statement of the conditions comprising the EEP is different in the two cases. Also experiments that would allow testing these conditions are conceptually very different, as not all classical concepts apply in quantum mechanics. This, however, does not invalidate the formulation of the principle, nor by itself entails that the principle is violated.

References

1. A. Einstein, Über das Relativitätsprinzip und die aus demselben gezogenen Folgerungen. *Jahrb. f. Rad. und Elekt.* 4, 411 (1907). *Jahrbuch der Radioaktivität* 4, 411–462 (1907)
2. J. Philoponus, *Corollaries on Place and Void* (University Press, Ithaca, New York, 1987). Translated by David Furley
3. C.M. Will, *Theory and Experiment in Gravitational Physics* (Cambridge University Press, 1993)

4. S. Fray, C.A. Diez, T.W. Hänsch, M. Weitz, Atomic interferometer with amplitude gratings of light and its applications to atom based tests of the equivalence principle. *Phys. Rev. Lett.* **93**, 240404 (2004)
5. R. Geiger, V. Ménotet, G. Stern, N. Zahzam, P. Cheinet, B. Battelier, A. Villing, F. Moron, M. Lours, Y. Bidel et al., Detecting inertial effects with airborne matter-wave interferometry. *Nat. Commun.* **2**, 474 (2011)
6. S. Herrmann, H. Dittus, C. Lämmerzahl et al., Testing the equivalence principle with atomic interferometry. *Class. Quantum Gravity* **29**, 184003 (2012)
7. D. Schlippert, J. Hartwig, H. Albers, L. Richardson, C. Schubert, A. Roura, W. Schleich, W. Ertmer, E. Rasel, Quantum test of the universality of free fall. *Phys. Rev. Lett.* **112**, 203002 (2014)
8. S. Schlamminger, K.-Y. Choi, T. Wagner, J. Gundlach, E. Adelberger, Test of the equivalence principle using a rotating torsion balance. *Phys. Rev. Lett.* **100**, 041101 (2008)
9. G. Amelino-Camelia, J. Ellis, N. Mavromatos, D.V. Nanopoulos, S. Sarkar, Tests of quantum gravity from observations of γ -ray bursts. *Nature* **393**, 763–765 (1998)
10. R. Maartens, K. Koyama, Brane-World gravity. *Living Rev. Relativ.* **13**, 5 (2010). [arXiv:1004.3962](https://arxiv.org/abs/1004.3962) [hep-th]
11. T. Damour, Theoretical aspects of the equivalence principle. *Class. Quantum Gravity* **29**, 184001 (2012)
12. R. Kaltenbaek, G. Hechenblaikner, N. Kiesel, O. Romero-Isart, K.C. Schwab, U. Johann, M. Aspelmeyer, Macroscopic quantum resonators (MAQRO). *Exp. Astron.* **34**, 123–164 (2012)
13. D. Aguilera, H. Ahlers, B. Battelier, A. Bawamia, A. Bertoldi, R. Bondarescu, K. Bongs, P. Bouyer, C. Braxmaier, L. Cacciapuoti et al., STE-QUEST—test of the universality of free fall using cold atom interferometry. *Class. Quantum Gravity* **31**, 115010 (2014)
14. B. Altschul, Q.G. Bailey, L. Blanchet, K. Bongs, P. Bouyer, L. Cacciapuoti, S. Capozziello, N. Gaaloul, D. Giulini, J. Hartwig, L. Iess, P. Jetzer, A. Landragin, E. Rasel, S. Reynaud, S. Schiller, C. Schubert, F. Sorrentino, U. Sterr, J.D. Tasson, G.M. Tino, P. Tuckey, P. Wolf, Quantum tests of the Einstein equivalence principle with the STE-QUEST space mission. *Adv. Space Res.* **55**, 501–524 (2015). doi:[10.1016/j.asr.2014.07.014](https://doi.org/10.1016/j.asr.2014.07.014)
15. J. Williams, S.W. Chiow, N. Yu, H. Müller, Quantum test of the equivalence principle and space-time aboard the international space station. *New J. Phys.* **18**, 025018 (2016)
16. A. Einstein, Ist die Trägheit eines Körpers von seinem Energieinhalt abhängig? *Annalen der Physik* **323**, 639–641 (1905)
17. S. Rainville, J.K. Thompson, E.G. Myers, J.M. Brown, M.S. Dewey, E.G. Kessler, R.D. Deslattes, H.G. Börner, M. Jentschel, P. Mutti, D.E. Pritchard, World year of physics: a direct test of $E = mc^2$. *Nature* **438**, 1096–1097 (2005). doi:[10.1038/4381096a](https://doi.org/10.1038/4381096a)
18. A.P. Lightman, D.L. Lee, Restricted proof that the weak equivalence principle implies the Einstein equivalence principle. *Phys. Rev. D* **8**, 364–376 (1973). doi:[10.1103/PhysRevD.8.364](https://doi.org/10.1103/PhysRevD.8.364)
19. D. Colladay, V.A. Kostelecký, CPT violation and the standard model. *Phys. Rev. A* **55**, 6760–6774 (1997). doi:[10.1103/PhysRevD.55.6760](https://doi.org/10.1103/PhysRevD.55.6760)
20. C. Lämmerzahl, Quantum tests of the foundations of general relativity. *Class. Quantum Gravity* **15**, 13 (1998)
21. M.P. Haugan, Energy conservation and the principle of equivalence. *Ann. Phys.* **118**, 156–186 (1979)
22. M.A. Hohensee, H. Müller, R. Wiringa, Equivalence principle and Bound Kinetic energy. *Phys. Rev. Lett.* **111**, 151102 (2013)
23. M. Gasperini, Testing the principle of equivalence with neutrino oscillations. *Phys. Rev. D* **38**, 2635 (1988)
24. R. Mann, U. Sarkar, Test of the equivalence principle from neutrino oscillation experiments. *Phys. Rev. Lett.* **76**, 865 (1996)
25. K. Nordtvedt Jr., Quantitative relationship between clock gravitational “red-shift” violations and nonuniversality of free-fall rates in nonmetric theories of gravity. *Phys. Rev. D* **11**, 245 (1975)

26. H. Müntinga, H. Ahlers, M. Krutzik, A. Wenzlawski, S. Arnold, D. Becker, K. Bongs, H. Dittus, H. Duncker, N. Gaaloul et al., Interferometry with Bose-Einstein condensates in microgravity. *Phys. Rev. Lett.* **110**, 093602 (2013)
27. M. Zych, F. Costa, I. Pikovski, Č. Brukner, Quantum interferometric visibility as a witness of general relativistic proper time. *Nat. Commun.* **2**, 505 (2011). doi:[10.1038/ncomms1498](https://doi.org/10.1038/ncomms1498)
28. I. Pikovski, M. Zych, F. Costa, Č. Brukner, Universal decoherence due to gravitational time dilation. *Nat. Phys.* **11**, 668–672 (2015)
29. D.M. Greenberger, The role of equivalence in Quantum Mechanics. *Ann. Phys.* **47**, 116–126 (1968). doi:[10.1016/0003-4916\(68\)90229-7](https://doi.org/10.1016/0003-4916(68)90229-7)
30. P.C.W. Davies, J. Fang, Quantum theory and the equivalence principle. *Proc. R. Soc. Lond. Ser. A Math. Phys. Sci.* **381**, 469–478 (1982). doi:[10.1098/rspa.1982.0084](https://doi.org/10.1098/rspa.1982.0084)
31. L. Viola, R. Onofrio, Testing the equivalence principle through freely falling quantum objects. *Phys. Rev. D* **55**, 455–462 (1997). doi:[10.1103/PhysRevD.55.455](https://doi.org/10.1103/PhysRevD.55.455)
32. C. Lämmerzahl, On the equivalence principle in quantum theory. *Gen. Relativ. Gravit.* **28**, 1043–1070 (1996). doi:[10.1007/BF02113157](https://doi.org/10.1007/BF02113157)
33. C. Alvarez, R. Mann, Testing the equivalence principle in the quantum regime. *Gen. Relativ. Gravit.* **29**, 245–250 (1997). doi:[10.1023/A:1010296229642](https://doi.org/10.1023/A:1010296229642)
34. G. Adunas, E. Rodriguez-Milla, D.V. Ahluwalia, Probing quantum violations of the equivalence principle. *Gen. Relativ. Gravit.* **33**, 183–194 (2001)
35. P.C. Davies, Quantum mechanics and the equivalence principle. *Class. Quantum Gravity* **21**, 2761 (2004)
36. E. Kajari, N. Harshman, E. Rasel, S. Stenholm, G. Süßmann, W. Schleich, Inertial and gravitational mass in quantum mechanics. *Appl. Phys. B* **100**, 43–60 (2010). doi:[10.1007/s00340-010-4085-8](https://doi.org/10.1007/s00340-010-4085-8)
37. E. Okon, C. Callender, Does quantum mechanics clash with the equivalence principle and does it matter? *Eur. J. Philos. Sci.* **1**, 133–145 (2011). doi:[10.1007/s13194-010-0009-z](https://doi.org/10.1007/s13194-010-0009-z)
38. A.M. Nobili, D. Lucchesi, M. Crosta, M. Shao, S. Turyshev, R. Peron, G. Catastini, A. Anselmi, G. Zavattini, On the universality of free fall, the equivalence principle, and the gravitational redshift. *Am. J. Phys.* **81**, 527–536 (2013)
39. R. Colella, A. Overhauser, S. Werner, Observation of gravitationally induced quantum interference. *Phys. Rev. Lett.* **34**, 1472–1474 (1975). doi:[10.1103/PhysRevLett.34.1472](https://doi.org/10.1103/PhysRevLett.34.1472)
40. U. Bonse, T. Wroblewski, Measurement of neutron quantum interference in noninertial frames. *Phys. Rev. Lett.* **51**, 1401 (1983)
41. N.D. Birrell, P.C.W. Davies, *Quantum Fields in Curved Space*. No. 7 (Cambridge university press, 1984)
42. B. Ziałyński, M. Zych, Generalization of the Margolus-Levitin bound. *Phys. Rev. A* **74**, 034301 (2006). doi:[10.1103/PhysRevA.74.034301](https://doi.org/10.1103/PhysRevA.74.034301)

Chapter 8

Clocks Beyond Classical Space-Time

Considering clocks as physical systems in quantum mechanics allows for operationally well-defined scenarios where proper time can display quantum properties—i.e. a single clock can run different proper-times in superposition or two clocks can be entangled in their proper times, as discussed in the preceding chapters.

This chapter discusses the regime where quantum theory has to be applied also to the massive systems—which according to General Relativity *define* casual relations between events. Crucially, events are here defined operationally: with respect to physical clocks, i.e. their positions and proper times. We will see that in the considered regime causal relations between events can display quantum properties. Results of this chapter show that using the formalism developed in this thesis, quantum superposition principle can be consistently applied to gravitational degrees of freedom and no inconsistencies arise—even if the resulting space-time is provably non-classical. Moreover, the formalism allows us to make quantitative predictions in simple scenarios involving quantum superpositions of distinct classical causal structures.

8.1 Superpositions of Temporal Order

Quantum mechanics forces us to question whether physical quantities (such as spin, positions or energy) have predefined values. Bell's theorem [1] shows that, if observable quantities were determined by some locally-defined variables, it would be impossible to accomplish certain tasks—such as the violation of the Bell inequalities—whereas such tasks are possible in quantum mechanics [2–7]. However, the time ordering of events is usually assumed to be predetermined in quantum mechanics. Whether an event A is in the past, in the future, or space-like separated from another event B is pre-defined by the location of these events in space-time. In general relativity, space-time itself is dynamical [8–11]. Even if dynamical, however, the causal

structure of classical general relativity is classically pre-defined: causal relations between any pair of events are uniquely determined by the metric, which itself is given by the distribution of matter-energy degrees of freedom in the past light-cone of the events. Causal relations are hence determined by local classical variables. The picture is on the one hand expected to change if one considers quantum states of gravitating degrees of freedom [12]. On the other hand, it is questioned whether it is at all possible to consistently apply quantum theory to gravitational degrees of freedom [13, 14]. Below it is shown explicitly that a preparation of a massive system in a superposition of two distinct states, each yielding a different causal structure for future events, allows for causal relations that display “quantum properties”. In the spirit of Bell’s theorem a task is then formulated which cannot be accomplished if the time ordering between events was pre-determined by some local variables, while the task becomes possible if the events are contained in a space-time region affected by the gravitational field of the massive object. A consistent quantitative treatment of such scenarios is enabled by the quantum “clock” framework, developed in the preceding Chapters of this thesis.

A space-time event can be meaningfully specified only in relation to some physical system, e.g. in terms of the time shown by a given clock. The presence of massive bodies can alter the relative rates at which different clocks tick. For example, in a weak-field approximation, a clock with spatial coordinate x (defined with respect to some fixed observer) in a gravitational potential arising from a mass M positioned at X will run slower by a factor $1 - \frac{\Phi(X-x)}{c^2}$ as compared to a clock at a far away location x' —where $\Phi(X - x') = -\frac{GM}{|X-x'|}$ effectively vanishes. Note, that only the relative distance between the clock and the mass has physical significance. There is no difference, (for the internal evolution of the clock) whether we think of the clock being positioned closer/further away from the mass or the mass being brought closer/further away from the clock. This simple observation shows that internal evolution of the clock which is put in a superposition of two locations: closer and further away from a massive body (studied in details in Chaps. 4 and 5) is analogous to the situation when the massive body is put in a superposition of different locations: further and closer to the clock, see Fig. 8.1. The analogy between the two scenarios is of course limited and Sect. 8.3 discusses some of the differences.

Consider two observers, a and b , with two initially synchronised clocks, and following two different pre-defined world lines.¹ A massive body is then brought in the vicinity of the two observers to induce time dilation between them. The position of the massive body is decided by a third observer, which chooses between two configurations, K_1 and K_2 . For the choice K_1 , the massive body is positioned such that the event A , defined by observer a measuring time $t_a = \tau^*$ on their local clock,

¹One can consider that the world lines are fixed with respect to some far away system, and thus are not affected by the position of the massive bodies in their vicinity. In general, this implies that different accelerations will have to be applied to the observers in order to keep them on the pre-defined world-lines, depending on the position of the mass. However, the latter is not necessary: one can consider spherical mass distributions with different radii placed around the clocks. They result in a potential difference—and thus in a gravitational time dilation between clocks—without exerting a force, leaving the clocks inertial.

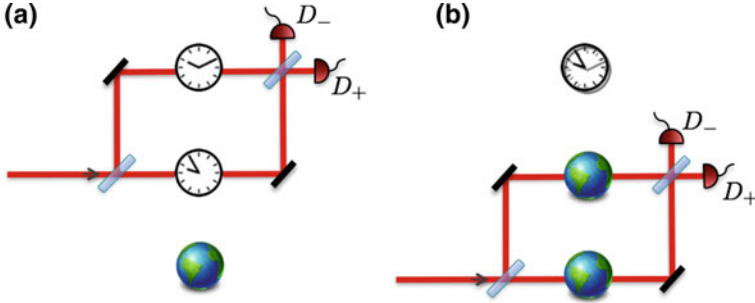


Fig. 8.1 Analogy between time shown by a clock which is **a** in a spatial superposition in a fixed space-time and **b** in a space-time that itself is in a “superposition”, due to a spatial superposition of a large mass. Due to time dilation the clock ticks slower near the massive object than further away from the mass. The state of the clock only depends on a relative distance from the mass. Both: detecting the mass in the detector D_+ (D_-) in (b) and not-detecting the clock in the detector D_- (D_+) in (a) prepare the clock in a state that corresponds to a superposition of two different elapsed proper times

ends up in the past light cone of the event B , defined by observer b measuring time $t_b = \tau^*$. If K_2 is chosen instead, the mass is prepared in a different configuration, such that the event B ends up in the past of event A .

A possible way to realise configuration K_1 is to place an approximately point-like body of mass M closer to b than to a , see Fig. 8.2. If a and b are at the respective fixed distances r_a and $r_b = r_a - h$ (in Schwarzschild coordinates) from the mass, the respective gravitational potentials are given by $\Phi(r_a) = -\frac{GM}{r_a}$ and $\Phi(r_b) \approx -\frac{GM}{r_a} (1 + \frac{h}{r_a})$. An infinitesimal proper time element along a fixed world line at distance r_i is given by

$$d\tau(r_i) = \sqrt{-g_{00}(r_i)} dt, \quad (8.1)$$

where t is the coordinate time and $g_{00}(r_i) \approx -(1 + 2\frac{\Phi(r_i)}{c^2})$ in Schwarzschild metric, to lowest order. Consider an event defined by b 's clock showing time t_b . When observed from a , this event will correspond to the proper time $\bar{t}_a = \sqrt{\frac{g_{00}(r_a)}{g_{00}(r_b)}} t_b$, which follows from Eq. (8.1). (The clocks of a and b are initially synchronised). For the considered metric $\bar{t}_a \approx (1 + \frac{GM}{r_a^2 c^2} h) t_b$. If t_b satisfies: $t_b \geq \frac{2r_a^2 c}{GM}$ there is enough time for a not-faster-than-light signal emitted at the event A , defined by $t_a = \tau^*$, to cover the distance h and reach observer b at the event B , defined by $t_b = \tau^*$. The condition on t_b above is obtained from a condition imposed on τ^* , which goes as follows: The coordinate time for which a photon travels from r_a to r_b reads $T_c = \frac{1}{c} \int_{r_b}^{r_a} dr' \sqrt{-\frac{g_{rr}(r')}{g_{00}(r')}} < 2h/c$ (c.f. Sect. 5.2.1) where $g_{rr}(r') \approx (1 + 2\frac{\Phi(r')}{c^2})^{-1}$ [11] is the radial component of the metric. Photon emitted from location r_a at time $t_a = \tau^*$ reaches r_b at $\bar{t}_b = \sqrt{-g_{00}(r_b)} (\frac{\tau^*}{\sqrt{-g_{00}(r_a)}} + T_c)$ according to the local clock at r_b . (Note that $\frac{\tau^*}{\sqrt{-g_{00}(r_a)}}$ is simply the coordinate time of the photon's emission.) One

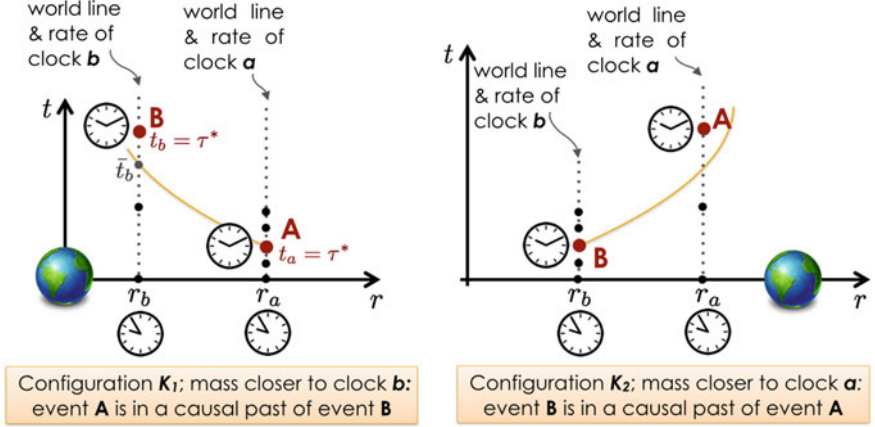


Fig. 8.2 Causal relations between events can be changed by placing mass in different configurations. The diagrams are drawn with respect to coordinate time t and radial distance r and depict world lines (dotted lines) of two clocks positioned at fixed locations r_b and r_a ; the big dots mark equal proper time intervals as measured by the two clocks; A, B label events defined as follows: Event A (B) is defined by the clock positioned at r_a (r_b) indicating proper time τ^* . In configuration K_1 a mass is placed closer to clock b than to clock a . Due to gravitational time dilation event A ends in a causal past of event B ; for a fixed configuration of the clocks and the mass (their relative distances) the time τ^* can be adjusted such that light emitted at event A reaches clock b at its proper time $\bar{t}_b < \tau^*$, i.e. before the event B . The yellow line from A is a null geodesic, a world line of a light pulse emitted at A . In configuration K_2 the mass is placed closer to clock a (at the same distance from a as it is from b in configuration K_1), the clocks remain at their fix positions. In full analogy to the previous configuration, in K_2 the event B ends up before the event A

further requires that $\bar{t}_b \leq \tau^*$ —and this gives the final condition on τ^* . Configuration K_2 can be similarly arranged by placing the mass closer to a than to b .

When A is in the past light-cone of B , a physical system could be transferred from A to B . One can consider a quantum system S initially prepared in a state $|\psi\rangle^S$ which undergoes a unitary operation U_A at event A and a unitary U_B at event B , and so the resulting final state is

$$|\tilde{\psi}_1\rangle^S = U_B U_A |\psi\rangle^S, \quad (8.2)$$

neglecting for simplicity any other time evolution between the two events. If event B is before event A , and we use the same initial state, and apply the same unitaries at the events A and B , the final state reads

$$|\tilde{\psi}_2\rangle^S = U_A U_B |\psi\rangle^S. \quad (8.3)$$

A situation can therefore be arranged such that state (8.2) is produced for configuration K_1 and (8.3) is produced for K_2 . If quantum mechanics applies with no restriction to the massive system, the mass configurations K_1, K_2 can be assigned

quantum states $|K_1\rangle^M$ and $|K_2\rangle^M$, respectively. If K_1, K_2 are macroscopically distinguishable configurations, the two quantum states $|K_1\rangle^M, |K_2\rangle^M$ can be assumed orthogonal. Furthermore, if the quantum states can indeed be assigned to the mass configurations, the superposition state $\frac{1}{\sqrt{2}}(|K_1\rangle^M + |K_2\rangle^M)$ also represents—at least in principle—a physical configuration of the masses. By a straightforward application of the superposition principle, the final state of the mass M and of the system S is then given by

$$\frac{1}{\sqrt{2}}(|K_1\rangle^M U_B U_A |\psi\rangle^S + |K_2\rangle^M U_A U_B |\psi\rangle^S). \quad (8.4)$$

At the formal level, the situation above corresponds to a *quantum control* [15–18] of the order between unitary operations performed at events A and B , which was introduced and studied in the context of information processing tasks and was shown to provide computational advantage over the strategies in which the order of applying operations is fixed [18, 19]. It would not be possible to prepare the superposition state Eq. (8.4) if the unitaries were applied in a fixed order, as in a quantum circuit,—i.e. if the temporal order of events A and B , at which the respective unitaries U_A and U_B are applied, was fixed.

Notice that, if the control system is discarded, the reduced state of the system reads

$$\frac{1}{2}(|\tilde{\psi}_1\rangle\langle\tilde{\psi}_1|^S + |\tilde{\psi}_2\rangle\langle\tilde{\psi}_2|^S). \quad (8.5)$$

The state (8.5) is indistinguishable from a *probabilistic mixture* of the two states $|\tilde{\psi}_1\rangle, |\tilde{\psi}_2\rangle$. This can be interpreted as a situation where the order between the events A and B is fixed, but not known. Hence, any scenario aimed at testing operationally a superposition of time order necessarily requires a measurement of the control system—here: the mass.

8.2 Bell Inequalities for Temporal Order

If the temporal order between the space-time events A and B was fixed, it would not be possible to prepare the state (8.4) by simply applying the unitaries U_A, U_B at the events A and B respectively. In the following section this argument is extended to a protocol that can rule out the existence of any pre-defined event order. The protocol is based on the operations and measurement outcomes of local observers—analogue in spirit to Bell’s argument against local classical variables [1]. It involves two space-like separated *pairs* of observers, which apply operations on two parts of a bipartite quantum system initially prepared in a separable state. If the time order between the operations is classically pre-determined, the final state of the system remains separable. If the event order is “entangled”, then by acting only with local operations

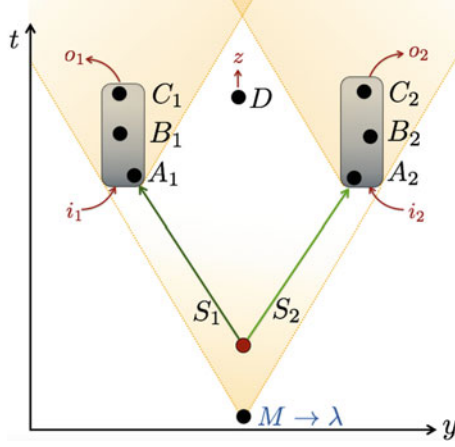


Fig. 8.3 Scenario allowing for the formulation of Bell-like argument for temporal order. A bipartite system, made of subsystems S_1 and S_2 is send to two groups of observers. Observers acting on S_1 at events A_1, B_1, C_1 are given an input bit i_1 , while observers acting on S_2 at events A_2, B_2, C_2 are given an input bit i_2 . The two groups of three events are space like separated from each other, the light cones correspond to the shaded areas in the figure. The observers in each region finally output one bit, denoted o_1, o_2 . The order of the events within each group is controlled by another system M through a variable λ . This system is measured at event D , space-like separated from other events, producing an output z . If the initial state of the joint system of S_1, S_2, M is a product state and λ controlling the order of events is a classical variable (which can be dynamical and probabilistic), then the bipartite statistics of the outcomes produced by the observers does not violate any Bell inequality (assuming that all the operations are faithfully described by quantum theory)

on subsystems in a product state, it is nevertheless possible to create an entangled state and, via appropriate measurements, use it to violate Bell's inequalities.

The following scenario will thus be considered: a bipartite system, with subsystems S_1 and S_2 , is prepared in a separable state; observers a_1 and b_1 perform unitary operations on system S_1 at the space-time events A_1, B_1 , respectively; analogously, observers a_2 and b_2 perform unitary operations on S_2 at events A_2, B_2 ; two additional observers c_1, c_2 perform (the Bell) measurements on the subsystems S_1, S_2 at events C_1, C_2 , respectively; finally, observer d measures the control system (i.e. the massive object) at the event D , see Fig. 8.3.

The notion of events with a pre-defined order is defined as follows:

Definition 1 A set of events is *classically ordered* if, for each pair of events A and B , there exists a space-like surface and a classical variable λ defined on it that determines the causal relation between A and B : for each given λ , either $A < B$ (A in the past causal cone of B), $B < A$ (A in the past causal cone of B), or $A || B$ (A and B space-like separated).

Notice that this definition leaves open the possibility that the order between two events depends on some operation performed in the past (i.e. some other observer can “prepare” λ). Moreover, the classical variable λ might not be fixed deterministically,

but distributed according to some probability. Thus, *classically ordered* events do not necessarily form a partially ordered set: classical order can be *dynamical* and *stochastic*. This is in agreement with classical general relativity, where causal structure of space time is determined by the distribution of mass-energy, via the Einstein equations.

For deriving Bell inequality for temporal order it is here assumed that every local operation performed by each observer is described by quantum mechanics² which can, however, be relaxed to a theory-independent argument.

Definition 2 A multipartite scenario is *locally quantum* if the operations and measurements of each observer are faithfully described by quantum mechanics, i.e. every local operation can be described as a completely positive (CP), trace non-increasing map acting on a space of density matrices.

Theorem 1 Assume that the following conditions hold:

1. The space-time events A_1 , B_1 , and C_1 are space-like separated from the events A_2 , B_2 , and C_2 . All of them are also space-like separated from the event D ;
2. No initially entangled state is shared between the three groups of observers acting at the above specified events;
3. Local quantum operations are performed at the above mentioned events and the resulting multipartite scenario is locally quantum;
4. The events are classically ordered;

then, no bipartite statistics produced at the events A_1 , B_1 , C_1 and A_2 , B_2 , C_2 can violate Bell inequalities, even if conditioned on possible measurement outcomes at event D .

Formal proof of the theorem is presented in the Appendix F.1. Below, only a simple argument is sketched: By assumption (2) no initially entangled state is shared by the three groups of observers; quantum mechanics is valid locally by assumption (3) and the three regions are space-like separated. Any shared resource, that could be used for a violation of Bell inequality, consists of a separable state of subsystems S_1 , S_2 and of a system on which observer d makes a measurement at event D . Because of assumption (4), operations in each region are always performed in a specific order. This order might depend on a classical variable λ defined on some space-like surface in the past and can thus be different for each λ . However, in each case the subsystems S_1 , S_2 are subject to a sequence of three local operations performed at events A_1 , B_1 , C_1 and A_2 , B_2 , C_2 , respectively. Under a sequence of local operations entanglement cannot increase [22], and thus also under a probabilistic mixture of differently ordered sequences. Thus the subsystems S_1 , S_2 remain in a separable state. Results of local measurements performed on S_1 and S_2 by observers c_1 , c_2 at events C_1 , C_2 , respectively, cannot violate Bell inequality; even when results are conditioned on the outcome of any measurement made at D , also when the measurement involves λ , which defines the order.

²The assumption of definite causal order is sufficient to derive *causal inequalities*: tasks that, without any additional assumption, cannot be performed if the causal structure is classical [20]. However, it is not possible to violate causal inequalities using quantum control of order [21].

8.2.1 Violation of Bell Inequalities for Temporal Order

Here it is shown that if the event order is “entangled”, then by acting only with local operations on separable subsystems, it is nevertheless possible to create an entangled state and, via appropriate measurements, use it to violate Bell inequalities.

A bipartite quantum system, initially in a product state $|\psi_1\rangle^{S_1}|\psi_2\rangle^{S_2}$, is sent to two different regions of space, such that: observers a_1, b_1 , and c_1 only interact with S_1 , while observers a_2, b_2 , and c_2 only interact with S_2 . Observers a_1, a_2 perform respectively the unitaries U_{A_1}, U_{A_2} at the events A_1, A_2 , while observers b_1, b_2 , perform the unitaries U_{B_1}, U_{B_2} at the events B_1, B_2 . Observers c_1 and c_2 measure the subsystems S_1 and S_2 at events C_1 and C_2 , respectively, as depicted in Fig. 8.4.

Now assume that a massive system can be prepared in two configurations, K_1 and K_2 , such that $A_1 \prec B_1 \prec C_1$ and $A_2 \prec B_2 \prec C_2$ for K_1 , while $B_1 \prec A_1 \prec C_1$ and $B_2 \prec A_2 \prec C_2$ for K_2 ; and such that the two groups of three events are always

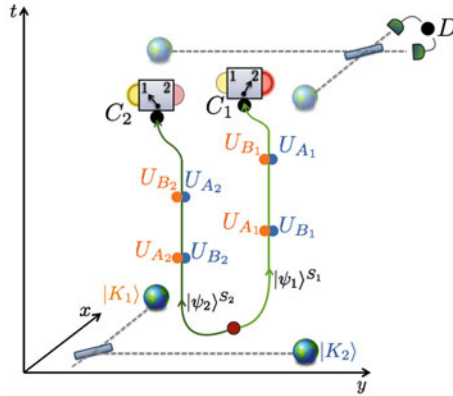


Fig. 8.4 Protocol for the preparation of an entangled state and for a violation of Bell’s inequalities, enabled by entanglement of temporal order of events. A bipartite system is prepared in a product state $|\psi_1\rangle^{S_1}|\psi_2\rangle^{S_2}$ of its two subsystems S_1, S_2 , which are then sent to two regions of space. One pair of observers perform unitary operations U_{A_1} and U_{B_1} on S_1 at the correspondingly marked space-time events; another pair act on S_2 with unitary operations U_{A_2} and U_{B_2} . Each operation is applied by the observer only once at an event defined by their local clock. Suppose a mass can be prepared in a spatial superposition of two macroscopically distinct states $|K_1\rangle$ and $|K_2\rangle$ which define different causal structure for future events, see Fig. 8.2 (the world lines of the two mass amplitudes are not depicted for better clarity). The following colour code is used: when amplitude $|K_1\rangle$ ($|K_2\rangle$) is realised, only events marked by orange (blue) dots occur. For the amplitude $|K_1\rangle$ the event when U_{A_i} $i = 1, 2$ is applied on S_i occurs in the causal past of the event when U_{B_i} is applied; and vice versa for the state $|K_2\rangle$. The operations can be chosen such that $U_{A_i} U_{B_i} |\psi_i\rangle^{S_i}$ is orthogonal to $U_{B_i} U_{A_i} |\psi_i\rangle^{S_i}$ and thus the final state of the subsystems is entangled. Bell measurements are performed at events C_1 and C_2 on S_1 and S_2 , respectively. At event D the mass, which controlled the order of events, is measured in a superposition basis. Conditioned on the outcome of the measurement at D , the results of the Bell test can be used to violate Bell’s inequalities. If the order of events is pre-defined it is not possible to prepare an entangled state by acting only locally on two uncorrelated subsystems and measurements of c_1, c_2 cannot violate any Bell inequality

space-like separated from each other. If the mass is prepared in the superposition $\frac{1}{\sqrt{2}}(|K_1\rangle^M + |K_2\rangle^M)$, the joint mass-system state after applying the unitaries (and before the measurements at C_1, C_2) reads

$$\frac{1}{\sqrt{2}}(|K_1\rangle^M U_{B_1} U_{A_1} |\psi_1\rangle^{S_1} U_{B_2} U_{A_2} |\psi_2\rangle^{S_2} + |K_2\rangle^M U_{A_1} U_{B_1} |\psi_1\rangle^{S_1} U_{A_2} U_{B_2} |\psi_2\rangle^{S_2}). \quad (8.6)$$

The observer d at the event D measures the massive system in the superposition basis $|\pm\rangle^M = \frac{1}{\sqrt{2}}(|K_1\rangle^M \pm |K_2\rangle^M)$. The state of the system conditioned on the outcome of the measurement at D , is

$$\frac{1}{\sqrt{2}}(U_{B_1} U_{A_1} |\psi_1\rangle^{S_1} U_{B_2} U_{A_2} |\psi_2\rangle^{S_2} \pm U_{A_1} U_{B_1} |\psi_1\rangle^{S_1} U_{A_2} U_{B_2} |\psi_2\rangle^{S_2}). \quad (8.7)$$

If the states $U_{B_1} U_{A_1} |\psi_1\rangle^{S_1}, U_{B_2} U_{A_2} |\psi_2\rangle^{S_2}$ are orthogonal to the states $U_{A_1} U_{B_1} |\psi_1\rangle^{S_2}, U_{A_2} U_{B_2} |\psi_2\rangle^{S_2}$, respectively, then (8.7) is a maximally entangled state. As a concrete example, consider a two-qubit system with initial state $|\psi_1\rangle^{S_1} \otimes |\psi_2\rangle^{S_2} \equiv |z+\rangle^{S_1} \otimes |z+\rangle^{S_2}$. As local unitaries one can choose

$$U_{A_1} = U_{A_2} \equiv U_A = \frac{\mathbb{1} + i\sigma_x}{\sqrt{2}}, \quad U_{B_1} = U_{B_2} \equiv U_B = \sigma_z, \quad (8.8)$$

where σ_x and σ_z are the usual Pauli matrices. Notice that $U_A U_B = \frac{\sigma_z + \sigma_y}{\sqrt{2}}$, while $U_B U_A = \frac{\sigma_z - \sigma_y}{\sqrt{2}}$. The final state (8.7) is in this case

$$\frac{1}{\sqrt{2}}(|x+\rangle^{S_1} |x+\rangle^{S_2} \pm |x-\rangle^{S_1} |x-\rangle^{S_2}), \quad (8.9)$$

where the sign depends on the outcome $|\pm\rangle$ of the measurement on the massive system.

Local measurements can be performed by c_1, c_2 on the state (8.9), which violate Bell inequalities, conditioned on the measurement outcome at D . In order to observe violation of Bell inequalities, the observer c_1 measures the observable $\mathcal{C}_1^0 = \frac{\sigma_y - \sigma_z}{\sqrt{2}}$ for the setting $i_1 = 0$ and the observable $\mathcal{C}_1^1 = \frac{\sigma_y + \sigma_z}{\sqrt{2}}$ for $i_1 = 1$, while c_2 measures $\mathcal{C}_2^0 = \sigma_y$ for $i_2 = 0$ and $\mathcal{C}_2^1 = \sigma_z$ for $i_2 = 1$. With these measurement choices, the expectation value for the CHSH correlation [23] reads

$$\langle CHSH \rangle_{\pm} = \langle \mathcal{C}_1^0 \otimes \mathcal{C}_2^0 + \mathcal{C}_1^0 \otimes \mathcal{C}_2^1 + \mathcal{C}_1^1 \otimes \mathcal{C}_2^0 - \mathcal{C}_1^1 \otimes \mathcal{C}_2^1 \rangle_{\pm} = \mp 2\sqrt{2}, \quad (8.10)$$

where the sign \pm corresponds to the outcomes of the measurement at D . Thus, conditioned on the outcome at D , the measurements at C_1 and C_2 violate the CHSH inequality which requires $|\langle CHSH \rangle| \leq 2$. In order to close a potential loophole that settings choices at C_1, C_2 are communicated to D , the event D is space-like separated

from other events involved in the protocol. Thus, the measurement settings at C_1 and C_2 are also independent of the outcome at D . The three measurements performed by c_1, c_2, d are realised at space-like separation, and the violation of the inequality is recovered when all the data are compared.

Ideas for physical implementation of the protocol The violation of the CHSH inequalities, Eq. (8.10) implies that at least one of the assumptions of the Theorem 1 does not hold. A physical realisation of the scenario is in principle possible where the preparation of the state of the system and masses satisfies all the assumptions and thus the violation of the inequalities leads to the conclusion that the assumption of a *classical order* of events is violated, i.e. the causal relation between the events cannot be classically defined. Two examples of a physical implementation of the scenario are depicted in Fig. 8.5. In all the scenarios the involved clocks are initially synchronised and the mass configurations K_1, K_2 are obtained by placing effectively point like body with a fixed mass at various locations with respect to the observers.

In the first example, the distance between observers $b_i, i = 1, 2$ and the mass is the same for both K_1 and K_2 , while observers a_i are closer to the mass in configuration K_2 than in K_1 , Fig. 8.5a. The subsystems S_i can be realised as two identically prepared, uncorrelated photons and the local operations can be performed on the photons' polarisation degrees of freedom. The source emitting the photons is equally distant from K_1 and K_2 —so that its local clock remains uncorrelated with the mass. At a pre-defined time T_s (as measured by the source) after the state of the mass has been prepared, the source emits the photon pair. One of the photons is directed towards observer a_1 then to b_1 again to a_1 back to b_1 and then exits towards observer c_1 (or observer c_1 replaces observer a_1), Fig. 8.5b. The other photon is reflected between a_2 and b_2 in exactly the same manner and is then reflected towards c_2 . Photon's emission time is chosen such that for the mass configuration K_1 event A_1 at which U_{A_1} is applied occurs when the photon reaches a_1 for the first time, and when K_2 —when the photon reaches a_1 for the second time. The event when the operation U_{B_1} is applied for both cases occurs when the photon reaches b_1 for the first time. The same holds for the other photon on which observers a_2, b_2 are acting. The scenario assumes that the observers interact with the photon only once, and only at a fixed, pre-agreed time which they measure with their local clocks. In general, the travel time of the photon between the observers will depend on the mass configuration (due to the Shapiro delay, see Sect. 5.2.1). In order to avoid this effect, the mass can be (coherently) moved far away from the region where the observers are located after the state of the local clocks defining events A_i and B_i have been prepared. In order to decorrelate the clocks from the state of the systems S_i a swap operation on the mass is preformed and it is brought back in the same location. After time T_s the clock of the observers a_i, b_i become synchronised again and de-correlate from the mass. The mass is then measured by observer d and the observers c_1, c_2 can perform Bell measurements as discussed above.

Another possibility for the realisation of the protocol is depicted in Fig. 8.5c, d. The mass distribution, Fig. 8.5c, is such that K_1 is closer to b_1 than to a_1 and for K_2 the relative distances are reversed. The same holds for observers a_2, b_2 who

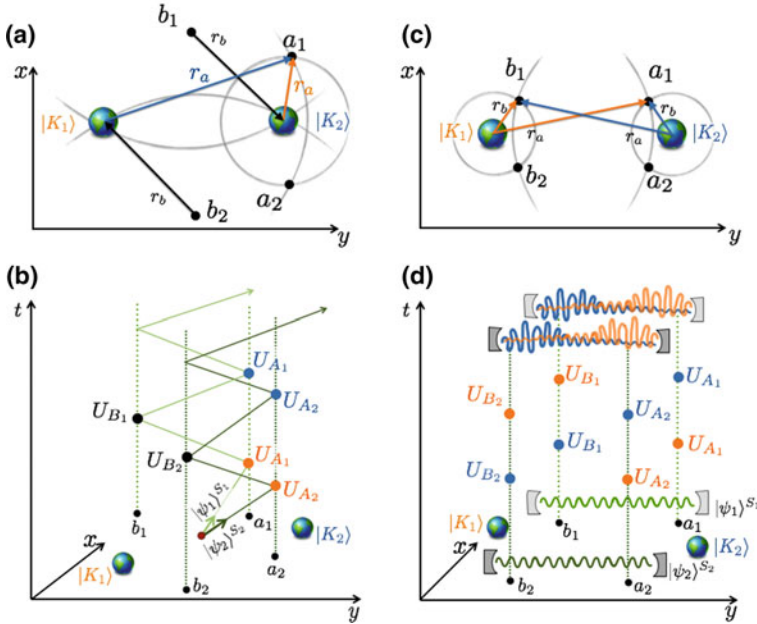


Fig. 8.5 Examples of two realisations of the protocol for violation of Bell's inequalities for temporal order of events. First example: **a** Locations of the mass in configurations K_1 , K_2 with respect to the observers a_i, b_i , $i = 1, 2$. Observers b_i are at a distance r_b from both K_i , while a_i is at a distance r_a from K_2 and $r'_a > r_a$ from K_1 . **b** Sketch of the world lines of the two subsystems S_i (green lines) and observers (dotted lines). The subsystem S_i is initially in a state $|\psi_i\rangle^{S_i}$. Events when the observers a_i act on S_i for the case when K_1 (K_2) is prepared are marked with an orange (blue) dot. They are labelled by the operation U_{A_i} which the observer a_i apply. Each operation is applied only once. Events when b_i apply unitary U_{B_i} on the subsystem S_i are marked by a black dot—they are independent of which configuration is prepared (in the specific case depicted in **a**). Second example: **c** In configuration K_1 the mass is at the same distance r_b from both b_i and at a distance $r_a < r_b$ from both a_i . For the configuration K_2 the mass is at the distance r_a from b_i , and at r_b from a_i . **d** The subsystems S_i are implemented in two regions of a vacuum state of an electromagnetic field. Observers a_i, b_i apply the operations U_{A_i}, U_{B_i} locally on the field. The notation for observers and labelling of events, including the colour code, are the same as in **b**. Likewise, for the case when configuration K_1 (K_2) is prepared the final state of the field is represented in orange (blue). The figure suggests that these field modes are orthogonal, in which case the final state of the subsystems (the two regions of the field) is maximally entangled

are placed symmetrically to observers a_1, b_2 with respect to the axis defined by the locations of the mass. The local operations can be performed in the Fock space of a photon field, more precisely in the two-level system spanned by the vacuum and a single-photon state. The photon field is prepared in mode a at event A_1 , and in mode b at event B_1 . The modes are chosen such, that the two possible final states of the field at event C_1 —corresponding to the order between events A_1, B_1 —are distinguishable. The situation for the observers a_2, b_2 is the same and they prepare the modes a, b , at the events A_2, B_2 , respectively, see Fig. 8.5d. One needs to note,

that vacuum of a relativistic quantum field is an entangled state [24–26] with respect to local subsystems. However, this entanglement is effectively inaccessible under coarse-grained operations [27]. Thus, if the operations performed by the observers are sufficiently coarse-grained, the initial state consisting of the local regions of a vacuum of a quantum field is effectively separable and does not violate the assumptions of the protocol. This implementation might offer an important advantage as compared to the first example, in that the states on which the observers act do not have to be distributed such as to enter their laboratories exactly when the operations need to be applied and also do not have to be actively exchanged between the observers multiple time.

8.3 Discussion

Space-time events used in the above argument were “attached” to coordinates defined by the local clocks of the observers. Instead, one could consider coordinates defined by the massive body, which is here in a spatial superposition, and define events with respect to these coordinates. In such a case, the operations performed by the observers will appear to be “in a superposition” of different space-time coordinates. The assumption that operations are local is then not satisfied and it is possible to re-interpret the violation of Bell inequalities as being embedded in a space-time with classically ordered events, but non-local coordinates. Physical meaning of such “quantum coordinate systems” is yet to be investigated.

Moreover, analogous “superposition” of the order of events can be achieved when the events are defined by clocks that were subject to the interferometric experiment discussed in Chaps. 4 and 5, see Fig. 8.1. In that case, however, these clocks are the only systems that can be used to label events for which temporal order is not classically defined. In the scenario considered in this chapter, any clock in the space-time region “affected” by the mass superposition will have classically undefined proper time. Thus, any pair of clocks will in general define events with non-classical causal relations. In both cases entanglement is created between the (internal) state of the clocks and their distance to the mass, however, in the case when the clock is fixed with respect to a far away observer and the mass is in a superposition with respect to him/her, the observer can violate Bell inequalities by making measurements on the internal states of the clock and the position of the mass. In the case of the interferometric experiment with clocks, both measurements would have to be realised on the clock—on its internal and position degrees of freedom (as the massive body has a well-defined position with respect to the observer). Despite the differences between these two scenarios, the analogy suggests that non-classical causal relations are a new feature already arising at the interplay between quantum theory and classical general relativity and one does need a quantum gravity framework to describe them; Neither they pose a challenge to the self-consistency of the theory.

The mass distributions can be prepared such, that the same force is exerted at the various events but the potential is different—such that there is time dilation between

local clocks, e.g. by using spherical shells of mass of different radii, instead of point-like mass distributions. In such a case, observers cannot detect, through local measurements, which of the two configurations was prepared. This is different from the realisations of quantum control of time order considered in the context of computations within an extended model of a quantum circuit: where gates acting on the system might be applied in different orders in superposition [15–18]. In the latter, one considers a situation in which, for example, a photon is sent to a beam splitter and if transmitted—it is directed first to an apparatus A and then to another apparatus B , while if it is reflected—it is directed first to B and then to A . Also in this case, the operations realised at A and at B are performed on the photon in a superposition of orders. However, one could, in principle, perform a non-demolition measurement on the photon, measuring its time of arrival at the devices A and B with local clocks. If the clocks are precise enough, the observers can distinguish whether the photon reached their station first or second, thus destroying the superposition. This is not possible in the gravitational scenario: all the observers a_1, b_1, a_2, b_2 perform their local operations when their local clocks show the same pre-established time t^* , thus no local measurement can tell whether they are acting first or second. Thus, there seems to be a fundamental difference between the laboratory and the time-dilation realisation of the control: in the first case, each operation is performed at two different times in superposition, while in the second each operation is performed at a fixed time, but the order between them is in a superposition. On the other hand, “two different times in superposition” means that there *cannot* be any information about the time at which the operation was performed in the quantum circuit scenario, since this will destroy the superposition and alter the outcomes of the protocol.

The effect considered in this chapter appears in a semi-classical, albeit non-perturbative, regime, where gravitational field is not explicitly quantised. Such an approach is complementary to the perturbative methods employed by most quantum gravity theories,³ see e.g. [29] for an overview. Entirely new conceptual features appear in this regime from the combination of general relativity and quantum mechanics; no inconsistency or conceptual tensions arise when considering superpositions of space-times with different time evolutions or even different causal structures, in contrast to Refs. [13, 14, 30]. Indeed, it is often presumed that it is not possible even in principle to address scenarios involving superpositions of space-time, and one postulates that intrinsic and fundamentally irreversible decoherence must then take place. This ideas date back to Feynman who speculated that quantum theory could break down at macroscopic scales [31], and to the work of Hawking [32] showing that non-unitary evolution is a generic feature of quantum gravity.⁴ Other approaches

³There are also attempts for a non-perturbative approach to Lorentzian quantum gravity within the causal dynamical triangulation method [28].

⁴In the reference [32] the non-unitarity is derived from considering fluctuations of space-time metric away from being globally hyperbolic, in which case the Green functions of any quantum field theory in such a space-time do not satisfy asymptotic completeness and thus (in general) there is no unitary evolution between states of the fields in the asymptotic past and future.

[13, 14] postulate a “gravitational collapse” of spatial superpositions of massive objects, which is attributed to time-energy uncertainty in the assumed gravitational self-interaction between the superposed amplitudes of a single mass. A different approach has been proposed in Ref. [30], where gravitational self-interaction is postulated within the path integral formulation of quantum mechanics, which also leads to suppression of spatial superpositions of massive particles.

Approach presented in this chapter challenges the very assumptions underlying intrinsic decoherence or collapse programs: that superposition principle of quantum theory cannot be consistently applied to space-time. The above sketched method based on the quantum “clock” framework allows analysing and making predictions in scenarios involving superpositions of macroscopically different backgrounds: For each probability amplitude, time-dilation effects introduced by gravity can be treated completely classically. The considered process involves a simple superposition of such amplitudes and the final probability is obtained from the Born rule applied to the sum of the involved amplitudes.

The formal motivation for intrinsic gravitational decoherence is that points on different manifolds cannot, in general, be uniquely mapped onto each other [14]. The present work challenges the physical relevance of this argument. It proposes an *operational* treatment of events—identified with physical objects—in contrast to defining events as points on an abstract space-time manifold. Furthermore, the approach of this thesis is to take the relations between physical systems as fundamental, and then abstract the notion of space-time that is compatible with them—rather than taking space-time as fundamental. Since non-classical relations between physical systems can readily be described within quantum and general relativistic frameworks, the present approach immediately yields quantitative description of non-classical space-times, such as those resulting from quantum superpositions of massive objects. This is in contrast with a viewpoint that the notion of space time is not only fundamental, but also necessarily classical.

Finally, one could object the very possibility of realising the proposed protocol in the manner satisfying all other assumptions (other than that of classical time order). One could also argue that the Bell inequality for temporal order can never, even in principle, be violated. Both these imply that one could always describe time order between events by some classical variable (e.g. by the parameter λ). Such a classical variable could then be used to define time parameter describing Schrödinger time evolution—even in scenarios involving quantum states of large masses. Such a position thus renders the very quest for a mechanism preventing, or destroying, quantum superpositions of massive systems completely obsolete, as such mechanisms are motivated by the expectation that no time parameter can consistently be defined that would describe time evolution in a region affected by macroscopic superposition states.

References

1. J.S. Bell, On the Einstein-Podolsky-Rosen paradox. *Physics* **1**, 195–200 (1964)
2. S.J. Freedman, J.F. Clauser, Experimental test of local Hidden-Variable theories. *Phys. Rev. Lett.* **28**, 938–941 (1972)
3. A. Aspect, P. Grangier, G. Roger, Experimental test of local Hidden-Variable theories via Bell's theorem. *Phys. Rev. Lett.* **47**, 460–463 (1981)
4. M. Giustina, A. Mech, S. Ramelow, B. Wittmann, J. Kofler, J. Beyer, A. Lita, B. Calkins, T. Gerrits, S.W. Nam, R. Ursin, A. Zeilinger, Bell violation using entangled photons without the fair-sampling assumption. *Nature* **497**, 227–230 (2013)
5. B. Hensen, H. Bernien, A. Dréau, A. Reiserer, N. Kalb, M. Blok, J. Ruitenbergh, R. Vermeulen, R. Schouten, C. Abellán et al., Loophole-free Bell inequality violation using electron spins separated by 1.3 kilometres. *Nature* **526**, 682–686 (2015)
6. M. Giustina, M.A.M. Versteegh, S. Wengerowsky, J. Handsteiner, A. Hochrainer, K. Phelan, F. Steinlechner, J. Kofler, J.-A. Larsson, C. Abellán, W. Amaya, V. Pruneri, M.W. Mitchell, J. Beyer, T. Gerrits, A.E. Lita, L.K. Shalm, S.W. Nam, T. Scheidl, R. Ursin, B. Wittmann, A. Zeilinger, Significant-Loophole-Free test of Bell's theorem with Entangled Photons. *Phys. Rev. Lett.* **115**, 250401 (2015)
7. L.K. Shalm, E. Meyer-Scott, B.G. Christensen, P. Bierhorst, M.A. Wayne, M.J. Stevens, T. Gerrits, S. Glancy, D.R. Hamel, M.S. Allman, K.J. Coakley, S.D. Dyer, C. Hodge, A.E. Lita, V.B. Verma, C. Lambrocco, E. Tortorici, A.L. Migdall, Y. Zhang, D.R. Kumor, W.H. Farr, F. Marsili, M.D. Shaw, J.A. Stern, C. Abellán, W. Amaya, V. Pruneri, T. Jennewein, M.W. Mitchell, P.G. Kwiat, J.C. Bienfang, R.P. Mirin, E. Knill, S.W. Nam, Strong Loophole-Free test of local Realism*. *Phys. Rev. Lett.* **115**, 250402 (2015)
8. A. Einstein, The foundation of the general theory of relativity. *Annalen der Physik* **40**, 284–337 (1916)
9. S.M. Carroll, *Spacetime and Geometry. An Introduction to General Relativity*, vol. 1 (Addison-Wesley, 2004)
10. C.W. Misner, K.S. Thorne, J.A. Wheeler, *Gravitation* (Macmillan, 1973)
11. S. Weinberg, *Gravitation and Cosmology: Principle and Applications of General Theory of Relativity* (Wiley, New York, 1972)
12. L. Hardy, Probability theories with dynamic causal structure: a new framework for quantum gravity. [arXiv:0509120](https://arxiv.org/abs/0509120) [gr-qc]
13. L. Diósi, Models for universal reduction of macroscopic quantum fluctuations. *Phys. Rev. A* **40**, 1165 (1989)
14. R. Penrose, On gravity's role in quantum state reduction. *Gen. Relativ. Gravit.* **28**, 581–600 (1996)
15. G. Chiribella, G.M. D'Ariano, P. Perinotti, B. Valiron, Quantum computations without definite causal structure. *Phys. Rev. A* **88**, 022318 (2013)
16. G. Chiribella, Perfect discrimination of no-signalling channels via quantum superposition of causal structures. *Phys. Rev. A* **86**, 040301 (2012)
17. T. Colnaghi, G.M. D'Ariano, S. Facchini, P. Perinotti, Quantum computation with programmable connections between gates. *Phys. Lett. A* **376**, 2940–2943 (2012)
18. M. Araújo, F. Costa, Č. Brukner, Computational advantage from Quantum-Controlled ordering of gates. *Phys. Rev. Lett.* **113**, 250402 (2014)
19. L.M. Procopio, A. Moqanaki, M. Araújo, F. Costa, I.A. Calafell, E.G. Dowd, D.R. Hamel, L.A. Rozema, Č. Brukner, P. Walther, Experimental superposition of orders of quantum gates. *Nat. Commun.* **6** (2015)
20. O. Oreshkov, F.M. Costa, Č. Brukner, Quantum correlations with no causal order. *Nat. Commun.* **3**, 1092 (2012)
21. M. Araújo, C. Branciard, F. Costa, A. Feix, C. Giarmatzi, and Č. Brukner, Witnessing causal nonseparability. *New. J. Phys.* **17**, 102001 (2015) doi:[10.1088/1367-2630/17/10/102001](https://doi.org/10.1088/1367-2630/17/10/102001)
22. M.A. Nielsen, Conditions for a class of entanglement transformations. *Phys. Rev. Lett.* **83**, 436–439 (1999)

23. J.F. Clauser, M.A. Horne, A. Shimony, R.A. Holt, Proposed experiment to test local Hidden-Variable theories. *Phys. Rev. Lett.* **23**, 880–884 (1969)
24. H. Reeh, S. Schlieder, Bemerkungen zur unitaeraequivalenz von lorentzinvarianten feldern. II *Nuovo Cimento* **22**, 1051–1068 (1961)
25. S.J. Summers, R. Werner, Bell's inequalities and quantum field theory. I. General setting. *J. Math. Phys.* **28**, 2440–2447 (1987)
26. S.J. Summers, R. Werner, Bell's inequalities and quantum field theory. II. Bell's inequalities are maximally violated in the vacuum. *J. Math. Phys.* **28**, 2448–2456 (1987)
27. M. Zych, F. Costa, J.J. Kofler, Č. Brukner, Entanglement between smeared field operators in the Klein-Gordon vacuum. *Phys. Rev. D* **81**, 125019 (2010)
28. J. Ambjoern, A. Goerlich, J. Jurkiewicz, R. Loll, Nonperturbative quantum gravity. *Phys. Rep.* **519**, 127–210 (2012)
29. C. Kiefer, *Quantum Gravity (General) and Applications* (Springer, Berlin, 2009)
30. P.C.E. Stamp, Environmental decoherence versus intrinsic decoherence. *Phil. Trans. R. Soc. A* **370**, 4429–4453 (2012)
31. R.P. Feynman, R.B. Leighton, M. Sands, *The Feynman Lectures on Physics. vol. 3: Quantum Mechanics* (Addison-Wesley Publishing Co., Inc., Reading, Mass.-London, 1965)
32. S.W. Hawking, The unpredictability of quantum gravity. *Commun. Math. Phys.* **87**, 395–415 (1982)

Chapter 9

Conclusions and Outlook

Quantum effects have been demonstrated with complex systems comprising tens of thousands of atoms [1–5]. The regime where general relativity affects internal dynamics of such systems might soon allow testing the interplay between quantum mechanics and general relativity.

This thesis aimed to take the first steps in developing a complete framework describing composite quantum systems in general background space-time, and to apply the framework for designing new experiments that would finally test of the overlap between quantum mechanics and general relativity. It has been shown that the framework of relativistic point-like particles with internal dynamics is a consistent theory (both in the classical and in the quantum case) with its own symmetry group (central extensions of the Poincaré group, and in the low energy regime—central extension of the Galilei group), physical effects and phenomenology required for testing its validity. In order to build physical intuition for this new regime, it has been shown that point-like particles with internal dynamics can be seen as ideal “clocks” and that the new physical effects arising from the relativistic quantum “clock” formalism can be understood in terms of time dilation and quantum complementarity principle.

Furthermore, the operational approach to proper time and clocks provided a quantitative description of scenarios where superposition principle is applied to the space-time itself, more precisely: to the massive degrees of freedom whose distribution influences the causal structure of space time according to general relativity. The identification of space-time events with physical systems (rather than with points on an abstract space-time manifold) combined with the “clock” framework led to the conclusion that on the one hand the resulting causal structure is provably non-classical—as it contains time-like events whose temporal order is in a quantum superposition of distinct classical possibilities, or even is entangled with the temporal order of other time-like events—and, on the other hand, that no tension or inconsistency arises between quantum superposition principle and general relativity, contrary to a common expectation [6–9].

Characterisation of the properties and limitations of the approach developed in the thesis is far from complete. For example, the regime where space-time curvature becomes relevant has not yet been addressed within this framework. Further research is also required for a complete understanding of the relation between this regime and quantum field theory in curved space-time. Further investigation of the decoherence mechanism caused by the time dilation is also still ahead. For example, the assumption of factorisable initial states and of fixed centre of mass trajectories should be relaxed and the interplay between effects that build up coherence of the superposition and the decoherence effects should be further investigated. Moreover, the decoherence basis in a general case—when time dilation between superposed amplitudes arises both from kinetic (special relativistic) and gravitational effects—is expected to be given by a combination of the position and momentum eigenstates. Whether time dilation results in decoherence into classical-like states, such as the Gaussian wave-packets, is not yet known. Finally, the regime where quantum superpositions of space-time are permitted, features effects which in key aspects are analogous to the effects arising in a fully classical space-time—where only the systems that define events require a quantum description. Further investigation of these analogies will likely sharpen our understanding of what a “genuine quantum gravity” stands for. Moreover, this analogy strongly suggests the necessity of extending the equivalence hypothesis to include equivalence between effects stemming from a superposition of distinct gravitational potentials and a corresponding superposition of differently accelerating reference frames. This would further require to extend the notion of covariance—physical equivalence of all coordinate systems—to include “quantum coordinate system”, which correspond to a “superposition” of different classical coordinates. A theory incorporating such quantum-extended covariance (i.e. invariant under transformations between “quantum coordinate systems”) would provide a new and potentially very useful approach to study joint foundations of general relativity and quantum mechanics.

Research on the interplay of quantum theory and general relativity can contribute to breaking new grounds in theory and trigger experimental exploration of new physical regimes. Moreover, a thorough understanding of this regime will eventually become necessary for the design and analysis of generic quantum experiments with complex quantum systems, as they will unavoidably reach the scale where effects of general relativity have to be considered. Future large-scale quantum technologies involving e.g. quantum communication through satellites [10–13] will have to account for relativistic gravity effects for their correct functioning—as much as the present-day technologies, such as the Global Positioning System, have to incorporate general relativistic effects for their proper work. Furthermore, the study of time dilation as a decoherence mechanism is directly relevant to the research on the origin of the “quantum-to-classical transition”—the emergence of classical physics from the quantum physical laws. In particular as it is conjectured that gravity can play a role in suppressing quantum effects in macroscopic systems [6, 7, 9, 14–16]. Research on the quantum-and-gravity interplay can also benefit studies in quantum gravity: New experiments will finally allow diminishing the gap between directly accessible regime and the supposed quantum gravity domain; Development of complemen-

tary formal methods, especially non-perturbative ones, for approaching conceptual questions in quantum gravity can reveal entirely novel features of this regime, not accessible by perturbative means. In particular, the study of novel features related to time and causality might allow answering whether (and how) recently discovered indefinite causal order [17–19] might be realised in nature. So far indefinite causal order—purported new resource for quantum information processing [20]—was studied from a purely information-theoretic perspective [21–24]. Further research can provide first answers to the question: what is the physical content of this new formalism and what is its relation to quantum gravity?

Besides bringing new results in fundamental science, studies of the joint foundation of quantum mechanics and general relativity can engage the public and can be highly beneficial in science outreach and education. Fundamental concepts of this field can easily be visualised and communicated in a non-technical way, inspiring even the youngest audience. Surprising and thought-provoking experiments that will eventually be triggered by such research, will likely catalyse public interest in basic science, which can further raise awareness and support for fundamental research.

References

1. M. Arndt, O. Nairz, J. Vos-Andreae, C. Keller, G. Van der Zouw, A. Zeilinger, Wave-particle duality of C60 molecules. *Nature* **401**, 680–682 (1999)
2. L. Hackermüller, K. Hornberger, B. Brezger, A. Zeilinger, M. Arndt, Decoherence of matter waves by thermal emission of radiation. *Nature* **427**, 711–714 (2004)
3. S. Gerlich, S. Eibenberger, M. Tomandl, S. Nimmrichter, K. Hornberger, P.J. Fagan, J. Tüxen, M. Mayor, M. Arndt, Quantum interference of large organic molecules. *Nat. Commun.* **2**, 263 (2011)
4. S. Eibenberger, S. Gerlich, M. Arndt, M. Mayor, J. Tüxen, Matter-wave interference of particles selected from a molecular library with masses exceeding 10000 amu. *Phys. Chem. Chem. Phys.* **15**, 14696–14700 (2013)
5. P. Haslinger, N. Dörre, P. Geyer, J. Rodewald, S. Nimmrichter, M. Arndt, A universal matter-wave interferometer with optical ionization gratings in the time domain. *Nat. Phys.* **9**, 144–148 (2013)
6. L. Diósi, Models for universal reduction of macroscopic quantum fluctuations. *Phys. Rev. A* **40**, 1165 (1989)
7. R. Penrose, On gravity’s role in quantum state reduction. *Gen. Relativ. Gravit.* **28**, 581–600 (1996)
8. L. Diósi, Intrinsic time-uncertainties and decoherence: comparison of 4 models. *Braz. J. Phys.* **35**, 260265 (2005)
9. P.C.E. Stamp, Environmental decoherence versus intrinsic decoherence. *Phil. Trans. R. Soc. A* **370**, 4429–4453 (2012)
10. D. Rideout, T. Jennewein, G. Amelino-Camelia, T.F. Demarie, B.L. Higgins, A. Kempf, A. Kent, R. Laflamme, X. Ma, R.B. Mann et al., Fundamental quantum optics experiments conceivable with satellites-reaching relativistic distances and velocities. *Class. Quantum Gravity* **29**, 224011 (2012)
11. T. Scheidl, R. Ursin, Space-QUEST: quantum communication using satellites. in *Proceedings of International Conference on Space Optical Systems and Applications (ICSOS)*, Ajaccio, Corsica, France, 2012, pp. 2–4 (2012)

12. T. Scheidl, E. Wille, R. Ursin, Quantum optics experiments using the international space station: a proposal. *New J. Phys.* **15**, 043008 (2013)
13. G. Vallone, D. Bacco, D. Dequal, S. Gaiarin, V. Luceri, G. Bianco, P. Villoresi, Experimental satellite quantum communications. *Phys. Rev. Lett.* **115**, 040502 (2014)
14. A. Bassi, K. Lochan, S. Satin, T.P. Singh, H. Ulbricht, Models of wave-function collapse, underlying theories, and experimental tests. *Rev. Mod. Phys.* **85**, 471 (2013)
15. C. Gooding, W.G. Unruh, Self-gravitating interferometry and intrinsic decoherence. *Phys. Rev. D* **90**, 044071 (2014)
16. C. Gooding, W.G. Unruh, Bootstrapping time dilation decoherence. *Found. Phys.* **45**, 1166–1178 (2015)
17. O. Oreshkov, F.M. Costa, Č. Brukner, Quantum correlations with no causal order. *Nat. Commun.* **3**, 1092 (2012)
18. T. Rudolph, Quantum causality: information insights. *Nat. Phys.* **8**, 860–861 (2012)
19. Č. Brukner, Quantum causality. *Nat. Phys.* **10**, 259–263 (2014)
20. L. Hardy, Probability theories with dynamic causal structure: a new framework for quantum gravity. [arXiv:0509120](https://arxiv.org/abs/0509120) [gr-qc]
21. G. Chiribella, G.M. D'Ariano, P. Perinotti, B. Valiron, Quantum computations without definite causal structure. *Phys. Rev. A* **88**, 022318 (2013)
22. G. Chiribella, Perfect discrimination of no-signalling channels via quantum superposition of causal structures. *Phys. Rev. A* **86**, 040301 (2012)
23. T. Colnaghi, G.M.D. Ariano, S. Facchini, P. Perinotti, Quantum computation with programmable connections between gates. *Phys. Lett. A* **376**, 2940–2943 (2012)
24. M. Araújo, F. Costa, Č. Brukner, Computational advantage from Quantum-Controlled ordering of gates. *Phys. Rev. Lett.* **113**, 250402 (2014)

Appendix A

A.1 Sketch of the Field Theory Derivation

The quantised Hamiltonian, Eq.(3.2), is here derived from a composite bosonic quantum field on a curved background. Denoting the field components $\varphi_J(x^0, \vec{x})$, $J = 1, \dots, N$ (and with $\hbar = 1$ for simplicity) the action of a quantum field reads [1, 2]

$$S = \int d^4x \sqrt{-g} \left(\sum_J g^{\mu\nu} \partial_\mu \varphi_J \partial_\nu \varphi_J + \sum_{J,K} M_{JK}^2 c^2 \varphi_J \varphi_K \right), \quad (\text{A.1})$$

where M_{JK} is the mass-matrix, which is positive and can be assumed symmetric without loss of generality; $g^{\mu\nu}$, $\mu, \nu = 0, \dots, 3$ is the space-time metric with signature $(-, +, +, +)$; and $\sqrt{-g}$ is the root of the determinant of $g_{\mu\nu}$. Einstein summation convention is employed. Assuming static and symmetric metric $\partial_{x^0} g^{\mu\nu} = 0$, and $g^{0i} = 0$, $i = 1, 2, 3$, the Euler-Lagrange equations reads

$$\left(\sqrt{-g}^{-1} \partial_\mu \sqrt{-g} g^{\mu\nu} \partial_\nu - \hat{M}^2 c^2 \right) \Phi = 0, \quad (\text{A.2})$$

where we introduced a vector notation for the field $\Phi^T := (\varphi_1, \dots, \varphi_N)$ and the operator \hat{M} for the mass-matrix M_{JK} . The first term in Eq.(A.2) is the curved space-time Laplacian [3], which written in terms of covariant derivatives ∇_μ gives

$$\left(g^{\mu\nu} \nabla_\mu \nabla_\nu - \hat{M}^2 c^2 \right) \Phi = 0. \quad (\text{A.3})$$

In terms of the four-momentum operators $\hat{P}_\mu = i\nabla_\mu$ Eq.(A.3) yields the familiar dispersion relation $g^{\mu\nu} \hat{P}_\mu \hat{P}_\nu = -\hat{M}^2 c^2$, where the rest mass-energy $c\hat{P}_0$ is given by the mass-matrix $\hat{M}c^2$, as e.g. for the neutrinos.

It is elementary to diagonalize Eq.(A.3) in the field components. Denoting by m_a , $a = 1, \dots, N$ the eigenvalues of \hat{M} (we assume non-degenerate spectrum for simplicity) we immediately obtain the Klein-Gordon equation for the corresponding

field $\tilde{\varphi}_a$: $(g^{\mu\nu}\nabla_\mu\nabla_\nu - m_a^2c^2)\tilde{\varphi}_a = 0$. For small energies, where particle creation and annihilation effects are negligible, the Klein-Gordon field can be treated as particle in first quantization and with the Ansatz $\tilde{\varphi}_a = e^{i[c^2S_0(x)+S_1(x)+c^{-2}S_2(x)+\dots]}$ one obtains that the solution satisfies Schrödinger-like equation with relativistic corrections [4, 5]. In particular, for a post-Newtonian metric $g_{00} = -(1 + 2\phi(x)/c^2 + 2\phi^2(x)/c^4)$, $g_{ij} = \delta_{ij}(1 - 2\phi(x)/c^2)$ following Ref. [5], for each component $\tilde{\varphi}_a$ one obtains

$$i\frac{\partial}{\partial t} = m_ac^2 + \frac{\hat{P}^2}{2m_a} + m_a\phi(x) - \frac{\hat{P}^4}{8m_a^3c^2} + \frac{m_a\phi^2(x)}{2c^2} + \frac{3}{2m_ac^2}\mathcal{F}(\hat{P}, \phi(x)), \quad (\text{A.4})$$

where $x^0 = ct$ and $\mathcal{F}(\hat{P}, \phi(x)) := \phi(x)\hat{P}^2 + [\hat{P}\phi(x)]\hat{P} + \frac{1}{2}[\hat{P}^2\phi(x)]$; notation: $[\hat{P}\phi(x)]$ denotes that \hat{P} as a differential operator acts only on $\phi(x)$.

In the low-energy limit the field components correspond to internal states of the composite particle with different rest mass-energies m_ac^2 . From Eq. (A.4) and linearity of quantum theory thus follows that the Hamiltonian for the external as well as internal states of the composity particle reads

$$\hat{H} = \hat{M}c^2 + \frac{\hat{P}^2}{2\hat{M}} + \hat{M}\phi(x) - \frac{\hat{P}^4}{8\hat{M}^3c^2} + \frac{\hat{M}\phi^2(x)}{2c^2} + \frac{3}{2\hat{M}c^2}\mathcal{F}(\hat{P}, \phi(x)),$$

Operator $\hat{M}c^2$ describes the total energy in the rest frame of the particle. \hat{M} (as well as any other operator) can be split into a constant part $\propto \hat{I}$ and the remaining dynamical part which we denote \hat{H}_{int} , i.e. we can always write $\hat{M} = m\hat{I}_{int} + \hat{H}_{int}/c^2$. Note that such defined parameter m can be identified with the mass-parameter of the particle, whereas the operator \hat{H}_{int} is the particle's rest frame Hamiltonian, which drives the dynamics of the internal degrees of freedom. Leaving only the lowest order terms in \hat{H}_{int}/mc^2 in the Hamiltonian \hat{H} yields

$$\begin{aligned} \hat{H} = mc^2 + \frac{\hat{P}^2}{2m} + m\phi(x) + \hat{H}_{int} \left(1 - \frac{\hat{P}^2}{2m^2c^2} + \frac{\phi(x)}{c^2} \right) \\ - \frac{\hat{P}^4}{8m^3c^2} + \frac{m\phi^2(x)}{2c^2} + \frac{3}{2mc^2}\mathcal{F}(\hat{P}, \phi(x)), \end{aligned} \quad (\text{A.5})$$

Appendix B

B.1 Evaluation of the Expected Photon Number

Consider the light source for the interferometer to be an ideal single photon source, which produces pulses propagating in the $+x$ (horizontal) direction each containing only one photon. In the local shell-frame on the earth's surface this can be represented by the quantum state (5.22). The use of plane-wave propagation is assumed justified by the paraxial approximation of a Gaussian spatial mode.

Detection of the horizontal output mode of the interferometer is assumed to be broadband (i.e. a frequency band-width much greater than the source) and time integrated (detection time is much longer than the pulse width) and thus can be described by an operator

$$a_o^\dagger a_o = \int \frac{d\tau_{r'}}{2\pi} \int d\nu e^{i\frac{\nu}{c}(x_{r'} - c\tau_{r'})} b_\nu^\dagger \int d\nu' e^{-i\frac{\nu'}{c}(x_{r'} - c\tau_{r'})} b_{\nu'} = \int d\nu b_\nu^\dagger b_\nu, \quad (\text{B.1})$$

where b_ν are single wave-number boson annihilation operators for the output mode. The expectation value $\langle a_o^\dagger a_o \rangle$ against the initial state (5.22) is calculated by finding the Heisenberg evolution of the detection operators. Quite generally the evolved single wave-number operators are of the form

$$b_\nu = \frac{1}{2} a_\nu (e^{-i\nu\phi_1} - e^{-i\nu\phi_2}) + \frac{1}{2} v_\nu (e^{-i\nu\phi_1} + e^{-i\nu\phi_2}), \quad (\text{B.2})$$

where v_ν are single wave-number boson annihilation operators from which the unoccupied input modes of the interferometer are constructed. Because they are initially in their vacuum state they will not contribute to the expectation value. The phases ϕ_i , $i = 1, 2$ are acquired propagating along the corresponding paths γ_i of the interferometer. Continuity at the mirror boundaries between the mode operator expressions along the different paths is assumed.

By symmetry, the contribution to the phases ϕ_i coming from the propagation along the radial part of the path is the same for both trajectories, as they are both

evaluated over an equal time-interval and have the same lengths as measured by a distant observer. Because they are common they will be eliminated since only the phase difference $\Delta\phi := \phi_1 - \phi_2$ will contribute to the final expression. From Eq. (5.22) and the metric Eq. (5.16) follows that the phases read $\phi_1 = \frac{1}{c}(l - c\tau_{r+h})$, $\phi_2 = \frac{1}{c}(l - c\tau_r)$ and thus

$$\Delta\phi = \Delta\tau, \quad (\text{B.3})$$

with $\Delta\tau$ given by the Eq. (5.21). Moreover, the locally measured radial distance h between the paths is found via

$$h_r = \int_r^{r+h} \frac{dr'}{\sqrt{1 - \frac{2GM}{c^2 r'}}}. \quad (\text{B.4})$$

Evaluating the photon number expectation value for the one-photon state $|1\rangle_f = \int d\nu f(\nu) e^{i\frac{\nu}{c}(x_r - c\tau_r)} a_\nu^\dagger |0\rangle$, Eq. (5.22), yields

$$\langle a_o^\dagger a_o \rangle = \langle 1 |_f \int d\nu b_\nu^\dagger b_\nu |1\rangle_f = \int d\nu |f(\nu)|^2 \frac{1}{4} |1 - e^{i\nu\Delta\tau}|^2, \quad (\text{B.5})$$

which is the same result as that of Eq. (5.23) for a single photon normalized wave packet.

Appendix C

C.1 Toy Models

Both experimental proposals discussed in Chap. 5 are formulated within the framework quantum mechanics on curved background. No effects specific to this theory have been experimentally verified so far—bridging this gap remains the principal motivation behind the present work. Quite generally, new physics is expected only at the scale where gravity itself could no longer be described as a classical theory. However, the tension between quantum mechanics and general relativity is of conceptual nature. Both theories stress that only operationally well defined notions may have physical meaning and this concerns also the notion of time (or proper time in general relativity). However, in contrast to general relativity, in quantum mechanics any degree of freedom of a physical system can be in a superposition and thus becomes undefined (beyond the classical probabilistic uncertainty). More generally—the theory allows for physical states that cannot be described within any local realistic model. If this applies to the degrees of freedom on which our operational treatment of time relies—the latter becomes classically undefined. This can be the case even when space-time itself can still be described classically, like in the proposals discussed in this thesis. One could, however, take an opposite view and assume that whenever space-time itself is classical, the time for any system, that constitutes an operationally defined clock, should admit a classical description as well. The tension between these two views motivates the investigation of theoretical frameworks alternative to quantum mechanics in curved space time. Here we sketch an explicit example of such an alternative toy theory, which can be tested by the experiments proposed in Chap. 5.

Relevant for the present problem is how the physical degrees of freedom evolve in a presence of time dilation. In the standard approach such evolution results in entanglement between the spatial mode of the wavefunction and other degrees of freedom. There is no well-defined time that such degrees of freedom experience and even a Bell-type experiment can be designed in which any local realistic model of time can be refuted. This entanglement results from the coupling $\hat{H}_{vis} = \hat{H}_s \frac{V(\hat{r})}{c^2}$, see

Eq. (5.29), and is the reason for the drop in the interferometric visibility (for both massive and massless cases). All so far observed gravitational effects can, however, be explained with one of two possible effective forms of such an interaction, which reproduce only specific features of (5.29) and correspond to different physical effects.

The effective coupling $\hat{H}_{phase} = \langle \hat{H}_s \rangle \frac{V(\hat{r})}{c^2}$, see Eq. (5.28), reproduces correctly the gravitational phase shift effect of the standard theory, but not the time dilation. Applying the operator (5.28) to the state of the clock degree of freedom $|\tau\rangle$ in a spatial superposition of two locations r_1 and r_2 , $|\Psi\rangle = \frac{1}{\sqrt{2}}(|r_1\rangle + |r_2\rangle)|\tau\rangle$, we get

$$\hat{H}_{phase}|\Psi\rangle = \frac{\langle \hat{H}_s \rangle}{\sqrt{2}} \left(\frac{V(r_1)}{c^2}|r_1\rangle + \frac{V(r_2)}{c^2}|r_2\rangle \right) |\tau\rangle,$$

where $\langle \hat{H}_s \rangle = \langle \tau | \hat{H}_s | \tau \rangle$. The full evolution in such a toy model is given by the Hamiltonian $\hat{H}_s + \hat{H}_{ps}$, which yields

$$|\Psi(t)\rangle = e^{-\frac{i}{\hbar}(\hat{H}_s + \hat{H}_{phase})t} |\Psi\rangle = \frac{1}{\sqrt{2}} \left[e^{-\frac{i}{\hbar}(\langle \hat{H}_s \rangle \frac{V(r_1)}{c^2})t} |r_1\rangle + e^{-\frac{i}{\hbar}(\langle \hat{H}_s \rangle \frac{V(r_2)}{c^2})t} |r_2\rangle \right] |\tau(t)\rangle, \quad (C.1)$$

where $|\tau(t)\rangle = e^{-\frac{i}{\hbar}\hat{H}_s t} |\tau\rangle$ and thus the evolution of the clock degree of freedom $|\tau\rangle$ does not depend on the position r . Hence, the coupling (5.28) predicts no general relativistic time dilation and no drop in the interferometric visibility—the clock degree of the freedom remains factorised from the spatial modes. However, each mode acquires a phase proportional to the gravitational potential and an effective mass defined by $\langle \hat{H}_s \rangle$, hence this effective coupling reproduces the relative phase shift measured in interference experiments. For a particle of mass m , $\hat{H}_s = mc^2 + \hat{H}_{int}$ (to first order in $1/c^2$), where \hat{H}_{int} is the Hamiltonian of the internal degrees of freedom and thus one obtains $m + \frac{\langle \hat{H}_{int} \rangle}{c^2}$ for the effective mass. The first term is simply the Newtonian mass, while the second is a relativistic correction. For a single photon mode with a frequency ω , $\hat{H}_s = \hbar\omega a^\dagger a$ and therefore the whole contribution to the phase shift comes from $\frac{\langle \hat{H}_s \rangle}{c^2} = \frac{\hbar\omega}{c^2}$. Thus, any measurement of the gravitational phase shift for photons would represent a signature of a non-Newtonian effective mass. However, no measurement of the phase shift (in the massive or massless case) could represent a measurement of the time dilation, since the phase shifts are explainable by the coupling (5.28) which does not cause clocks at different potentials to tick at different rates.

A different effective coupling can explain all classical general relativistic effects observed so far. It includes an effective gravitational potential $\langle V(\hat{r}) \rangle$ —gravitational potential smeared over the support of the wavefunction of a single physical system. Such a coupling reads

$$\hat{H}_{loc} = \hat{H}_s \frac{\langle V(\hat{r}) \rangle}{c^2} \quad (C.2)$$

and it accounts for gravitational experiments in which the relevant degrees of freedom are sufficiently well localized. These include not only classical tests of general rela-

tivity [6–10], but also experiments measuring the time dilation between two *localized* atomic clocks, each at a different gravitational potential.

More generally, one can construct a toy model by combining the above effective couplings \hat{H}_{phase} and \hat{H}_{loc} , for example

$$\hat{H}_i^{eff} = \hat{H}_s \left(1 + \frac{\langle V(\hat{r}) \rangle}{c^2} \right) + \frac{\Delta N_i}{\langle \hat{N}_i \rangle} \left(\langle \hat{H}_s \rangle \frac{V(\hat{r})}{c^2} - \hat{H}_s \frac{\langle V(\hat{r}) \rangle}{c^2} \right), \quad (\text{C.3})$$

which governs the evolution of the *i*th mode of a quantum state (one can associate different modes to e.g., different paths of a Mach-Zehnder interferometer). \hat{N}_i is the number operator in mode *i* and ΔN_i is its standard deviation. The parameter $\frac{\Delta N_i}{\langle \hat{N}_i \rangle}$ quantifies how well the quantum state is localised. It vanishes for Fock states (e.g. for a pair of atoms or photons, each in one, localised mode), and in the limit of large coherent states (for a coherent state $|\alpha\rangle$ in mode *i* we have $\frac{\Delta N_i}{\langle \hat{N}_i \rangle} = \frac{1}{|\alpha|} \rightarrow 0$ for $\alpha \rightarrow \infty$), which for photons corresponds to classical light. In both cases the Hamiltonian (C.3) reduces to $\hat{H}_s \left(1 + \frac{\langle V(\hat{r}) \rangle}{c^2} \right)$. In the other limit, when the parameter $\frac{\Delta N_i}{\langle \hat{N}_i \rangle} = 1$, which is the case for a single particle in a superposition of two modes, the effective Hamiltonian reduces to $\hat{H}_s + \langle \hat{H}_s \rangle \frac{V(\hat{r})}{c^2}$. The toy model (C.3) predicts no drop in the interferometric visibility for a particle in a spatial superposition (since in the relevant limit the energy operator \hat{H}_s does not couple to the potential) but is still consistent with the experiments carried out so far. (Moreover, Eq. (C.3) can be generalised beyond the above weak energy limit).

The difference between the standard extension of quantum mechanics to curved space-time and the toy model (C.3) can only be tested with a quantum system from which the time can be read out and which is put in a coherent spatial superposition at different gravitational potentials. Even though this model is artificial (e.g., it shares the difficulties of all quantum nonlinear models) it highlights the conceptual difference between gravitational phase shift experiments and measurements of the visibility loss. (While the former only probe the semi-classical coupling of energy to the gravitational potential, the latter directly test the full quantum form of such a coupling). Most importantly, the toy model emphasises the necessity of probing quantum mechanics in curved space-time: the results of current experiments cannot necessarily be extrapolated to this regime.

Appendix D

D.1 Mixed Internal States as Clocks

The time dilation induced coupling between internal degrees of freedom and the centre of mass causes decoherence of the latter. The complementarity principle between the visibility V of interference and the which-path information D is given by the inequality $V^2 + D^2 \leq 1$. The equal sign holds for pure states, i.e. for well-defined clocks as considered in Chap. 5. For mixed states, it is possible to have loss of visibility with no accessible which-path information, as is the case here (as well as in most other decoherence models such as in quantum Brownian motion [11, 12]). Mixed state of internal degrees of freedom can be seen as a mixture of clock-states that each measure the proper time along their path. To highlight this, consider for example a particle with a single 2-level internal degree of freedom which is in a clock-state, i.e. in a superposition of the ground and excited state with transition frequency $\omega = 1/t_\perp$ and an arbitrary relative phase ϕ : $|E_\phi\rangle = \frac{1}{\sqrt{2}}(|g\rangle + e^{i\phi}|e\rangle)$. If the particle moves along a path with overall proper time τ , the internal state will evolve to $|E_\phi(\tau)\rangle = \frac{1}{\sqrt{2}}(|g\rangle + e^{i\phi+\omega\tau}|e\rangle)$. For the particle in superposition along two paths with proper time difference $\Delta\tau$, the internal clock state will therefore acquire which-path information, thus leading to a loss in visibility given by $|\langle E_\phi(\tau_1)|E_\phi(\tau_2)\rangle| = |\cos(\omega\Delta\tau/2)|$, independent of the phase ϕ . For a fully mixed internal state (analogous to a thermal state),

$$\rho = \frac{1}{2} (|E_\phi\rangle\langle E_\phi| + |E_{\phi+\pi}\rangle\langle E_{\phi+\pi}|), \quad (\text{D.1})$$

the relative phase between $|g\rangle$ and $|e\rangle$ is unknown and thus no which-path information is available, but it still results in a drop in visibility. The above state can be equivalently written in the basis

$$\rho = \frac{1}{2} (|g\rangle\langle g| + |e\rangle\langle e|). \quad (\text{D.2})$$

Since it represents the same state, it will cause the same loss of visibility, the two situations (D.1) and (D.2) cannot be discriminated. The states $|g\rangle$ and $|e\rangle$ individually, however, are not clock-states, thus no time dilation can be read out directly. The interpretation of the visibility drop in this representation is the phase scrambling between $|g\rangle$ and $|e\rangle$ due to the red shift, since the states $|e\rangle$ acquire a different phase than the states $|g\rangle$. Irrespective of the state representation, time dilation causes loss of coherence of composite particles with internal degrees of freedom.

Appendix E

E.1 The Lowest Energy Limit of “Clock” Hamiltonian

Chapter 7 discusses the regime where kinetic and potential energies of test particles are low, such that relativistic corrections to the external motion of the particle (second line of Eq. (A.5)) are negligible, but where relativistic corrections to the internal dynamics $\hat{H}_{int}(-\frac{\hat{p}^2}{2m^2c^2} + \frac{\phi(x)}{c^2})$ cannot be neglected. In such a regime Eq. (A.5) becomes

$$\hat{H} = mc^2 + \frac{\hat{p}^2}{2m} + m\phi(x) + \hat{H}_{int} \left(\hat{I} - \frac{\hat{p}^2}{2m^2c^2} + \frac{\phi(x)}{c^2} \right), \quad (\text{E.1})$$

(which is the Hamiltonian in Eq. (7.2)).

Below it is shown how Eq. (E.1) can be derived directly from a simple WKB approximation to the Klein-Gordon equation (A.3). It suffices to take the following Ansatz for a solution:

$$\Phi(x^0, \vec{x}) = e^{-i\hat{M}cx^0} \psi(x^0, \vec{x}). \quad (\text{E.2})$$

It gives $\partial_0 \partial_0 \Phi \approx -\hat{M}^2 c^2 e^{-i\hat{M}cx^0} \psi - 2i\hat{M}c e^{-i\hat{M}cx^0} \partial_0 \psi$, where $e^{-i\hat{M}cx^0} \partial_0 \partial_0 \psi$ has been neglected as small compared to the other terms. We thus have

$$g^{00}(\hat{M}^2 c^2 \Phi + 2i\hat{M}c e^{-i\hat{M}cx^0} \partial_0 \psi) \approx (g^{ij} \hat{\nabla}_i \hat{\nabla}_j - \hat{M}^2 c^2) \Phi.$$

Introducing again $t = x^0/c$ and denoting $\dot{\psi} \equiv \partial_t \psi$ yields

$$i\dot{\Phi} \approx \left(\hat{M}c^2 + \frac{1}{2\hat{M}} g_{00} g^{ij} \hat{\nabla}_i \hat{\nabla}_j + \frac{1}{2\hat{M}} (-g_{00} - 1) \hat{M}^2 c^2 \right) \Phi. \quad (\text{E.3})$$

For a post-Newtonian metric introduced above and using again the notions of mass and internal energy defined through $\hat{M} = m\hat{I}_{int} + H_{int}/c^2$, Eq. (E.3) immediately reduces to Eq. (E.1) (when keeping terms of order H_{int}/mc^2).

E.2 Einstein's Hypothesis of Equivalence

This appendix shows, that the conditions derived in Sect. 7.2—imposed by the EEP on the dynamics of a massive system with internal degrees of freedom—are equivalent to conditions stemming directly from requiring the validity of the Einstein's hypothesis of equivalence.

As in the main text, the rest mass-energy operator of a massive system with internal degrees of freedom is denoted by $\hat{M}_r = m_r\hat{I}_{int} + \hat{H}_{int,r}/c^2$ and the inertial mass-energy operator by $\hat{M}_i = m_i\hat{I}_{int} + \hat{H}_{int,i}/c^2$. In an inertial coordinate system (x, t) and in the absence of external gravitational field, the low energy limit of a Hamiltonian of such system reads

$$i\hbar\frac{\partial}{\partial t} = \hat{M}_r c^2 - \frac{\hbar^2}{2\hat{M}_i} \nabla^2, \quad (\text{E.4})$$

where $-i\hbar\nabla \equiv -i\hbar\frac{\partial}{\partial x} = \hat{P}$ is the center of mass momentum operator and where $1/\hat{M}_i \approx \frac{1}{m_i}(\hat{I}_{int} - \hat{H}_{int,i}/m_i c^2)$. Lorentz boost is generated by $\hat{K} = i\hbar t\nabla + i\hbar\frac{x}{c^2}\frac{\partial}{\partial t}$ and to lowest order in the boost parameter v , the resulting new coordinates read $(x' \approx x + vt, t' \approx t + \frac{vx}{c^2})$ [1], thus

$$\begin{cases} \nabla = \nabla' + \frac{v}{c^2} \frac{\partial}{\partial t'}, \\ \frac{\partial}{\partial t} = v\nabla' + \frac{\partial}{\partial t'}, \end{cases} \quad (\text{E.5})$$

The Hamiltonian in Eq. (E.4) transforms into

$$i\hbar\frac{\partial}{\partial t'} = \hat{M}_r c^2 - \frac{\hbar^2}{2\hat{M}_i} \nabla'^2 + i\hbar v \left(\frac{\hat{M}_r}{\hat{M}_i} - 1 \right) \nabla' + \mathcal{O}(c^{-4}). \quad (\text{E.6})$$

and is invariant under the Lorentz boost if $\hat{M}_i = \hat{M}_r$. Since the rest mass parameter m_r can be assigned arbitrary value without introducing observable consequences (as long as the gravitational field produced by the system is not considered—which is the case here), the physical requirement imposed by demanding Lorentz invariance in this limit reads $\hat{H}_{int,i} = \hat{H}_{int,r}$, as derived the main text.

Requiring the validity of the Einstein's hypothesis of equivalence—the total physical equivalence between laws of relativistic physics in a non-inertial, constantly accelerated, reference frame and in a stationary frame subject to homogeneous gravity—imposes further conditions. A transformation from the initial inertial frame (x, t) to

an accelerated coordinate system ($x'' \approx x + \frac{1}{2}gt^2$, $t'' \approx t + \frac{gtx}{c^2}$), with g denoting the acceleration, gives (to lowest order):

$$\begin{cases} \nabla = \nabla'' + \frac{gt}{c^2} \frac{\partial}{\partial t''}, \\ \frac{\partial}{\partial t} = gt \nabla'' + \left(1 + \frac{gt}{c^2}\right) \frac{\partial}{\partial t''}. \end{cases} \quad (\text{E.7})$$

Schrödinger equation Eq. (E.4) transforms under Eq. (E.7) into

$$i\hbar \frac{\partial}{\partial t''} = \hat{M}_r c^2 - \hat{M}_r gx + i\hbar gt \left(\frac{\hat{M}_r}{\hat{M}_i} - 1 \right) \nabla'' - \frac{\hbar^2}{2\hat{M}_i} \nabla''^2. \quad (\text{E.8})$$

For a massive particle subject to a homogeneous gravitational potential $\phi(x) = gx$ its coupling to gravity is given by its gravitational charge—the total gravitational mass-energy $\hat{M}_g = m_g \hat{f}_{int} + \hat{H}_{int,g}/c^2$, where m_g describes the gravitational mass parameter and $\hat{H}_{int,g}$ contribution to the mass from internal energy. The Hamiltonian of such a system reads

$$i\hbar \frac{\partial}{\partial t'} = \hat{M}_r c^2 - \hat{M}_g gx - \frac{\hbar^2}{2\hat{M}_i} \nabla'^2. \quad (\text{E.9})$$

Thus, for the validity of the Einstein's Hypothesis of Equivalence in addition to $\hat{H}_{int,i} = \hat{H}_{int,r}$ it is also required that $\hat{M}_g = \hat{M}_i$ —in full agreement with the derivation in the main text. Moreover when the hypothesis of equivalence holds, the Hamiltonians of a composed quantum system subject to weak gravity reduces to the Hamiltonian in Eq. (7.2).

E.3 Fully Classical Test Theory of the EEP

In classical physics Hamiltonian of a composite system is a function of phase space variables of the centre of mass (Q, P) and of the internal degree of freedom (q, p) with the internal mass-energies $M_\alpha = m_\alpha c^2 + E_\alpha$ and reads

$$\tilde{H}_{test}^C = M_r + \frac{P^2}{2M_i} + M_g \phi(Q) \approx m_r c^2 + E_r + \frac{P^2}{2m_i} + m_g \phi(Q) - E_i \frac{P^2}{2m_i c^2} + E_g \frac{\phi(Q)}{c^2}. \quad (\text{E.10})$$

Time evolution of a classical variable is obtained from its Poisson bracket with the total Hamiltonian: $d/dt = \{\cdot, \tilde{H}_{test}^C\}_{PB}$. The acceleration of the center of mass Q reads

$$\ddot{Q} = -M_g M_i^{-1} \nabla \phi(Q), \quad (\text{E.11})$$

where ∇ is derivative with respect to Q . Equation (E.11) recovers the result that free fall is universal if $M_g = M_i = 1$ (or more generally, M_g/M_i can be any positive

number, the same for all physical systems, but such a numerical factor would just redefine the gravitational potential).

The time evolution of the internal variable q (keeping only first order terms in $H_{int,\alpha}/m_\alpha c^2$) reads

$$\dot{q}(Q, P) = \dot{q}_r - \dot{q}_i \frac{P^2}{2m_i^2 c^2} + \dot{q}_g \frac{\phi(Q)}{c^2}, \quad (\text{E.12})$$

where $\dot{q}_\alpha := \{q, H_\alpha\}_{PB}$ are in principle different velocities. The gravitational time dilation factor $\Delta\dot{q}/\dot{q} := \frac{\dot{q}(Q+h, P) - \dot{q}(Q, P)}{\dot{q}(Q, P)}$ reads

$$\Delta\dot{q}/\dot{q} \approx \frac{\dot{q}_g}{\dot{q}_r} \frac{\nabla\phi(Q)h}{c^2}, \quad (\text{E.13})$$

and it reduces to that predicted by general relativity $\Delta\dot{q}/\dot{q} \approx \frac{\nabla\phi(Q)h}{c^2}$ if $H_{int,r} = H_{int,g}$. Similarly, universality of special relativistic time dilation is recovered if $H_{int,r} = H_{int,i}$.

Conditions for the validity of the EEP (and the number of parameters to test) are the same in the fully classical case above and in the model H_{test}^C which describes a system with quantised centre of mass degrees of freedom. Since the EEP imposes equivalence conditions on the mass-energies of the system, it is the quantisation of the internal energy which is relevant for the difference between the classical and the quantum formulation of the EEP.

E.4 Lagrangian Formulation of the Test Theory

Lagrangian formulation of the test theory is obtained from the Legendre transform of the test Hamiltonian. The derivation is valid for both the classical and the quantum model; we will thus write for brevity $H_{test} = m_r c^2 + H_{int,r} + \frac{P^2}{2m_i} + m_g \phi(Q) - H_{int,i} \frac{P^2}{2m_i^2 c^2} + H_{int,g} \frac{\phi(Q)}{c^2}$.

For the centre of mass degree of freedom the canonically conjugate velocity is given by

$$\dot{Q} = \frac{\partial H_{test}}{\partial P} = \frac{P}{m_i} \left(1 - \frac{H_{int,i}}{m_i c^2} \right).$$

We formally introduce position q and momentum p of the internal degrees of freedom, which dynamics is given by the Hamiltonians $H_{int,\alpha} = H_{int,\alpha}(q, p)$. The conjugate internal velocity is thus defined as $\dot{q} = \frac{\partial H_{test}}{\partial p}$ and reads

$$\dot{q} = \frac{\partial H_{int,r}}{\partial p} - \frac{\partial H_{int,i}}{\partial p} \frac{P^2}{2m_i^2 c^2} + \frac{\partial H_{int,g}}{\partial p} \frac{\phi(Q)}{c^2}.$$

Lagrangian of the test theory can now be obtained through the Legendre transform of H_{test} : $L_{test} := P\dot{Q} + p\dot{q} - H_{test}$. We first introduce the total internal Lagrangians L_α via the Legendre transform of the total internal mass-energies $m_\alpha c^2 + H_{int,\alpha}$:

$$L_\alpha := \frac{\partial H_{int}}{\partial p} p - m_\alpha c^2 - H_{int,\alpha} \equiv -m_\alpha c^2 + L_{int,\alpha},$$

which leads the test Lagrangian in the form:

$$L_{test} = L_r - L_i \frac{\dot{Q}^2}{2c^2} + L_g \frac{\phi(Q)}{c^2}. \quad (\text{E.14})$$

Note, that $-m_\alpha c^2$ is the non-dynamical part of the internal Lagrangian and $L_{int,\alpha}$ is its dynamical part—in a full analogy to the Hamiltonian picture where mc^2 is the non-dynamical and $H_{int,\alpha}$ the dynamical part of the internal mass-energy. The conditions for the validity of the EEP derived in the main text for the internal Hamiltonians now translate to $L_i = L_r = L_g$. Indeed, when the internal dynamics is universal $L_\alpha \equiv L_0$ the Eq. (E.14) reduces to

$$L_{test} \xrightarrow{L_\alpha \equiv L_0} L = L_0 \left(1 - \frac{\dot{Q}^2}{2c^2} + \frac{\phi(Q)}{c^2}\right). \quad (\text{E.15})$$

Equation (E.15) is the lowest order approximation to the dynamics of a particle in space-time given by e.g. the Schwarzschild metric. Indeed, $L \approx L_0 \sqrt{-g_{\mu\nu} \dot{x}^\mu \dot{x}^\nu}$ with metric elements $g_{00} \approx -(1 + 2\phi(x)/c^2)$, $g_{ij} \approx c^{-2} \delta_{ij}$, $g_{0i} = g_{i0} = 0$ $i, j = 1, 2, 3$. In the limit $L_0 \approx -mc^2$ the non-relativistic Lagrangian of a massive particle in Newtonian potential is recovered $L \approx -mc^2 + m\dot{Q}^2/2 - m\phi(Q)$.

In contrast to thus far considered test theories of the EEP for composed systems, which only incorporate internal (binding) energy as fixed parameters, test theory given by the Lagrangian in Eq. (E.14) incorporates the dynamics of the associated degrees of freedom.

E.5 Quantum Test of the Classical WEP

Assume that WEP holds but only in the Newtonian limit, $m_i = m_g \equiv m$, and that LLI is valid ($\hat{H}_{int,r} = \hat{H}_{int,i}$) but $\hat{H}_{int,i} \neq \hat{H}_{int,g}$. In particular, we restrict to classical violations of the WEP, i.e. $[\hat{H}_{int,i}, \hat{H}_{int,g}] = 0$. For an internal energy eigenstate $|E_j\rangle$ we have $\hat{M}_i |E_j\rangle = M_{1,i} |E_j\rangle$ and $\hat{M}_g |E_j\rangle = M_{j,g} |E_j\rangle$ where $M_{j,\alpha} = m + E_{j,\alpha}/c^2$. From Eq. (7.6) we obtain $\hat{Q} |E_j\rangle = -g_j |E_j\rangle$ ($j = 1, 2$) where $g_j = g M_{j,g}/M_{j,i}$ where we assumed homogeneous gravitational field g . Parameters describing possible violations are $\eta_j := M_{j,g}/M_{j,i}$ (which can be seen as the diagonal elements of the matrix $\hat{\eta}$ introduced in Sect. 7.3). When $\eta_1 \neq \eta_2$ for some two internal states

$|E_1\rangle, |E_2\rangle$ the centre of mass will have the free-fall acceleration that depends on the internal state. Consider now a coherent superposition of the two internal energy eigenstates, semi-classically localised at some height h :

$$|\Psi(0)\rangle = 1/\sqrt{2}(|E_1\rangle + |E_2\rangle)|h\rangle. \quad (\text{E.16})$$

Under free-fall it evolves into

$$|\Psi(t)\rangle = 1/\sqrt{2}(e^{i\phi_1}|E_1\rangle|h_1\rangle + e^{i\phi_2}|E_2\rangle|h_2\rangle), \quad (\text{E.17})$$

where $h_j = h - 1/2g_jt^2$, $j = 1, 2$ is the position of the centre of mass correlated with the internal state $|E_j\rangle$ after time t of free fall and $\phi_j(t)$ is the free propagation phase for a particle with a total mass $M_{j,i}$ under gravitational acceleration g_j , which can be found e.g. in [13]. Initial superposition in a presence of classical violations evolves into an entangled state, with the internal degree of freedom entangled to the position. As a result the reduced state of the internal degrees of freedom $\hat{\rho}_{int}(t)$ becomes mixed: $\hat{\rho}_{int}(t) := \text{Tr}[|\Psi(t)\rangle\langle\Psi(t)|] = 1/2(|E_1\rangle\langle E_1| + |E_2\rangle\langle E_2| + e^{i\phi_1 - i\phi_2}\langle h_2|h_1\rangle|E_1\rangle\langle E_2| + h.c.)$. The amplitude of the off-diagonal elements

$$\mathcal{V} := |\langle h_2|h_1\rangle| \quad (\text{E.18})$$

quantifies the coherence of the reduced state and it decreases with the position amplitudes becoming distinguishable, in agreement with the quantum complementarity principle for pure states, see e.g. [14]. When the position amplitudes become orthogonal we have $\mathcal{V} = 0$ and the reduced state becomes maximally mixed. The classical violations of the WEP and the superposition principle of quantum mechanics thus entail decoherence of any freely falling system into its internal energy eigenbasis.

Since we assumed the validity of the LLI but a violation of the WEP we shall also observe a related violation of the LPI. Indeed, a coherent superposition of different energy states evolves in time and thus constitutes a “clock”. A frequency of such a “clock” is given by the inverse of the energy difference between the superposed states. The internal state in Eq. (E.16) when trapped at a height h evolves in time at a rate $\omega(h) = \omega(0)(1 + (E_{2,g} - E_{1,g})/(E_{2,i} - E_{1,i})gh/c^2)$ where $\omega(0) = (E_{2,i} - E_{1,i})/\pi\hbar$, in violation of the LPI. In case of no violations this rate would read $\omega(h)_{GR} = \omega(0)(1 + gh/c^2)$. An anomalous frequency dependence on the system’s position in the laboratory frame $\omega(h)$ would be the only consequence of the classical violations of the LPI for classical clocks. However, for a quantum “clock” there is an additional effect: The final state of the internal degree of freedom in Eq. (E.17) is stationary (because it becomes fully mixed). Classical violations discussed above thus result in a decoherence of any time evolving state, a “clock” into a stationary mixture.

Decoherence effect and entanglement between internal and external degrees of freedom, that would arise as a result of the classical violations of the WEP, cannot be described within a fully classical theory. Quantum test theory of the EEP is therefore necessary in order to describe all effects of the EEP violations on quantum systems, even if the violations themselves are assumed to be classical.

Realisation of such a quantum test of the classical WEP in principle takes place in interferometric experiments where atoms propagating in the two arms of the interferometer are in different energy eigenstates (Raman beam-splitting). As an example we consider a recent experiment performed by the group of P. Bouyer [15]. In this experiment Mach-Zehnder interferometer with ^{87}Rb was operated during a ballistic flight of an airplane with the aim to provide a proof of principle realisation of an inertial sensor in microgravity. We approximate the centre of mass position of the atoms by a Gaussian distribution $\langle x|h_j \rangle \propto e^{-(h_j-x)^2/2l_c^2}$ where l_c is the coherence length of the atom's wave-function. Assuming small violations the visibility in Eq. (E.18) can be approximated to $\mathcal{V} \approx 1 - (\Delta\eta \frac{gT^2}{l_c})^2$, where $\Delta\eta = |\eta_1 - \eta_2|$. From the experimental parameters estimated in [15]: $\mathcal{V} \approx 0.65$, $T = 20$ ms and estimating $l_c \approx 10 \mu\text{m}$ we can infer a bound $\Delta\eta < 8 \times 10^{-3}$.

Appendix F

F.1 Proof of the Bell Theorem for Temporal Order

More formally, the thesis of the theorem 1 in Sect. 8.2 can be expressed in the following way: assume that the observers a_1, b_1, c_1 are given as an input a bit i_1 and produce, through their local operations and measurements, a single bit of output o_1 , while the observers a_2, b_2, c_2 have a bit i_2 as input and a bit o_2 as output. The observer d produces an arbitrary variable z as a result of a local measurement. Then, given the assumptions of the theorem, the conditional probability

$$P(o_1, o_2 | i_1, i_2, z) \quad (\text{F.1})$$

does not violate Bell inequalities for any value of z .

By assumption, no initially entangled state is shared by the three groups of observers. Since quantum mechanics is valid locally, and the three regions are space-like separated, any shared resource can be described as a tri-partite separable state $\rho^{S_1 S_2 d}$, where S_1 represents the subsystem on which the operations at events A_1, B_1, C_1 are performed, S_2 is the subsystem on which the operations at events A_2, B_2, C_2 are performed, and d is the part of the system on which a measurement at D is performed. Because of assumption (4), the operations in each region are always performed in a specific order, although this order might depend on a classical variable λ defined on some space-like surface in the past. Thus, for each λ , the sequence of the three operations performed at events A_1, B_1, C_1 is represented by a POVM $\{E_{o_1}^\lambda(i_1)\}_{o_1}$; similarly a POVM $\{F_{o_2}^\lambda(i_2)\}_{o_2}$ describes the operations performed at events A_2, B_2, C_2 , and $\{G_z\}_z$ represents the D measurement.

More generally, the value of λ might be modified by a local operation. For example, given a λ such that A_1 is before B_1 and C_1 , the order between the latter two can depend on the operation performed in A_1 . However, the choice of operation on A_1 can only depend on the local input i_1 . Thus, for each value of i_1 the result of the three operations is still described by a POVM $\{E_{o_1}^\lambda(i_1)\}_{o_1}$. Even if, for a given i_1 , $B_1 \preceq C_1$ with some probability $0 < q(i_1) < 1$, (and $C_1 \preceq B_1$ with

probability $1 - q(i_1)$), the resulting effect can be described by the mixture of POVMs $\{q(i_1)E_{o_1}^{\lambda, B_1 \leq C_1}(i_1) + [1 - q(i_1)]E_{o_1}^{\lambda, C_1 \leq B_1}(i_1)\}_{o_1}$, which is still a POVM.

The probability distribution resulting from the local measurements is thus given by:

$$P(o_1, o_2, z|i_1, i_2) = \int d\lambda p(\lambda) \text{Tr} [E_{o_1}^{\lambda}(i_1) \otimes F_{o_2}^{\lambda}(i_2) \otimes G_z \rho^{S_1 S_2 d}], \quad (\text{F.2})$$

where $p(\lambda)$ is an arbitrary probability distribution for λ . Consider in particular a product state $\rho^{S_1 S_2 d} = \rho_1^{S_1} \otimes \rho_2^{S_2} \otimes \rho_3^d$. Then (F.2) takes the form

$$P(o_1, o_2, z|i_1, i_2) = \int d\lambda p(\lambda) \text{Tr} [E_{o_1}^{\lambda}(i_1) \rho_1^{S_1}] \text{Tr} [F_{o_2}^{\lambda}(i_2) \rho_2^{S_2}] \text{Tr} [G_z \rho_3]$$

and the conditional probability (F.1) is

$$P(o_1, o_2|i_1, i_2, z) = \int d\lambda p(\lambda) P(o_1|i_1, \lambda) P(o_2|i_2, \lambda), \quad (\text{F.3})$$

where $P(o_1|i_1, \lambda) = \text{Tr} [E_{o_1}^{\lambda}(i_1) \rho_1^{S_1}]$ and $P(o_2|i_2, \lambda) = \text{Tr} [F_{o_2}^{\lambda}(i_2) \rho_2^{S_2}]$. Since the probability distribution (F.3) satisfies the hypothesis of Bell's theorem [16], it cannot violate any Bell inequality. For an arbitrary separable state, the conditional probability (F.1) will be a convex combination of probabilities of the form (F.3), so it will still respect the hypothesis of Bell's theorem and will not allow any violation of Bell's inequalities.

References

1. S. Weinberg, *The Quantum Theory of Fields*, vol 2 (Cambridge University Press, 1996)
2. N. D. Birrell, P.C.W. Davies, *Quantum Fields in Curved Space*, vol 7 (Cambridge University Press, 1984)
3. S. Weinberg, *Gravitation and cosmology: principle and applications of general theory of relativity* (Wiley, New York, 1972)
4. C. Kiefer, T.P. Singh, Quantum gravitational corrections to the functional Schrödinger equation. *Phys. Rev. D* **44**, 1067–1076 (1991)
5. C. Laemmerzahl, A Hamilton operator for quantum optics in gravitational fields. *Phys. Lett. A* **203**, 12–17 (1995)
6. R. Pound, G. Rebka, Apparent weight of photons. *Phys. Rev. Lett.* **4**, 337–341 (1960)
7. J.C. Hafele, R.E. Keating, Around-the-world atomic clocks: predicted relativistic time gains. *Science* **177**, 166–168 (1972)
8. J.C. Hafele, R.E. Keating, Around-the-world atomic clocks: observed relativistic time gains. *Science* **177**, 168–170 (1972)
9. I.I. Shapiro, Fourth test of general relativity. *Phys. Rev. Lett.* **13**, 789–791 (1964)
10. I.I. Shapiro, M.E. Ash, R.P. Ingalls, W.B. Smith, D.B. Campbell, R.B. Dyce, R.F. Jurgens, G.H. Pettengill, Fourth test of general relativity: new radar result. *Phys. Rev. Lett.* **26**, 1132–1135 (1971)

11. A.O. Caldeira, A.J. Leggett, Path integral approach to quantum Brownian motion. *Phys. A Stat. Mech. Appl.* **121**, 587–616 (1983)
12. H.-P. Breuer, F. Petruccione, *The Theory of Open Quantum Systems* (Oxford University Press, 2002)
13. P. Storey, C. Cohen-Tannoudji, The Feynman path integral approach to atomic interferometry. *J. Phys.* **II**(4), 1999–2027 (1994). A tutorial
14. B.-G. Englert, Fringe visibility and which-way information: an inequality. *Phys. Rev. Lett.* **77**, 2154–2157 (1996)
15. R. Geiger, V. Ménotet, G. Stern, N. Zahzam, P. Cheinet, B. Battelier, A. Villing, F. Moron, M. Lours, Y. Bidel et al., Detecting inertial effects with airborne matter-wave interferometry. *Nat. Commun.* **2**, 474 (2011)
16. J.S. Bell, On the Einstein-Podolsky-Rosen paradox. *Physics* **1**, 195–200 (1964)